EPFL

Bionic artificial limbs (2nd part)

Translational neuroengineering

Silvestro Micera,
silvestro.micera@epfl.ch
Bertarelli Foundation Chair in Translational Neuroengineering,
Center for Neuroprosthetics, EPFL, Geneva

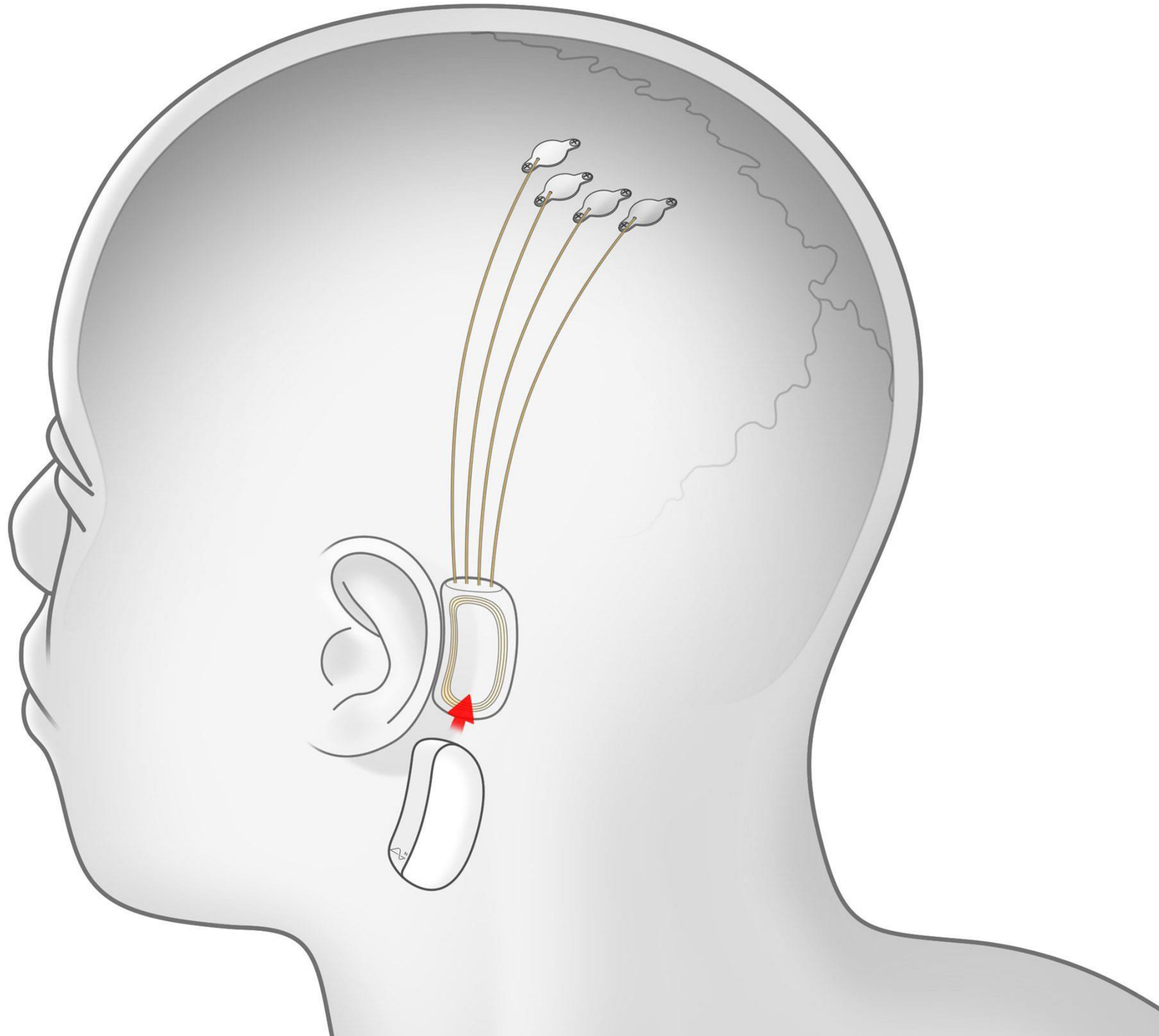

Translational NeuroEngineering

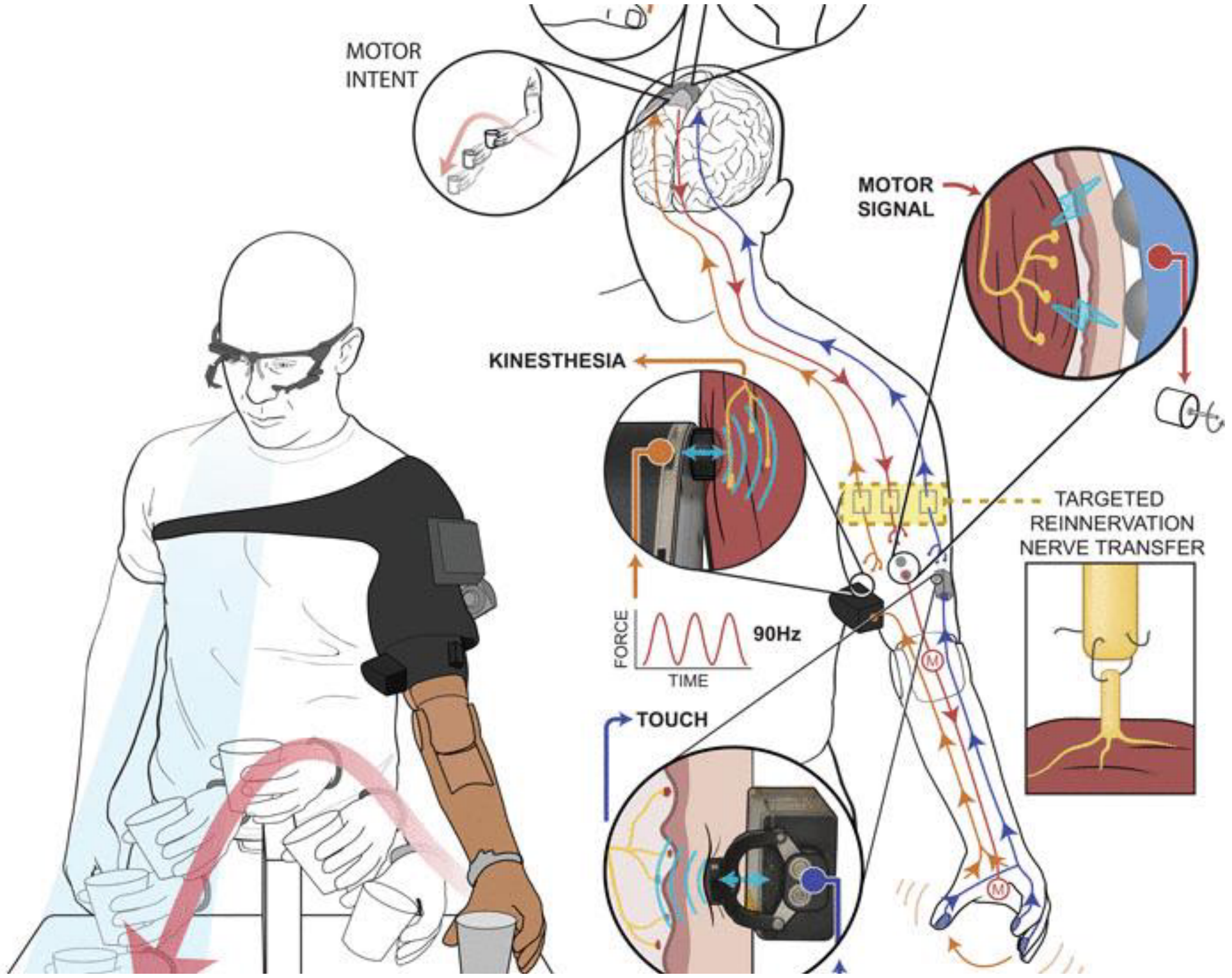
MOTOR
INTENT
MOTOR
SIGNAL
KINESTHESIA
TARGETED
REINNERVATION
NERVE TRANSFER
FORCE
TIME
90Hz
TOUCH

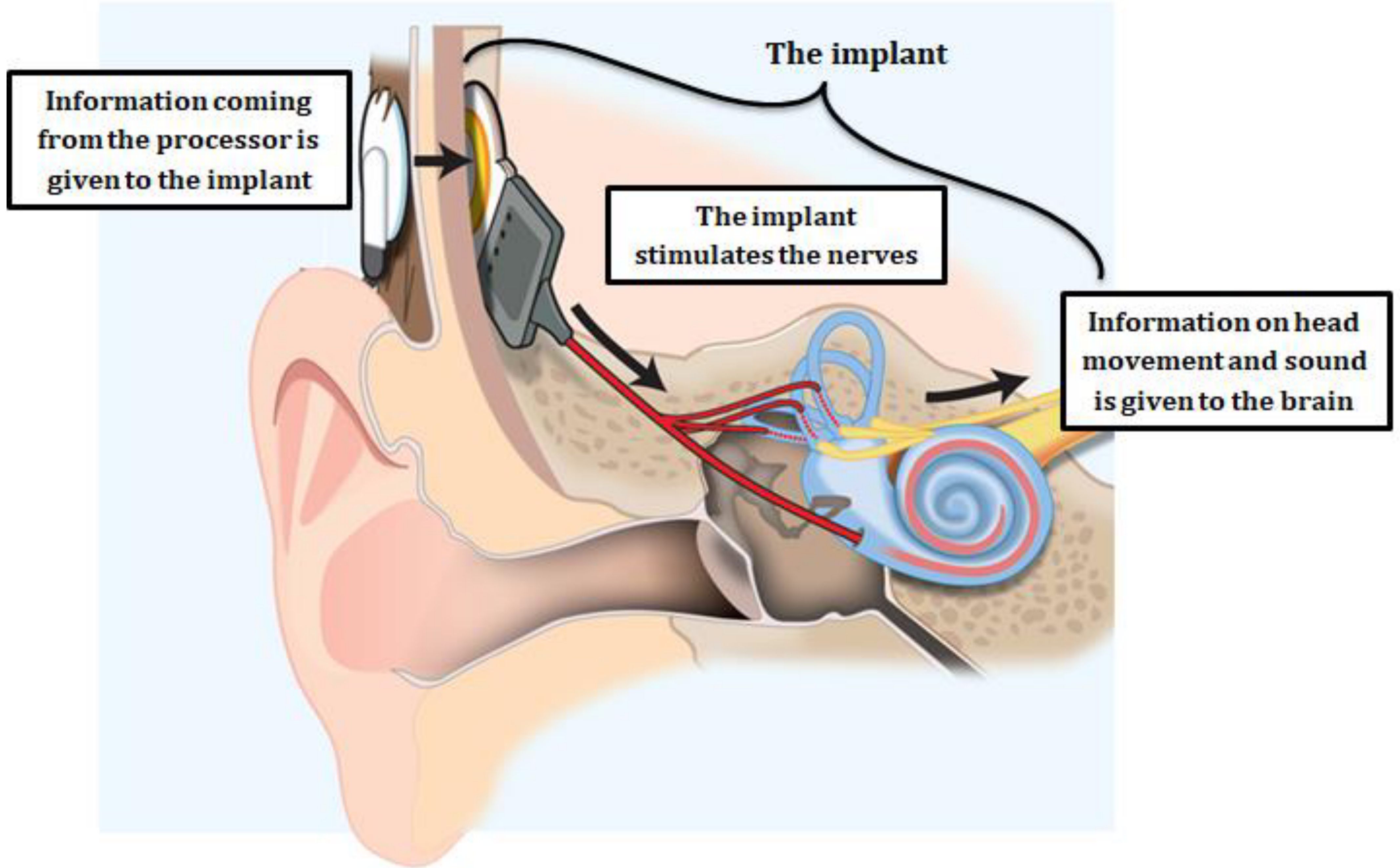
The implant
Information coming from the processor is given to the implant
The implant stimulates the nerves
Information on head movement and sound is given to the brain

Bionic artificial hand

What can an amputee get today?

Hand Prosthesis

- Prosthetic Hands
  - Passive
    - Cosmetic
  - Active
    - Body-powered
    - Myoelectric

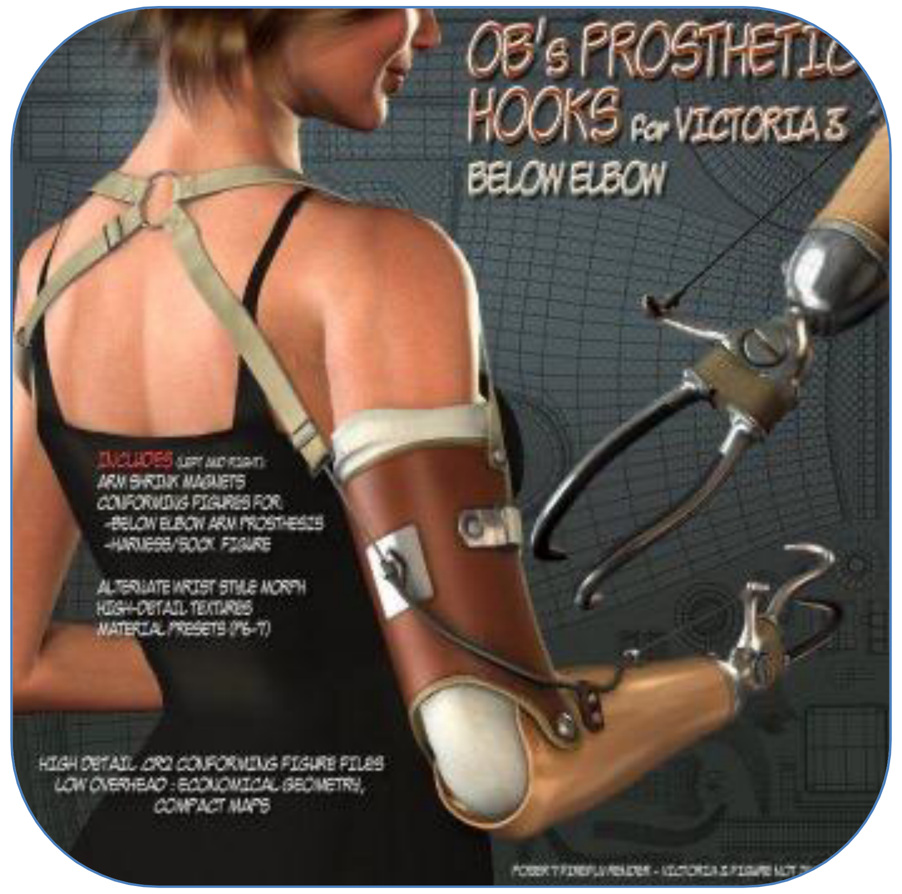

Mechatronic

Design issues: adaptability

Problem: It's an hard task to **design, actuate, and control** a self-contained artificial hand with a number of degrees of freedom (DoF) equal or close to those in the biological human hand!

22 muscles … + 18

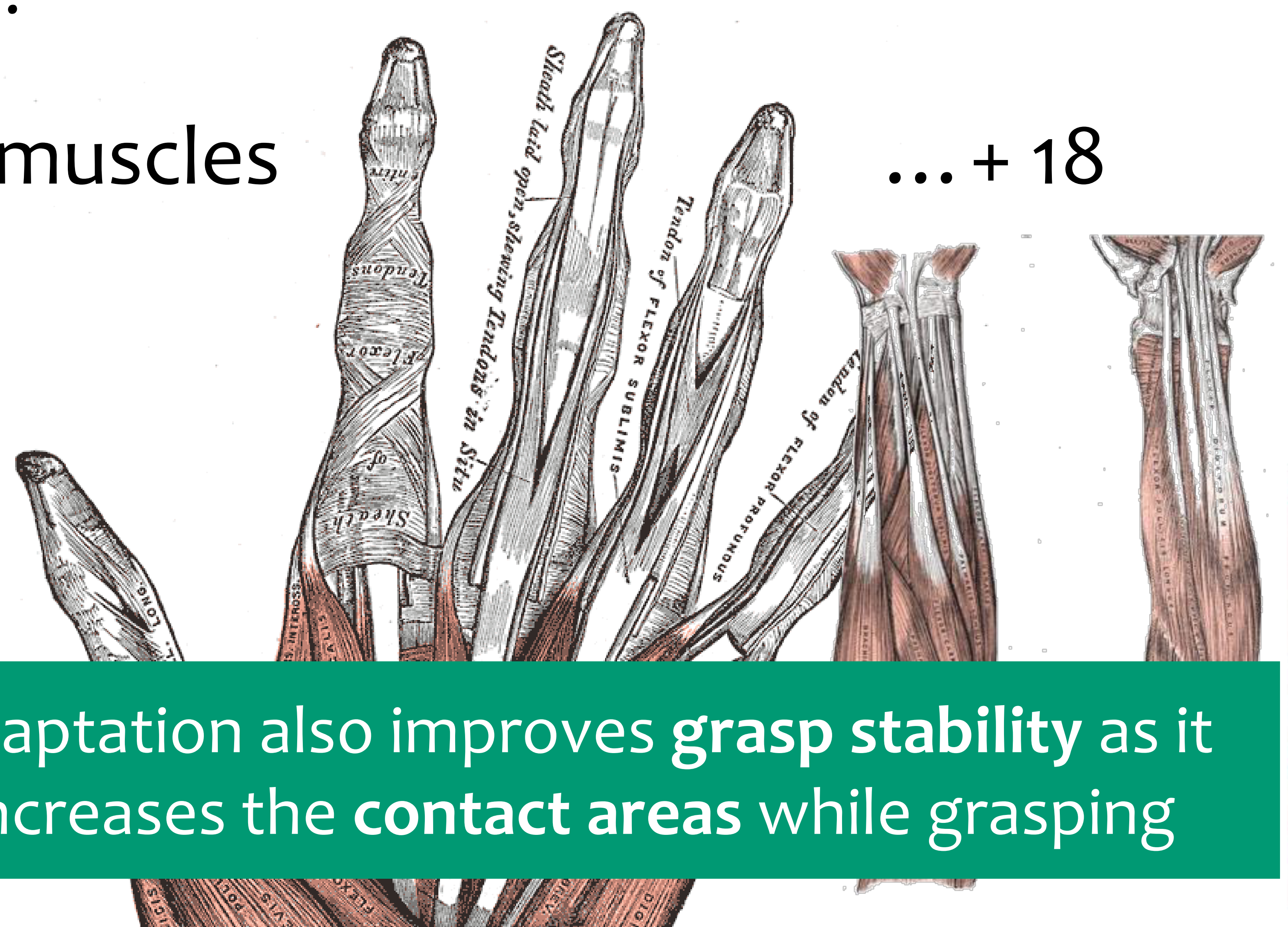

Adaptation also improves **grasp stability** as it increases the **contact areas** while grasping

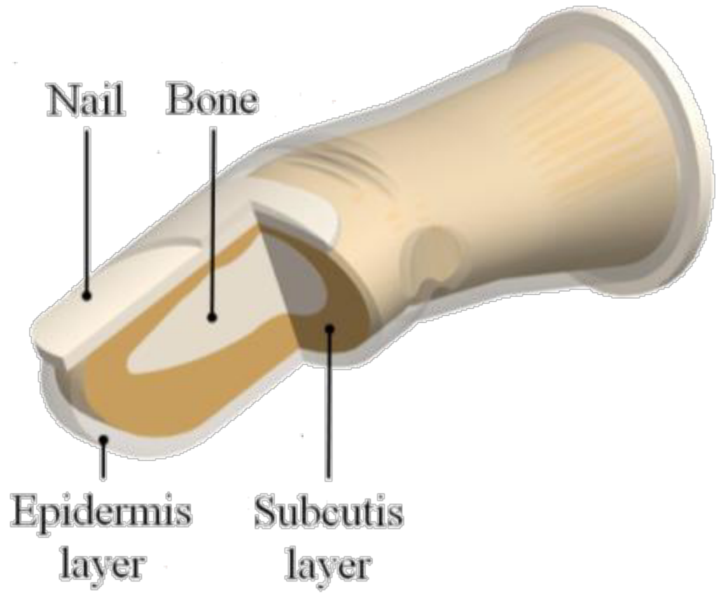

Phalanx adaptation mechanisms

Possible solutions (to simplify the problem):

- Cut DoFs; Rigidly couple DoFs;
- Implement adaptable mechanisms.

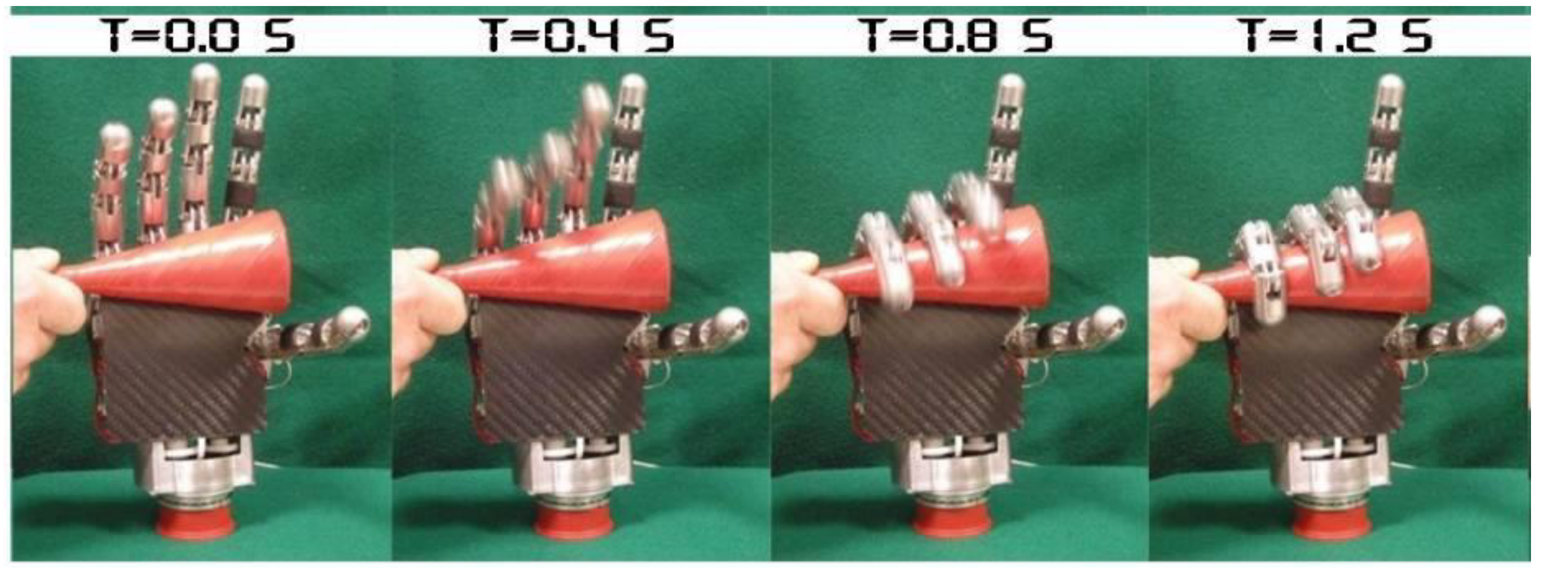

Hand adaptation mechanisms

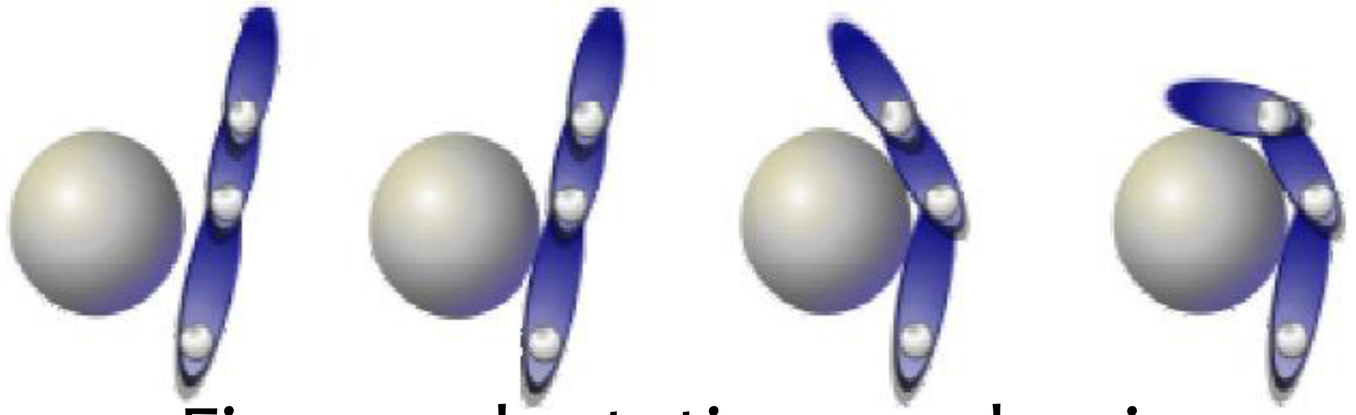

Finger adaptation mechanisms

Underactuated mechanisms

Mechatronic

Design issues: non back drivability

Mechanisms wherein motions generated by the input (motor) drive are transmitted to the output (i.e. fingers) and wherein motions originated from the output are blocked

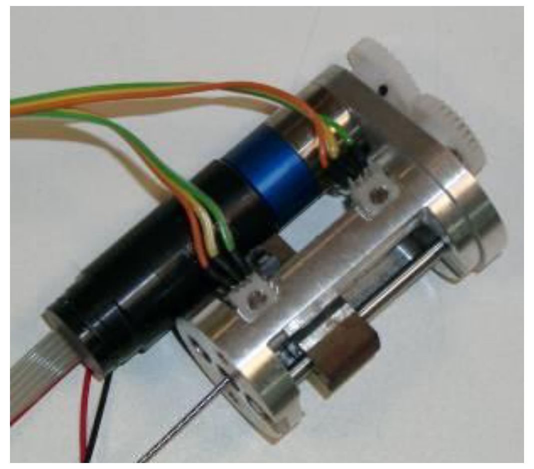

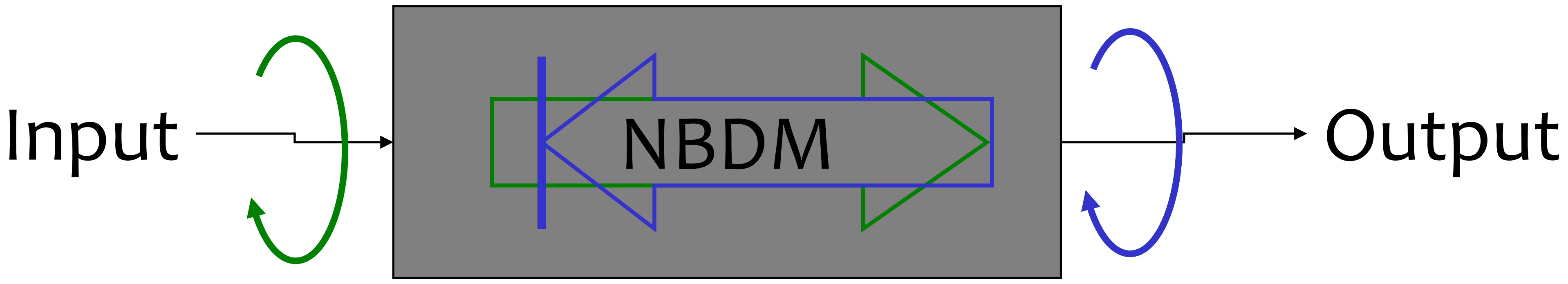

In a prosthesis it allows to maintain the grasp once the power supply is switched off

Non back drivable transmission = Power saving!= key in prosthetics!

Lead Screw

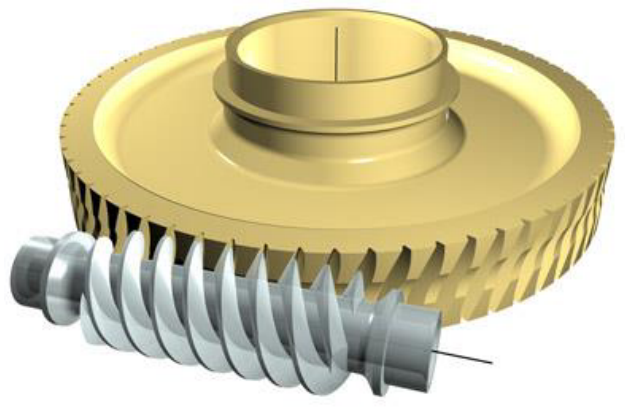

Worm Gear

Gear heads with high reduction rate

Brakes/ clutches

Interfaces with the PNS

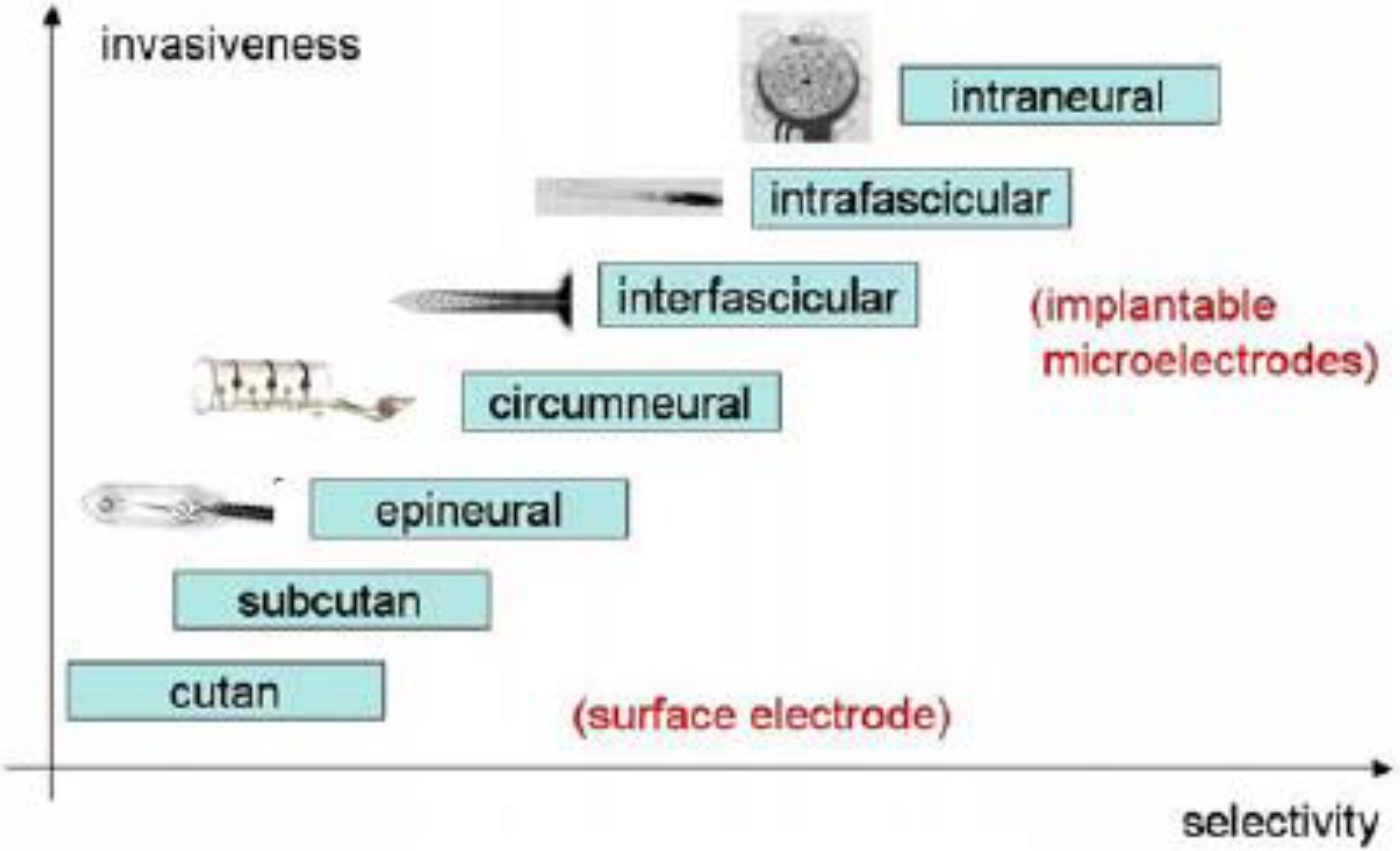

Sensory feedback

Real-time, and natural feedback from the hand prosthesis to the user is essential in order to enhance the control and functional impact of prosthetic hands in daily activities, prompting their full acceptance by the users

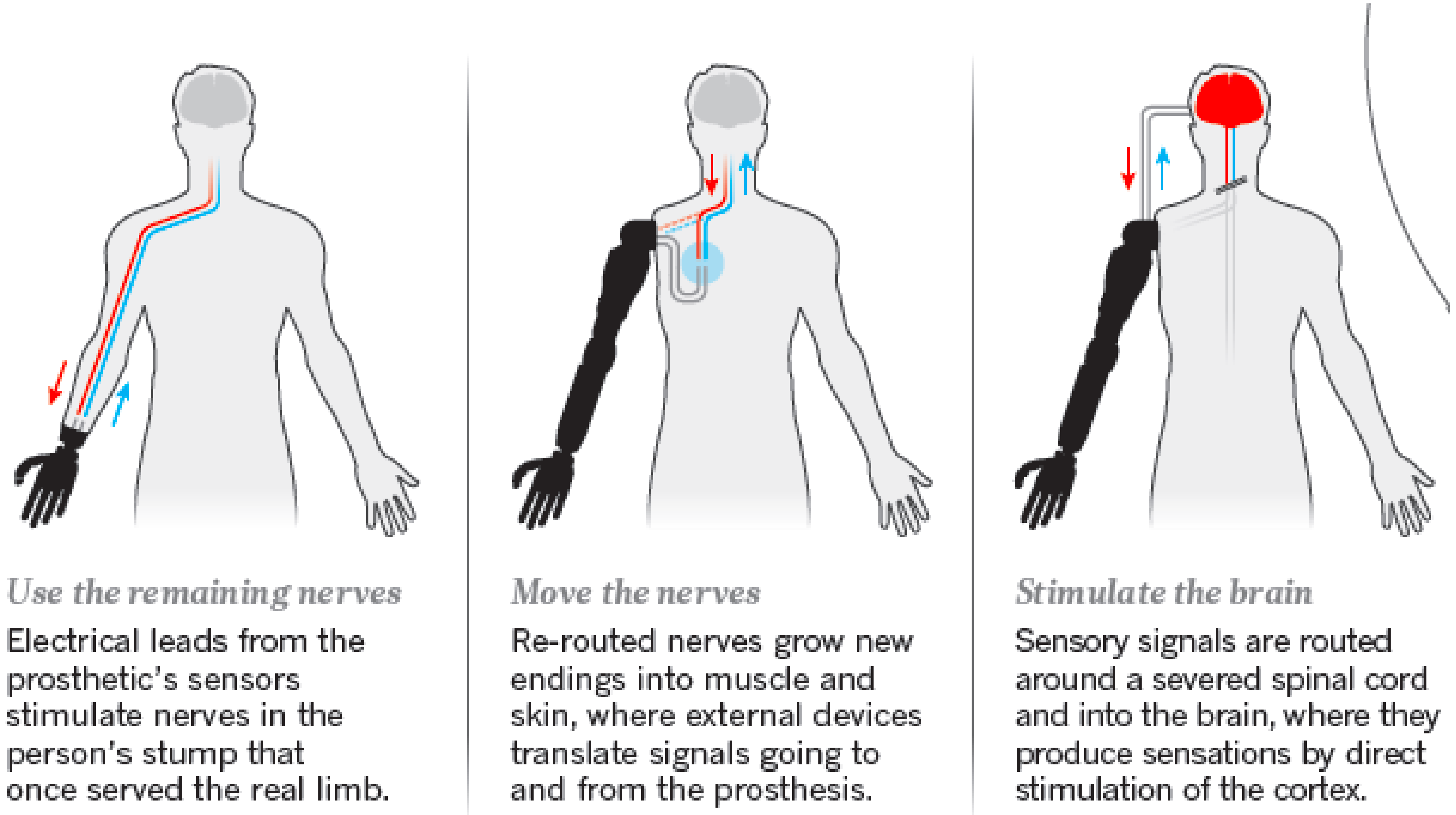

Kwok, Nature, 2013

Targeted Muscle Reinnervation

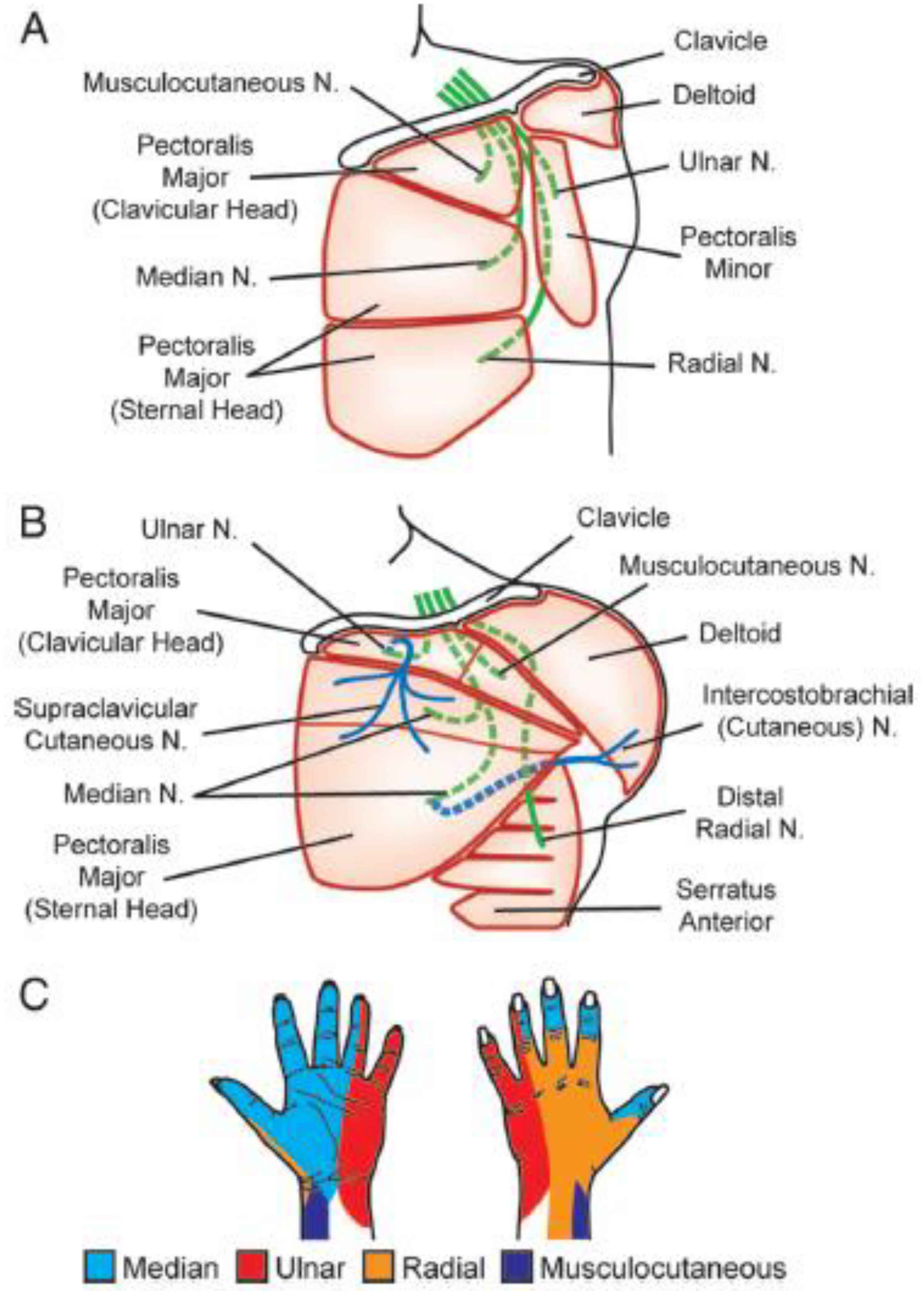

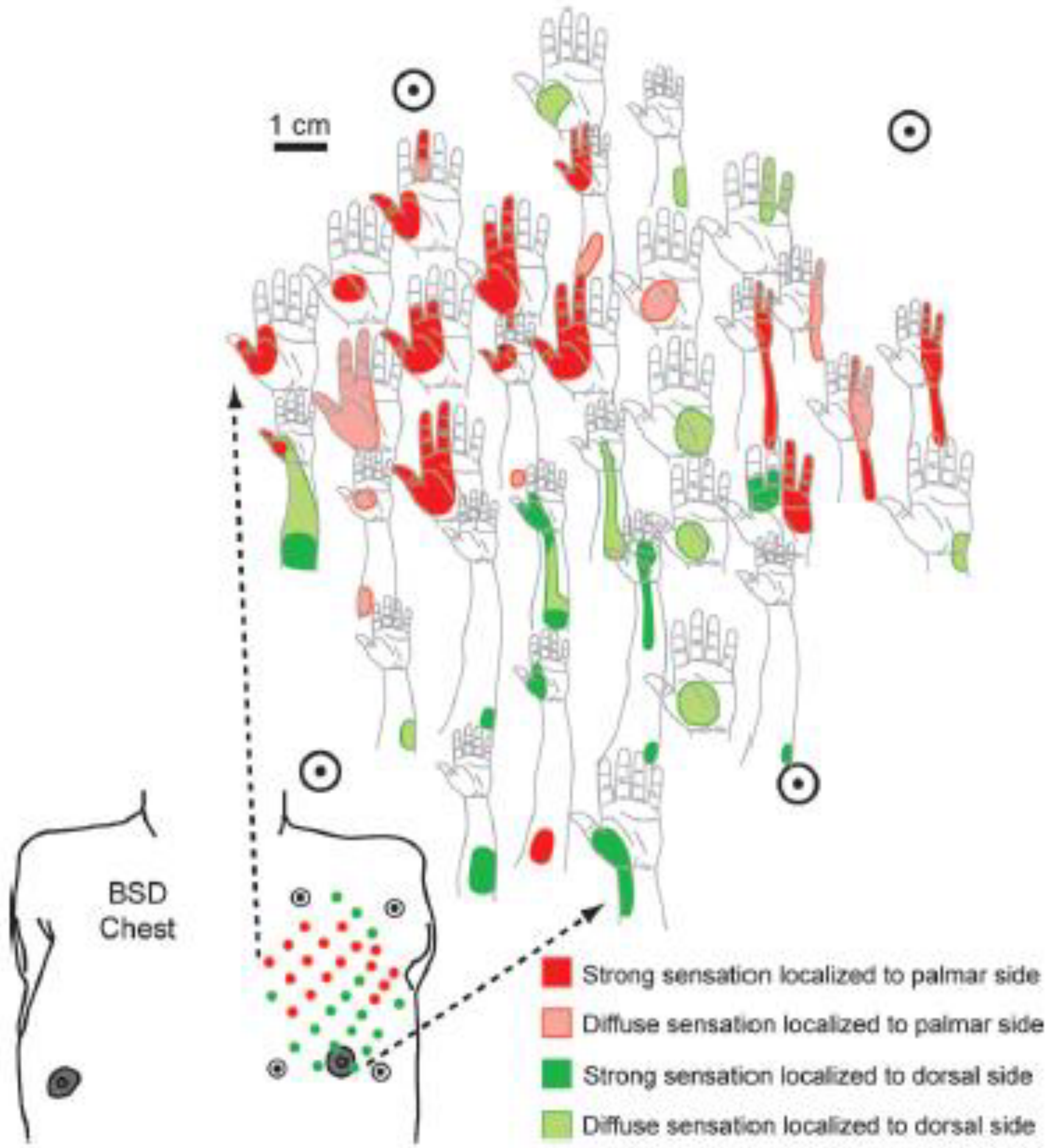

Kuiken et al., 2007, 2008

First intraneural experiment

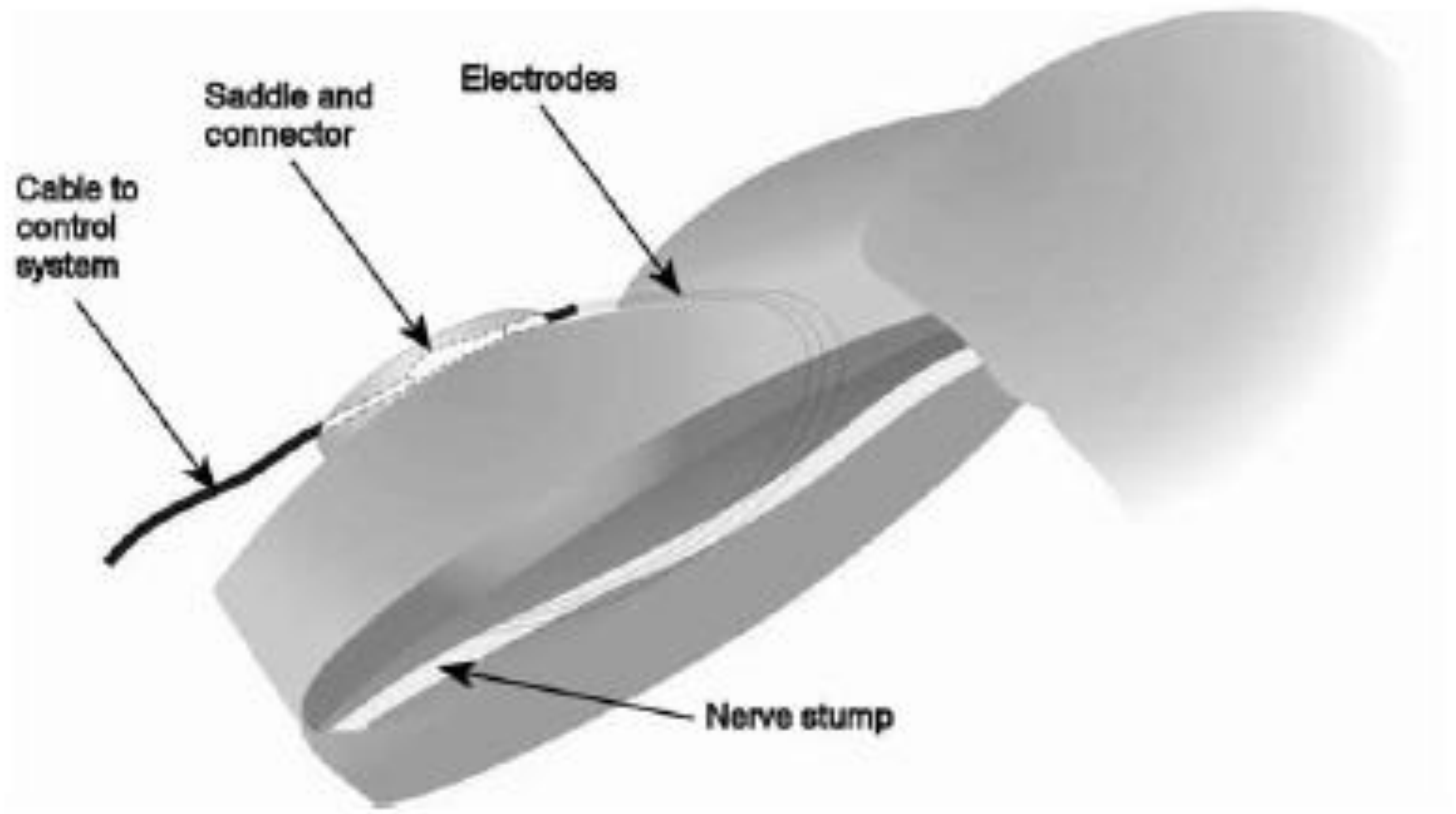

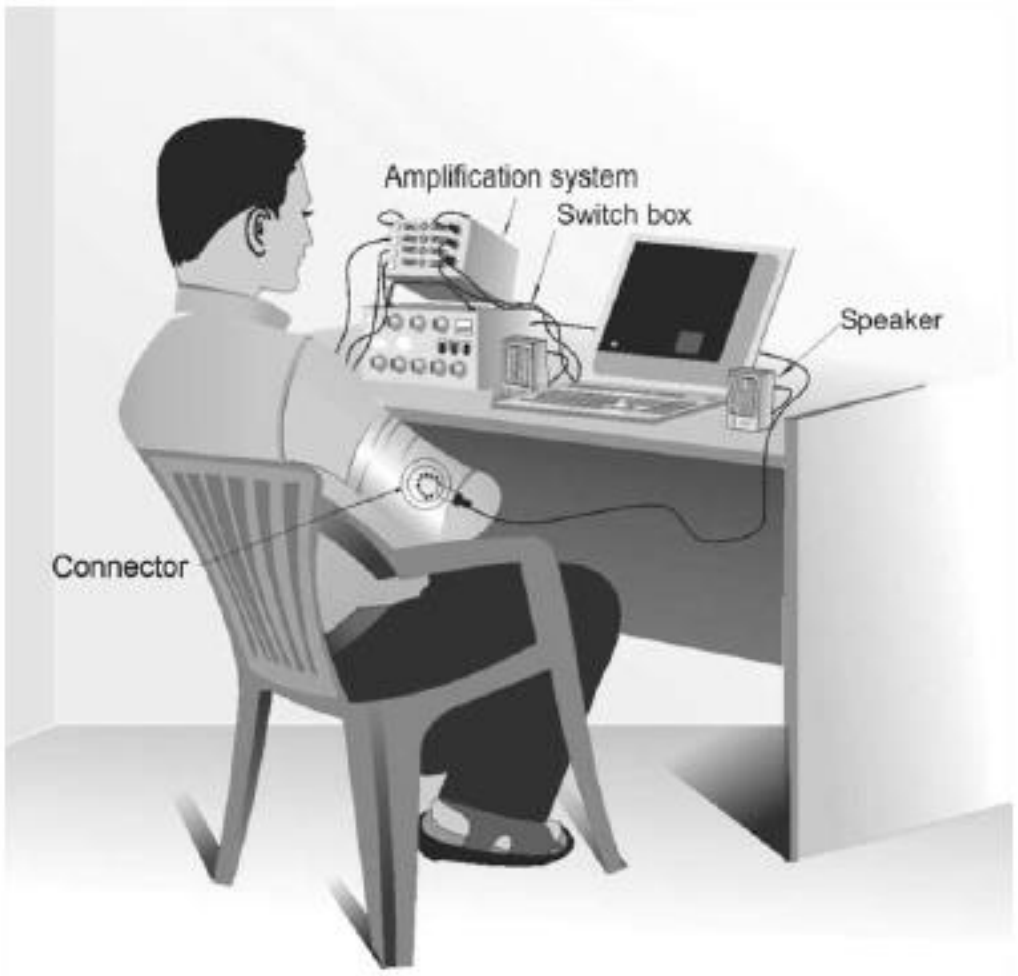

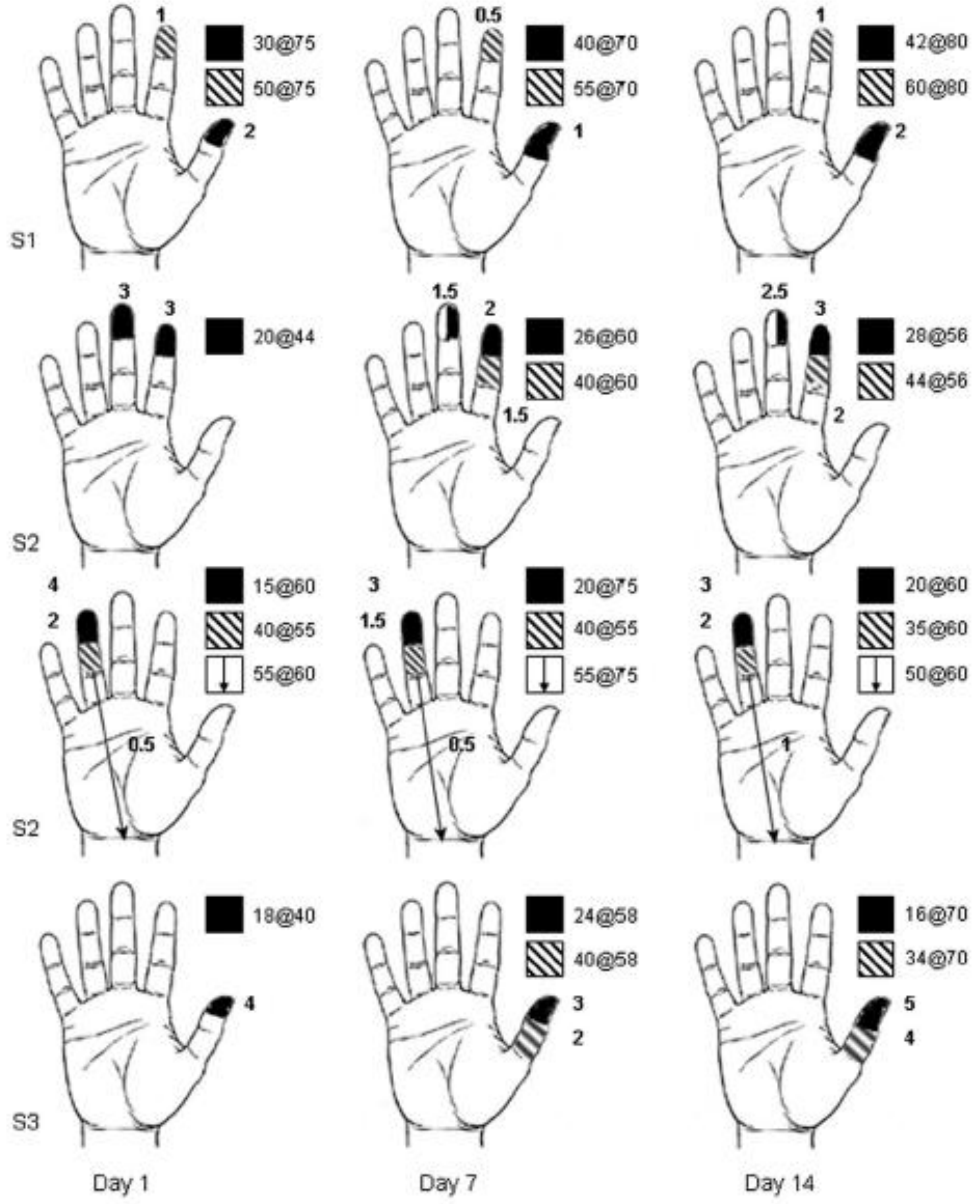

Closed-loop control based on sensory feedback

- Test the possibility for the subject to use the sensory information during closed-loop control and manipulation experiments

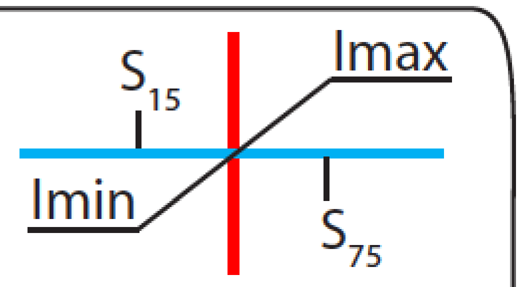

$$\mathbf{I} = (\mathbf{I}_{\mathbf{max}} - \mathbf{I}_{\mathbf{min}}) \cdot \frac{(S - S_{15})}{(S_{75} - S_{15})} + \mathbf{I}_{\mathbf{min}}$$

Current/Sensor relationship

Azzurra dexterous hand (Prensilia srl)

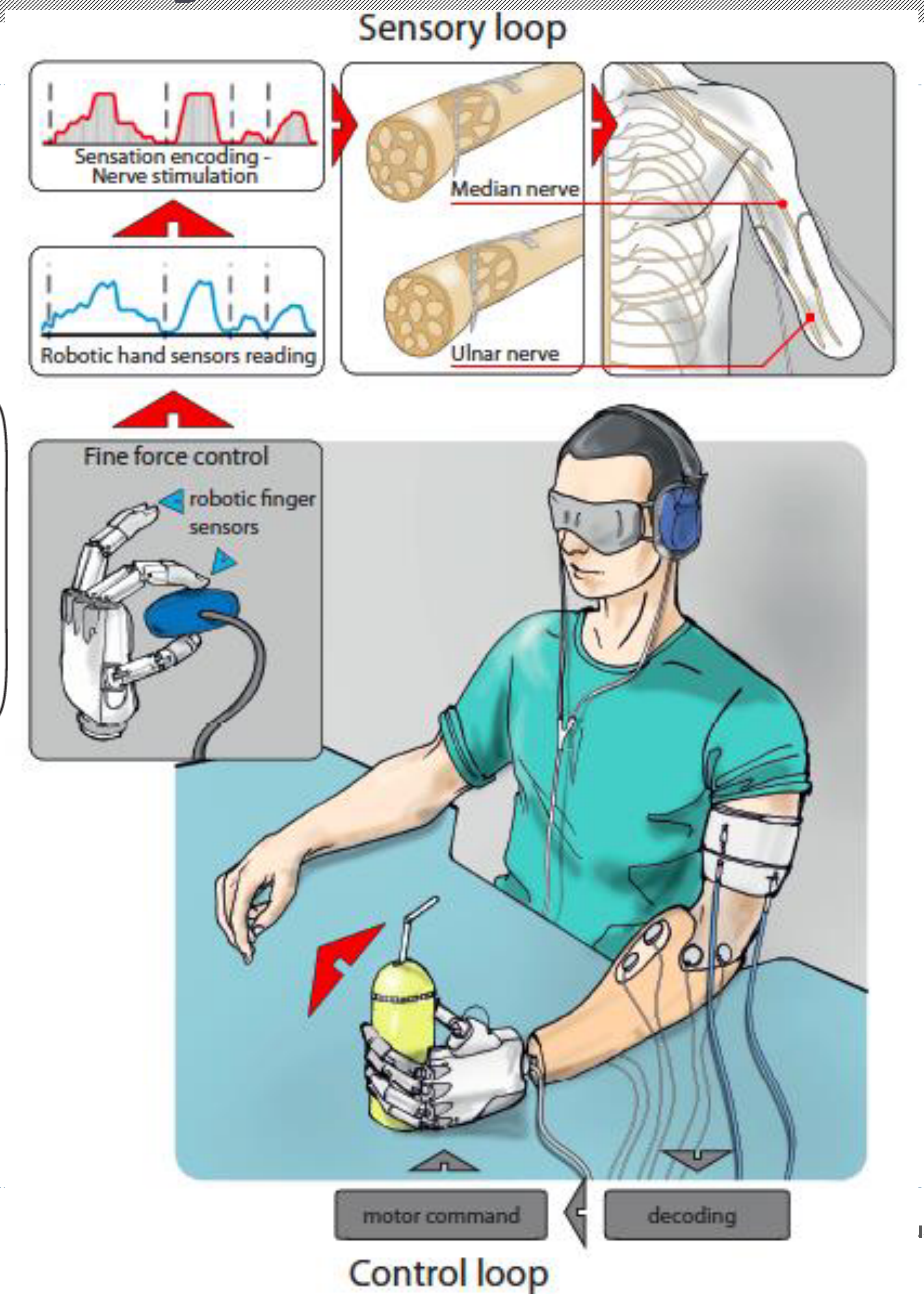

Restoration of proprioception and tactile feedback

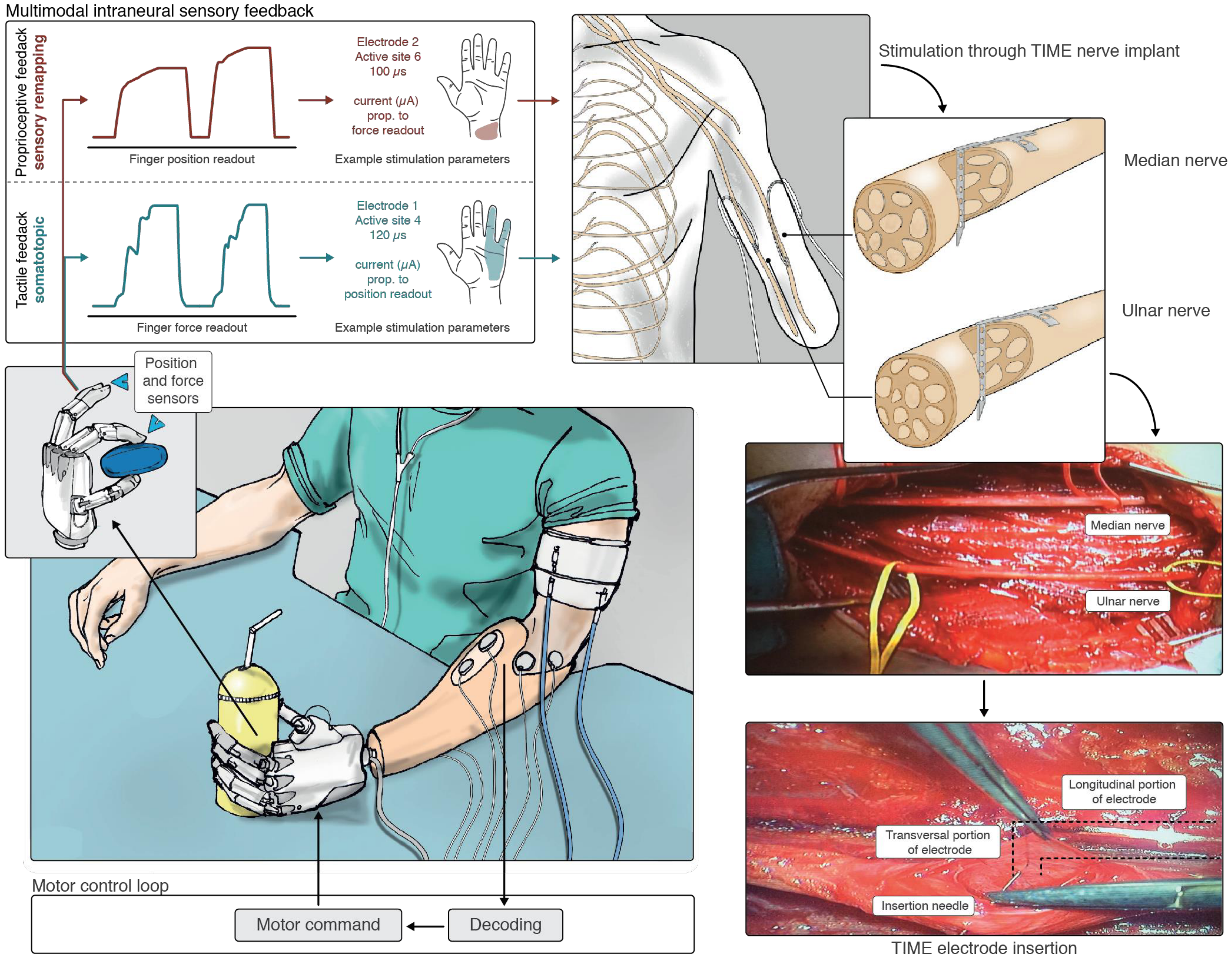

Embodiment

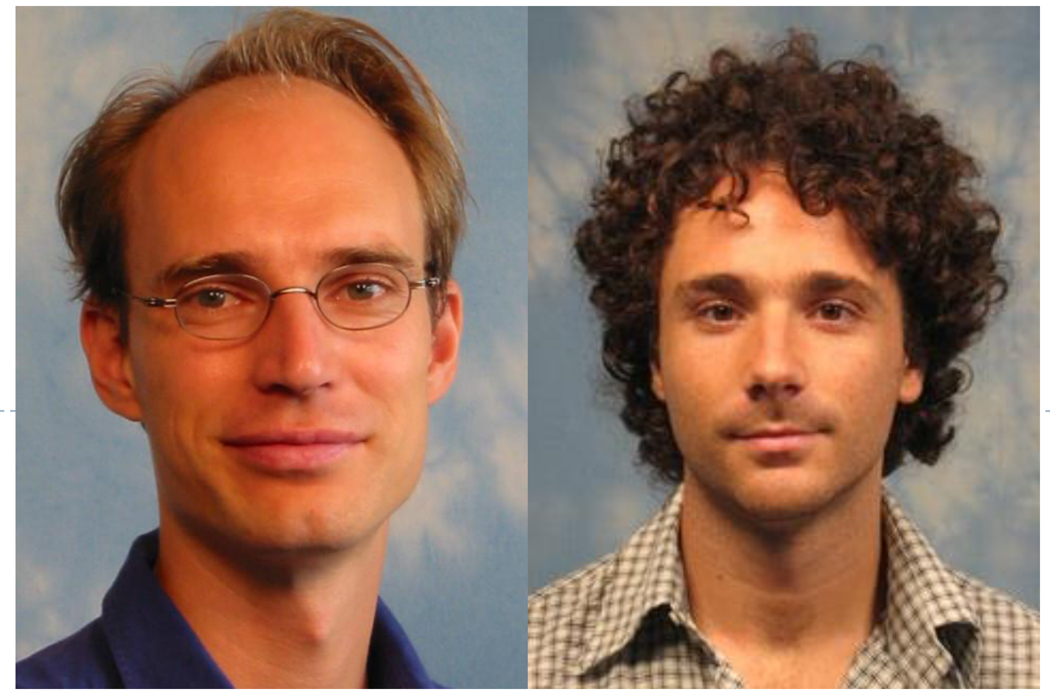

O. Blanke G. Rognini

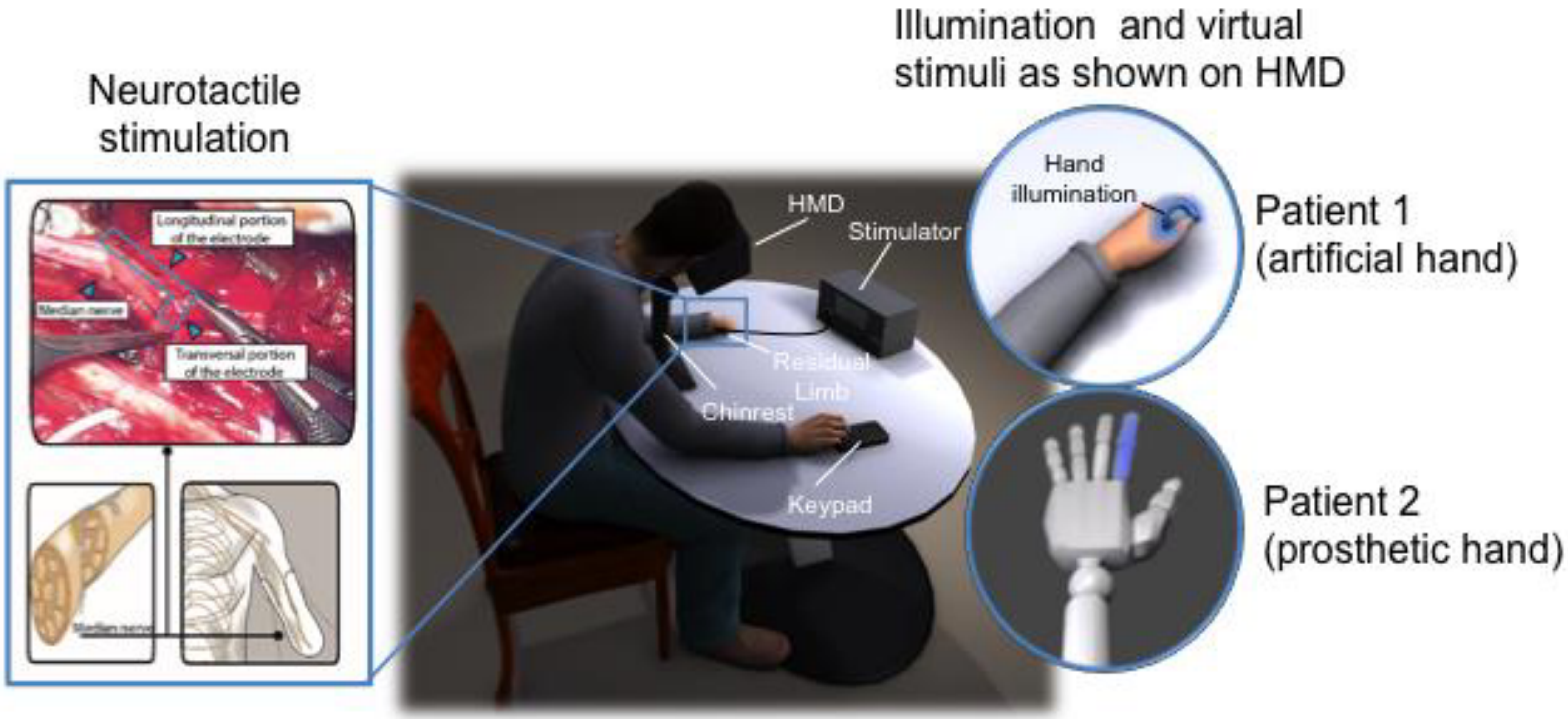

Human touch system

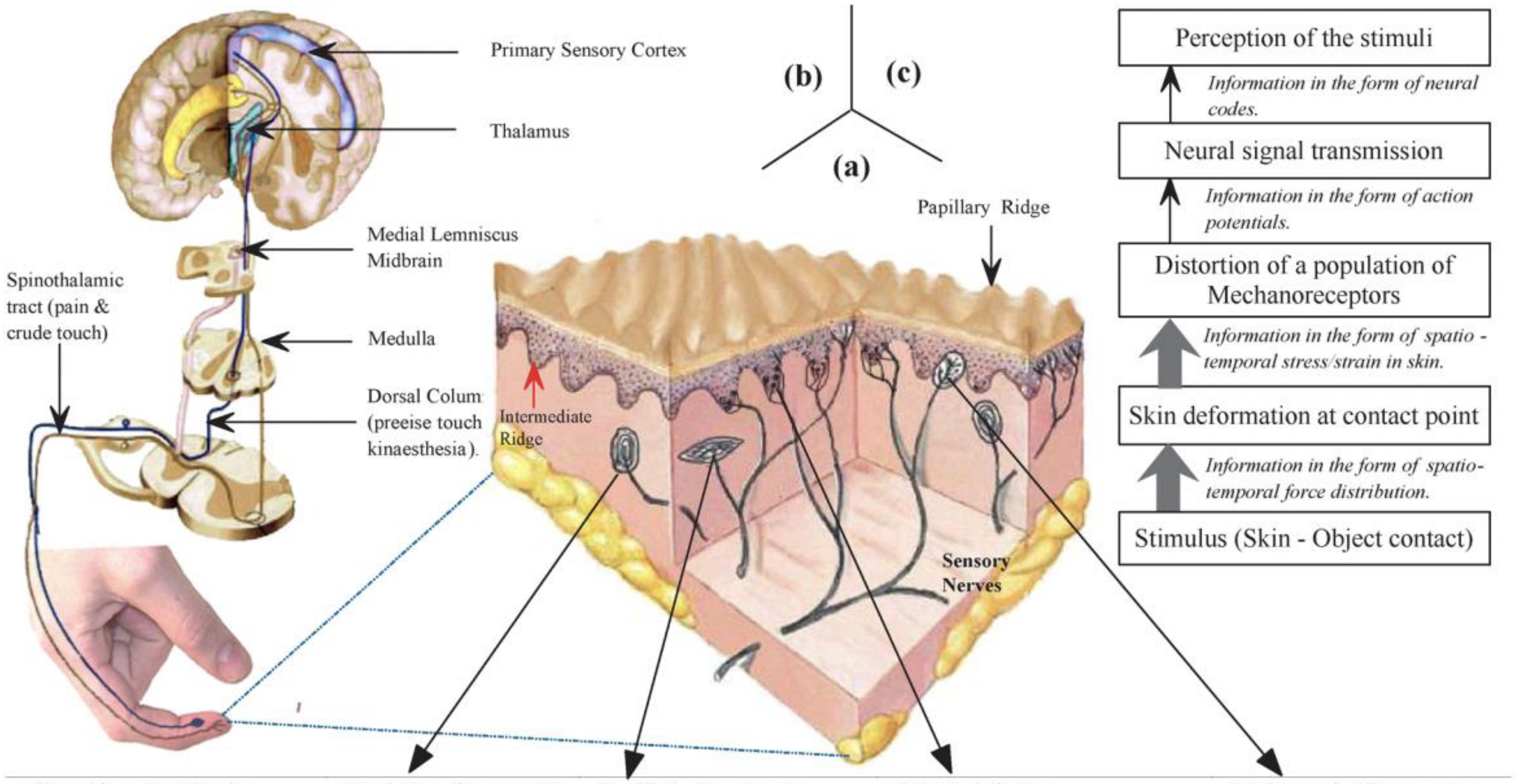

Classification Basis		Pacinian Corpuscle	Ruffini Corpuscle	Merkel Cells	Meissner's Corpuscle
Type		FA II	SA II	SA I	FA I
Adaptation Rate		Fast	Slow	Slow	Fast
Spatial Acuity (mm)		10+	7+	0.5	3-4
Vibration/rapid indent. threshold	Best(μm)	0.01	40	8	2
	Mean(μm)	0.08	300	30	6
Stimuli Frequency (Hz)		40-500+	100-500+	0.4-3	3-40
Conduction Velocity (m/s)		35-70	35-70	40-65	35-70
Effective Stimuli		Temporal changes in the skin deformation	Sustained downward Pressure; Lateral skin stretch; Skin slip.	Spatial deformation; Sustained pressure; Curvature, edge, corners.	Temporal changes in skin deformation
Sensory Function		High frequency vibration detection; Tool use.	Finger position; Stable grasp; Tangential Force; Motion direction	Pattern/form detection; texture perception; Tactile flow perception.	Low frequency vibration & motion detection; Grip control; Tactile flow perception.

- Natural sensors fibers convey detailed information about contact events and provide us with an exquisite sensitivity to the form and surface properties of grasped objects
- During object manipulation and tactile exploration, the glabrous skin of the hand undergoes complex spatiotemporal mechanical deformations, which in turn, drive very precise spiking responses in individual afferents
- Coarse object features, such as edges and corners, are reflected in spatial patterns of activation in slowly adapting type I (SA1) and rapidly adapting (FA) fibers, which are densely packed in the fingertip
- At the same time, interactions with objects and surfaces elicit high-frequency, low-amplitude sur-face waves that propagate across the skin of the finger and palmand excite vibration-sensitive Pacinian (PC) afferents all over thehand

Biomimetic encoding strategy

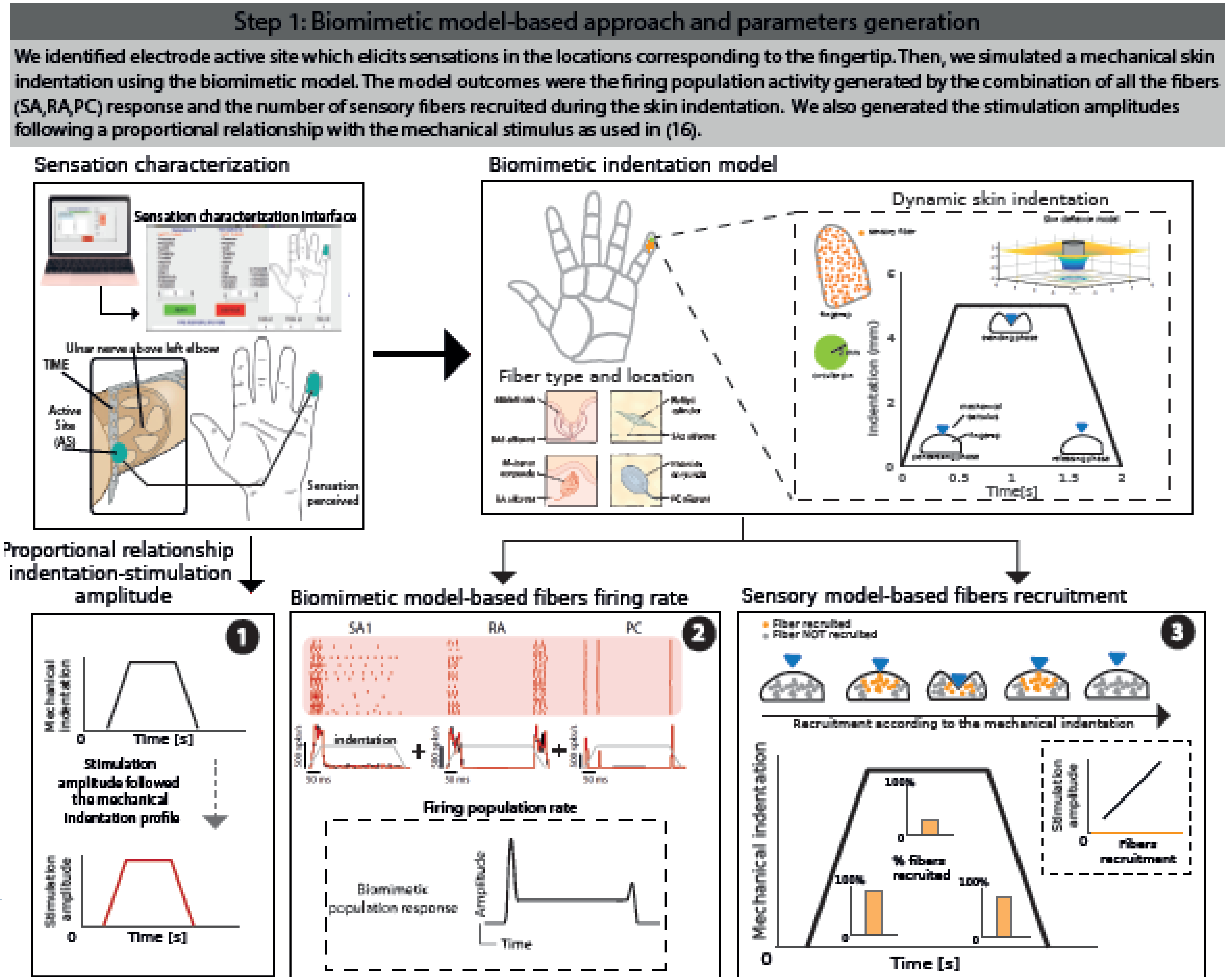

Biomimetic encoding strategy

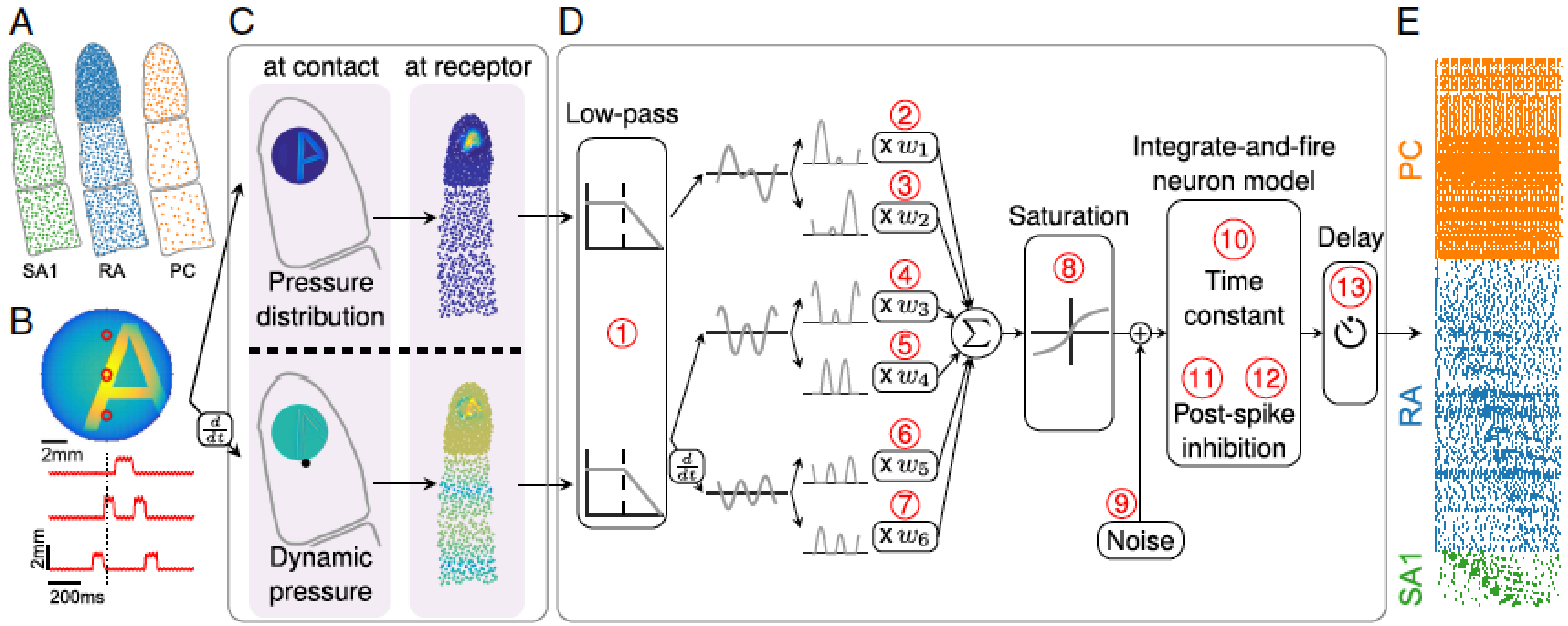

Fig. 1. Overview of the model. (*A*) Receptors are distributed across the skin given the known innervation densities of SA1, RA, and PC afferents. (*B*) The stimulus—in this case, a vibrating embossed letter A scanned across the skin—is defined as the time-varying depth at which each small patch of skin (here dubbed a pin) is indented (with a spatial resolution of 0.1 mm). The traces in *Lower* show the time-varying depth at the three locations on the skin indicated by the red dots in *Upper*. (*C*) The mechanics model relies on two parts: (*Upper*) modeling the distribution of stresses using a quasistatic elastic model and (*Lower*) modeling dynamic pressure and surface wave propagation. *Left* shows the surface deformation of the skin, and *Right* shows the resulting pattern of stresses at the location of the receptors. (*D*) The spiking responses are determined by leaky IF models using different sets of up to 13 parameters (marked in red numbers) for individual SA1, RA, and PC afferents fit based on peripheral recordings to skin vibrations. Adapted from ref. 71. (*E*) The output of the model is the spike train of each afferent in the population. Raster of the response of the afferent population sampled as in *A* to the stimulus shown in *B* (only active afferents are included). Note that the SA1s (in contact) only encode the spatial aspect of the stimulus, that the PCs encode from the whole finger phase-lock with the 200-Hz vibration, and that the RAs show mixed spatial and vibration responses.

Saal et al., PNAS, 2017

Biomimetic encoding strategy

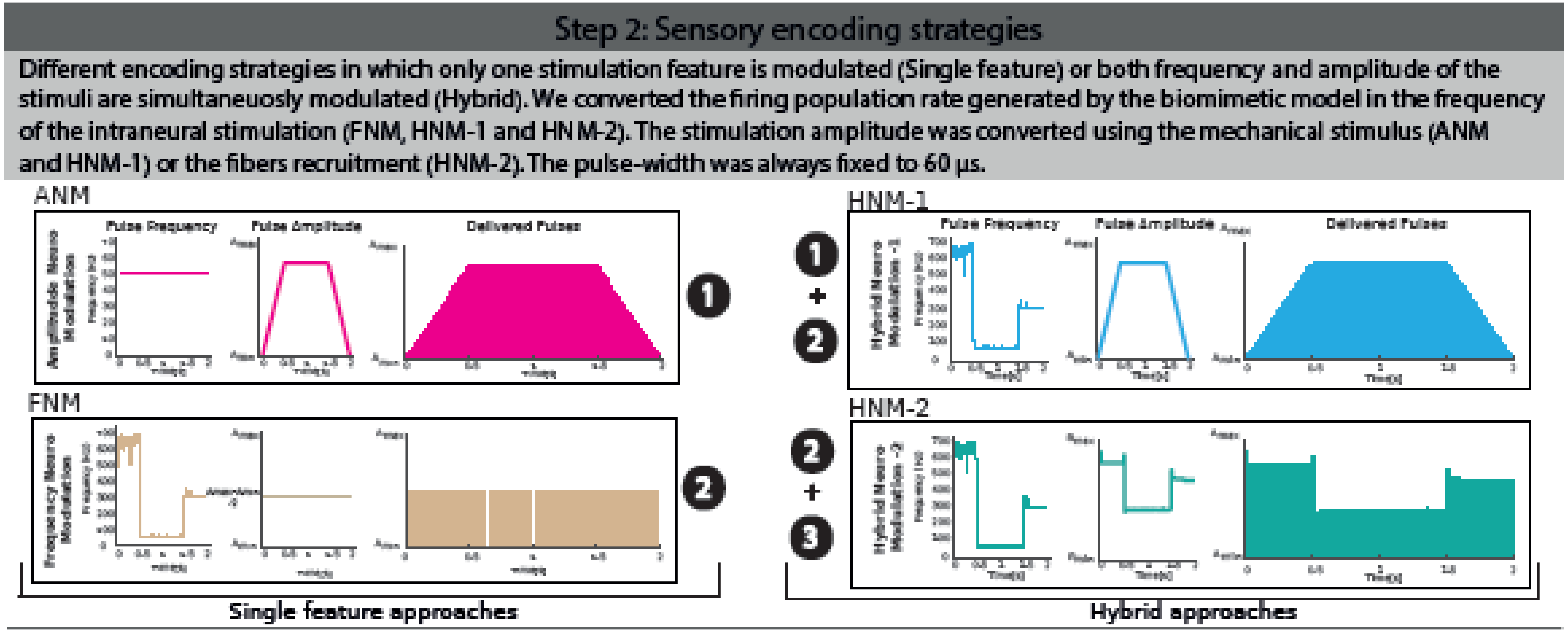

Valle et al., Neuron, 2018

Biomimetic encoding strategy

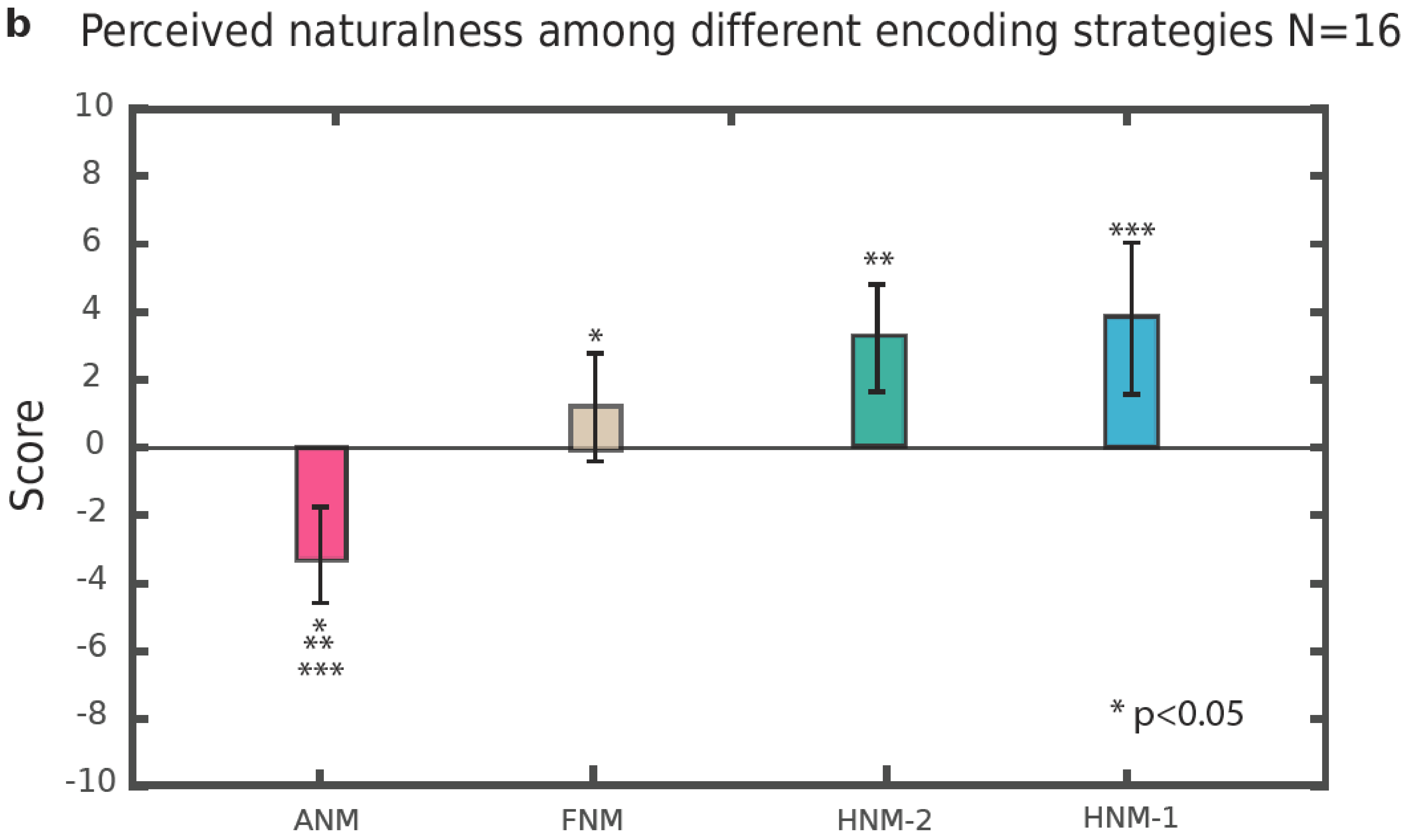

a

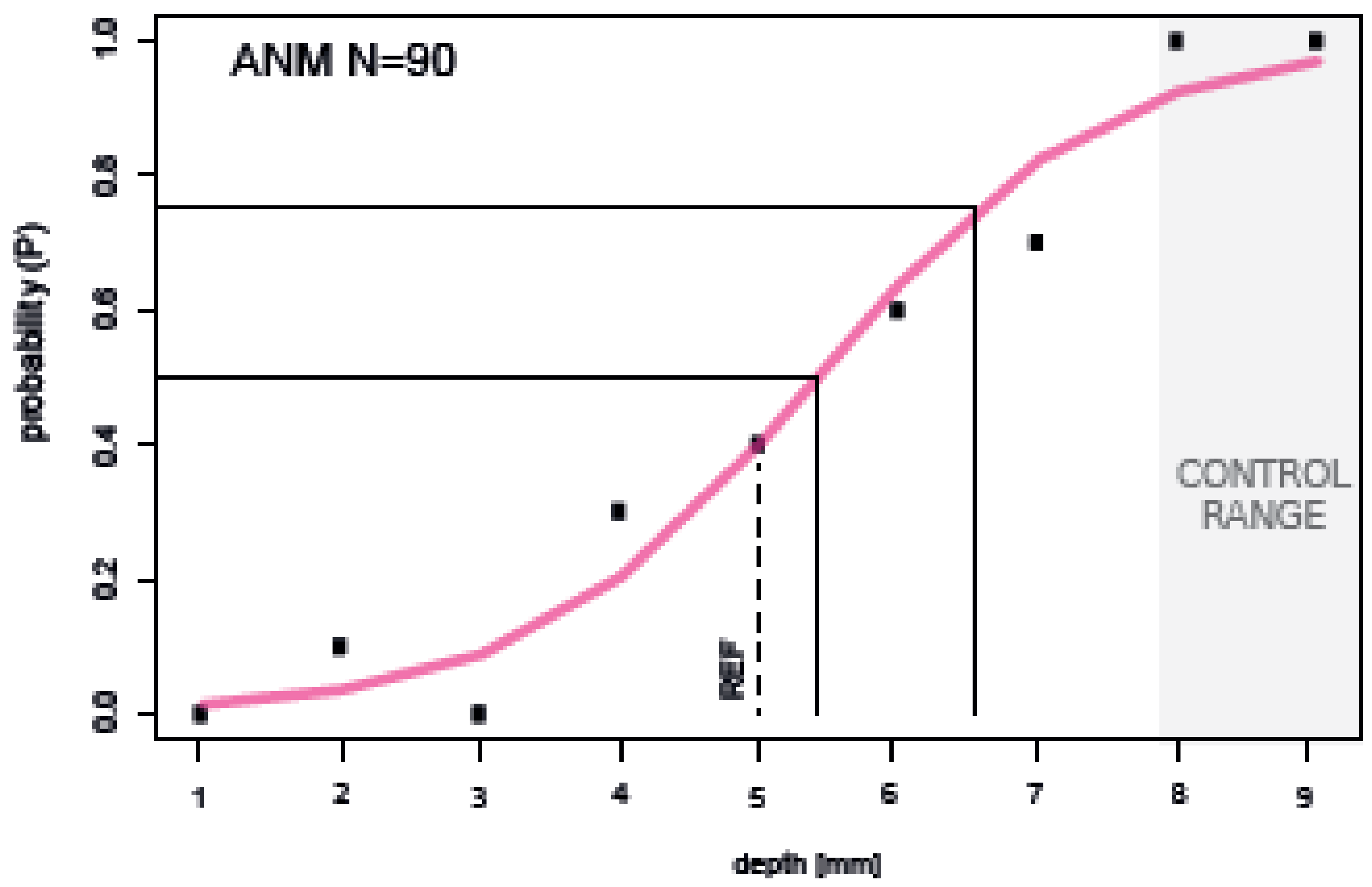

Point of Subjective Equality (PSE): **5.51** mm

Just-Noticeable Difference (JND): **1.01** mm

b

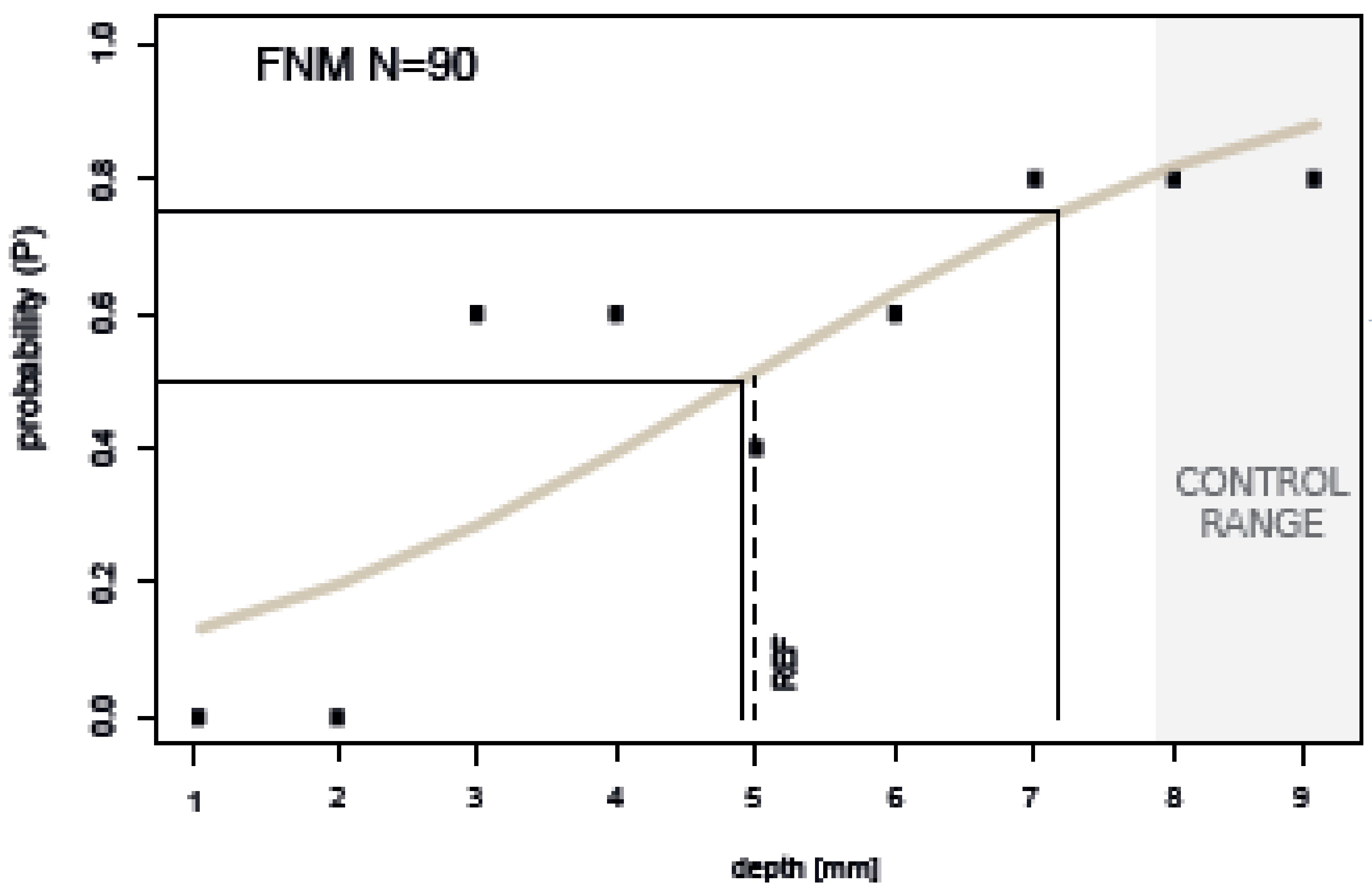

Point of Subjective Equality (PSE): **4.87** mm

Just-Noticeable Difference (JND): **2.26** mm

c

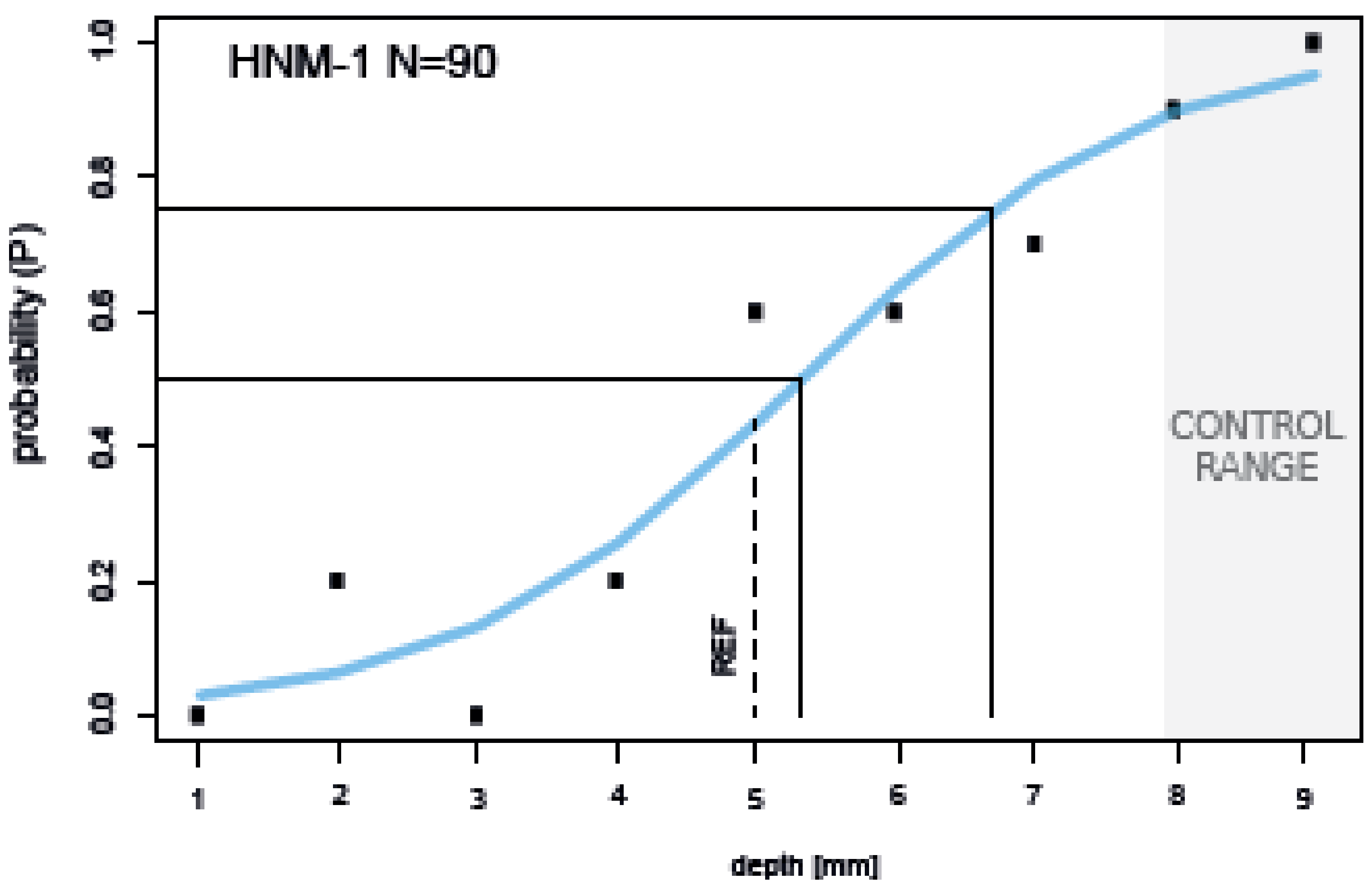

Point of Subjective Equality (PSE): **5.31** mm

Just-Noticeable Difference (JND): **1.35** mm

d

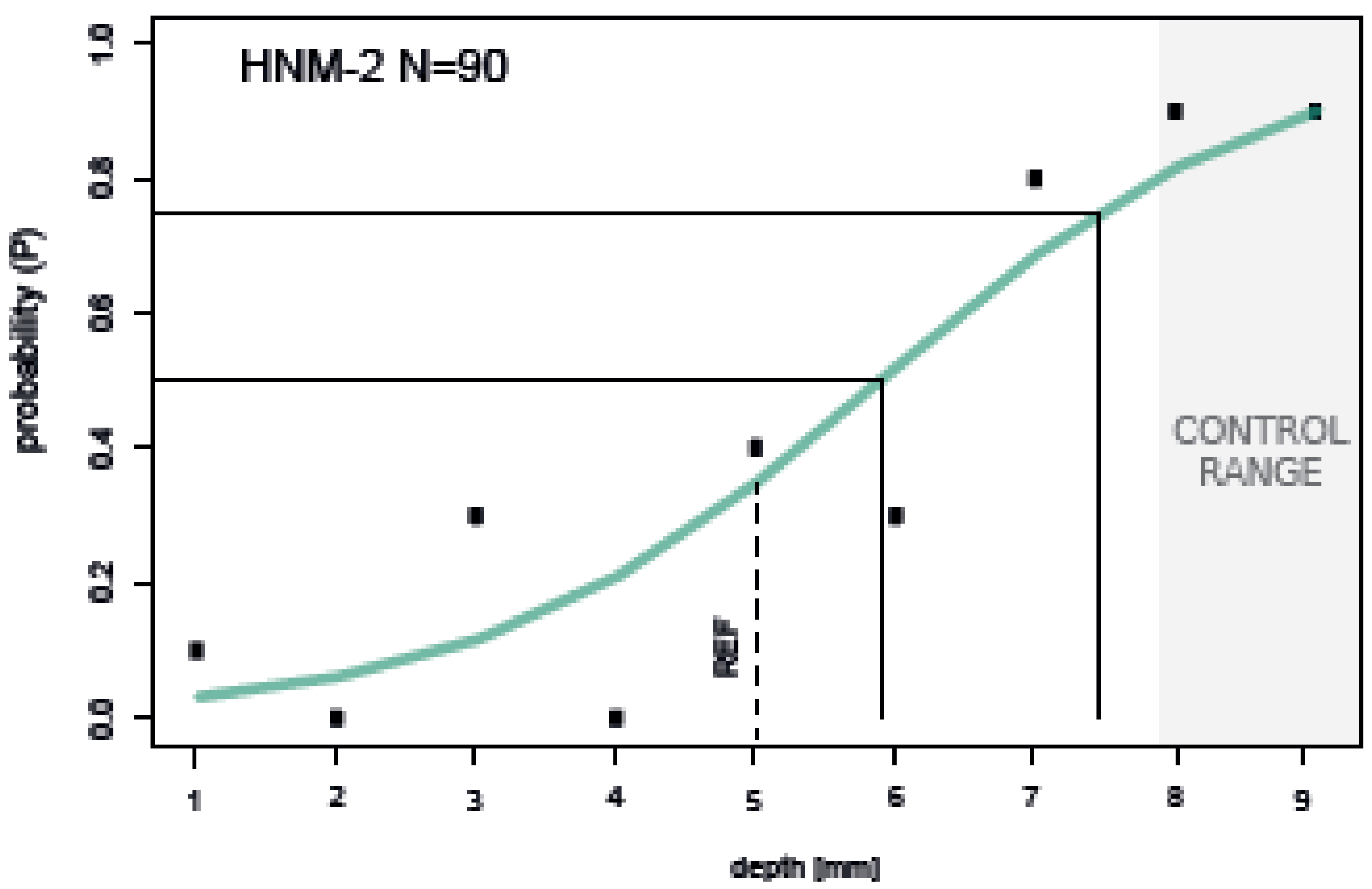

Point of Subjective Equality (PSE): **5.87** mm

Just-Noticeable Difference (JND): **1.55** mm

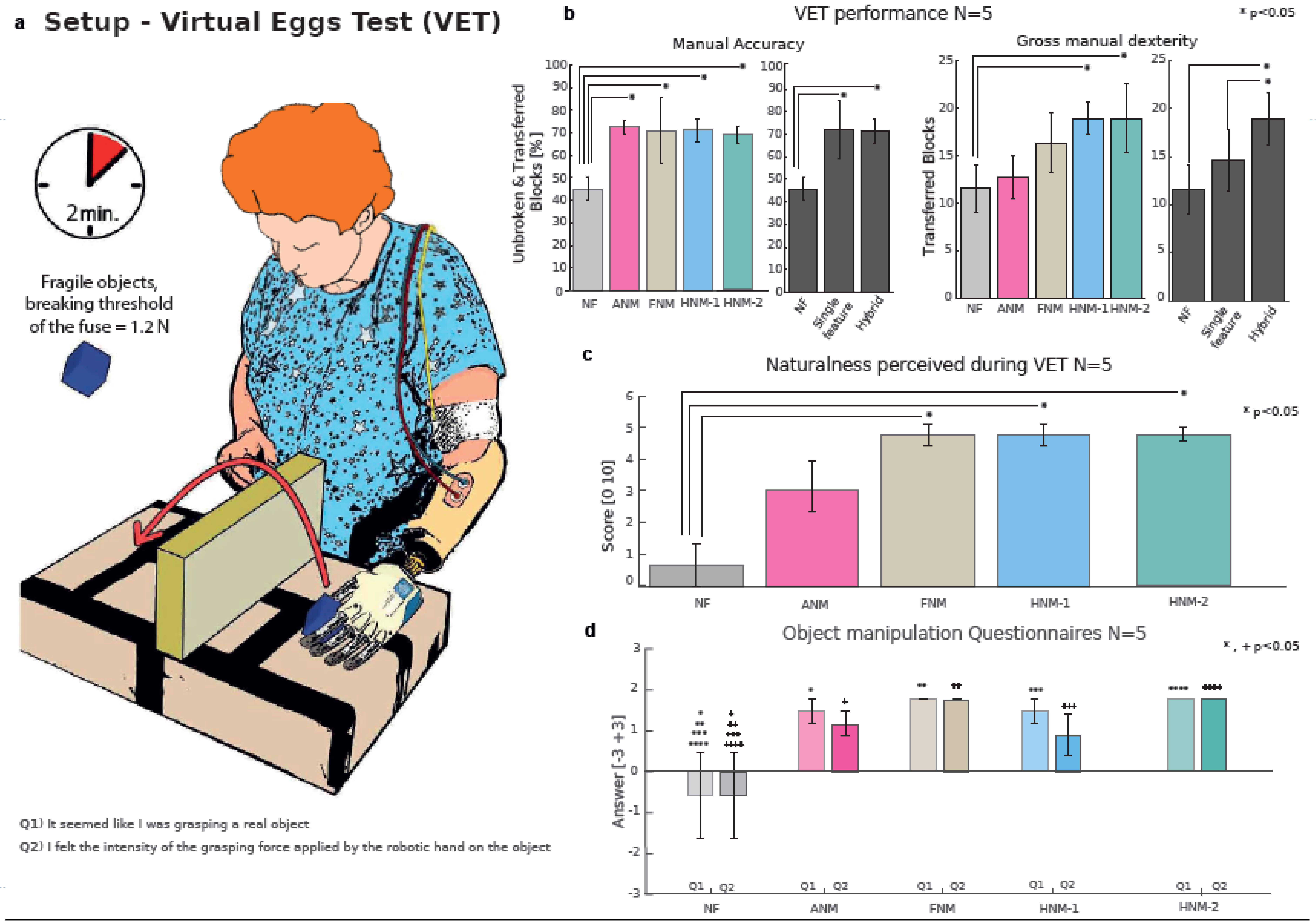

a Setup - Virtual Eggs Test (VET)
2min.
Fragile objects, breaking threshold of the fuse = 1.2 N
Q1) It seemed like I was grasping a real object
Q2) I felt the intensity of the grasping force applied by the robotic hand on the object
b VET performance N=5
* p<0.05
Manual Accuracy
Unbroken & Transferred Blocks [%]
NF ANM FNM HNM-1 HNM-2
NF Single feature Hybrid
Gross manual dexterity
Transferred Blocks
NF ANM FNM HNM-1 HNM-2
NF Single feature Hybrid
c Naturalness perceived during VET N=5
* p<0.05
Score [0 10]
NF ANM FNM HNM-1 HNM-2
d Object manipulation Questionnaires N=5
*, + p<0.05
Answer [-3 +3]
Q1 Q2
NF ANM FNM HNM-1 HNM-2

Biomimetic encoding strategy

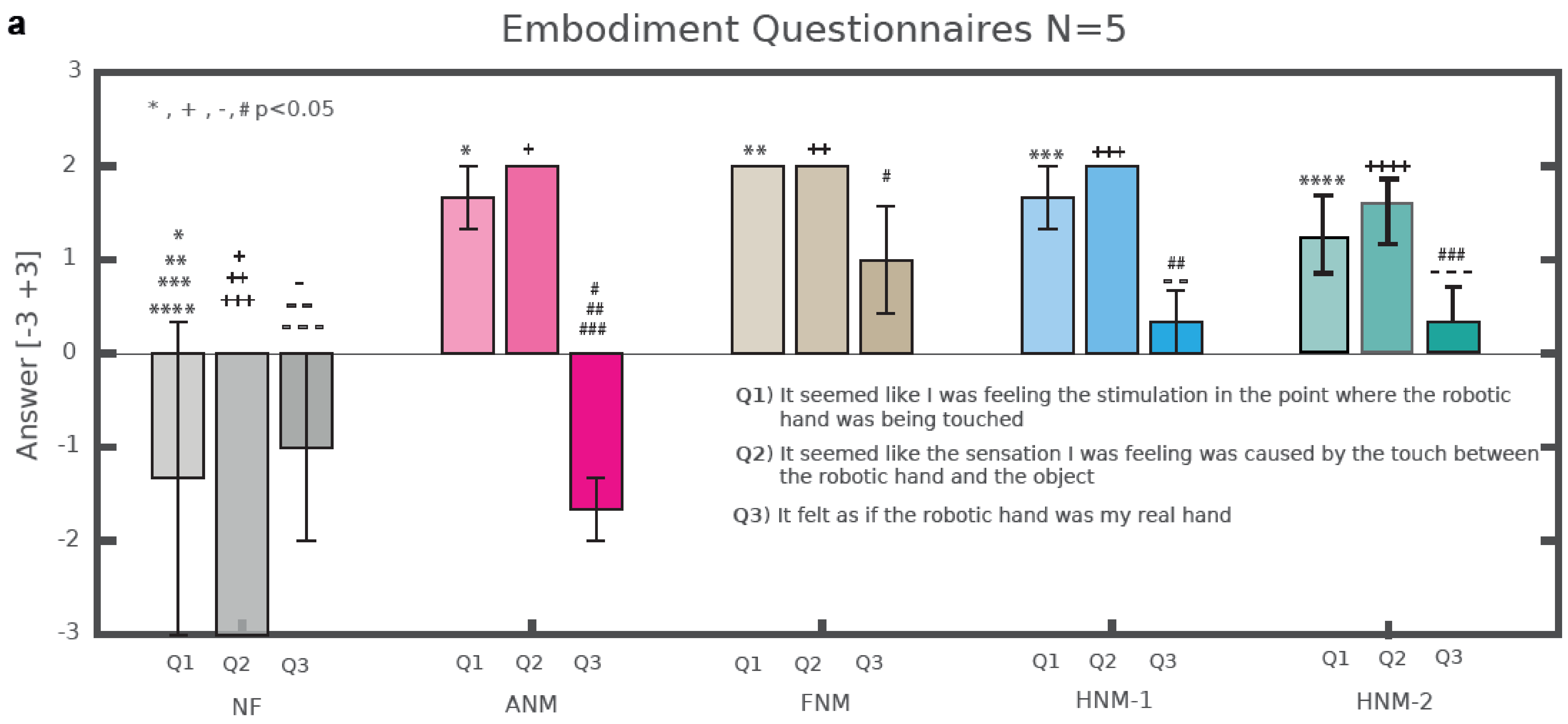

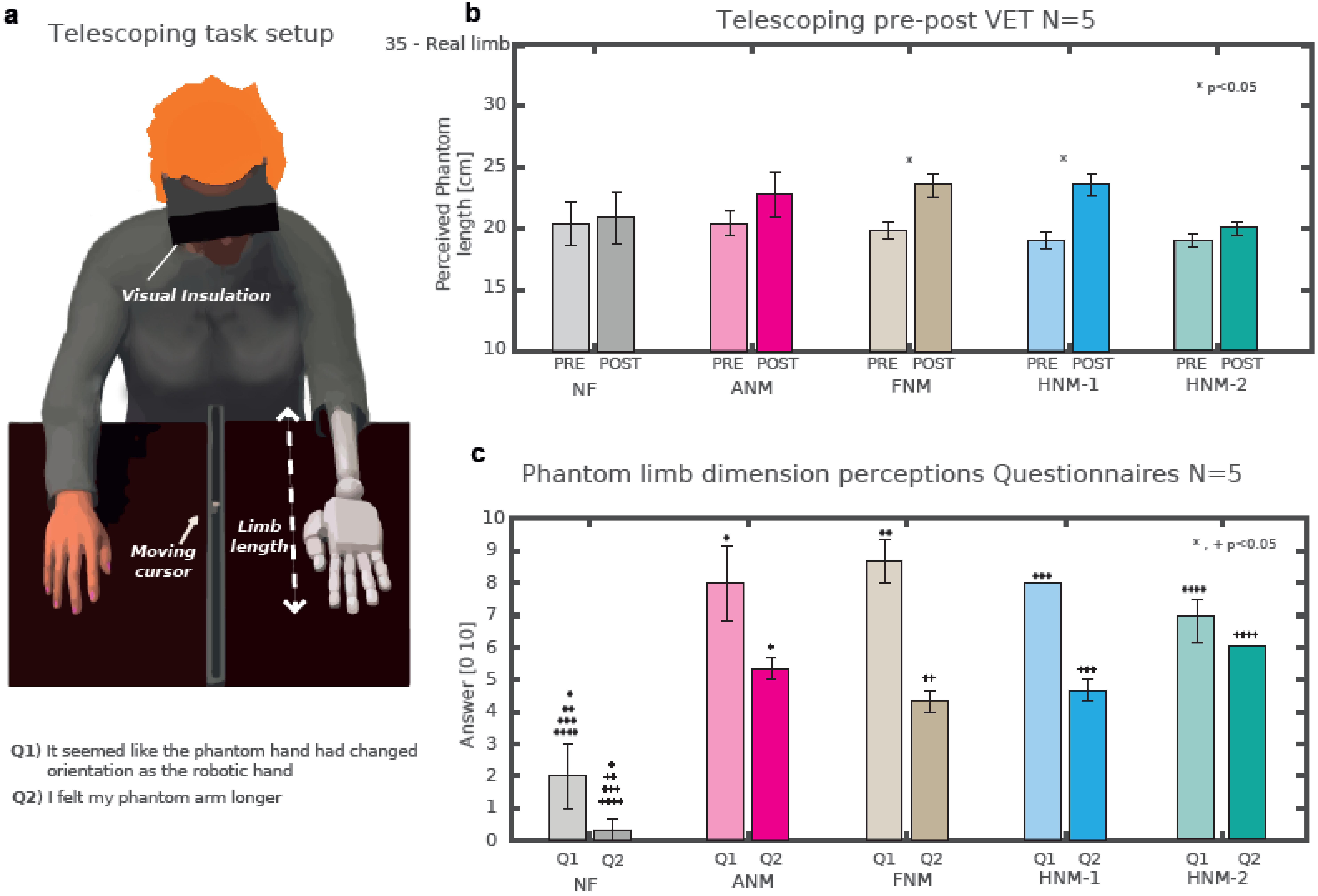
a
Telescoping task setup
Visual Insulation
Moving cursor
Limb length
Q1) It seemed like the phantom hand had changed orientation as the robotic hand
Q2) I felt my phantom arm longer
b
Telescoping pre-post VET N=5
35 - Real limb
Perceived Phantom length [cm]
x p<0.05
PRE POST
NF
ANM
FNM
HNM-1
HNM-2
c
Phantom limb dimension perceptions Questionnaires N=5
Answer [0 10]
x , + p<0.05
Q1 Q2
NF
ANM
FNM
HNM-1
HNM-2

Restoring perception of real textures

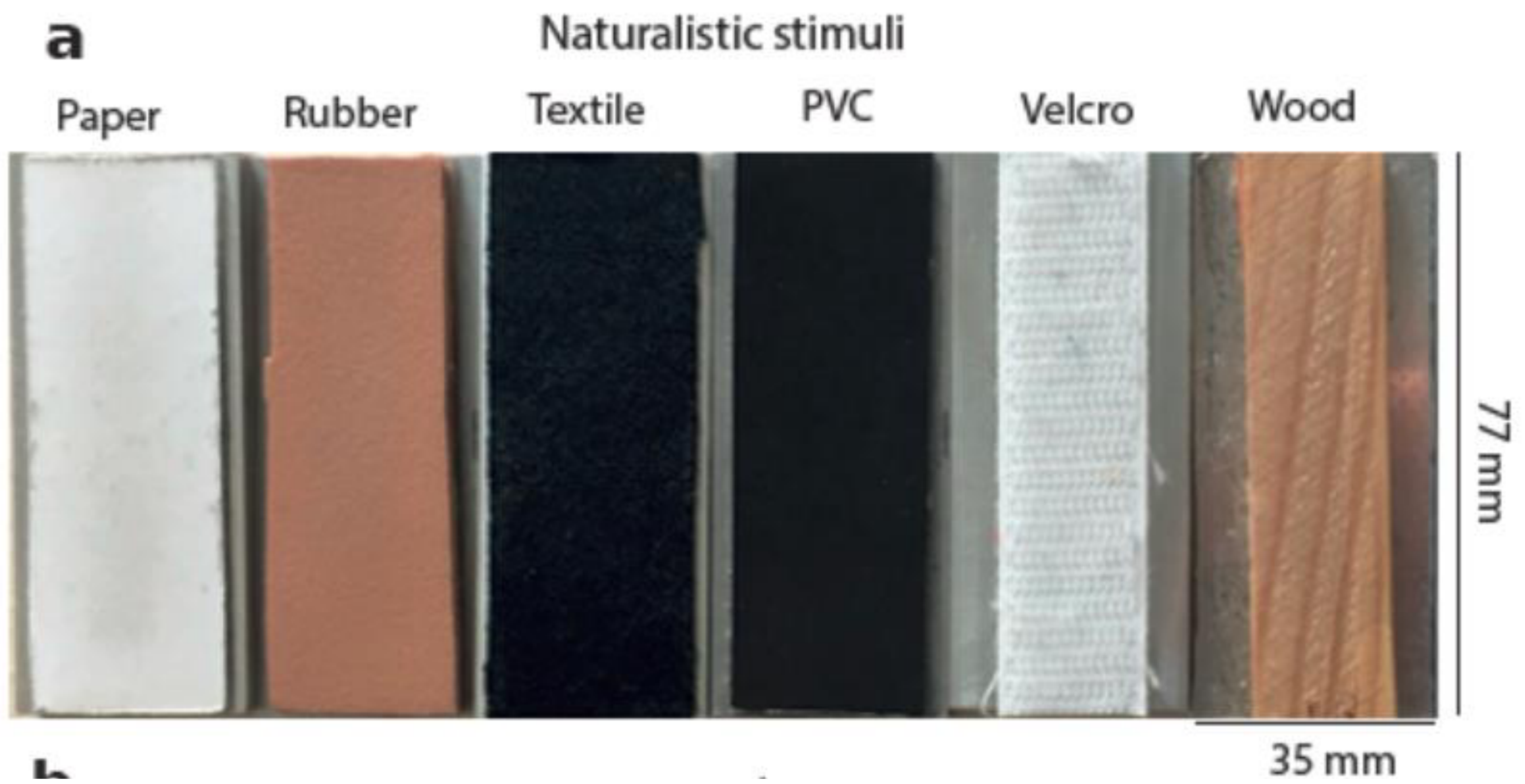

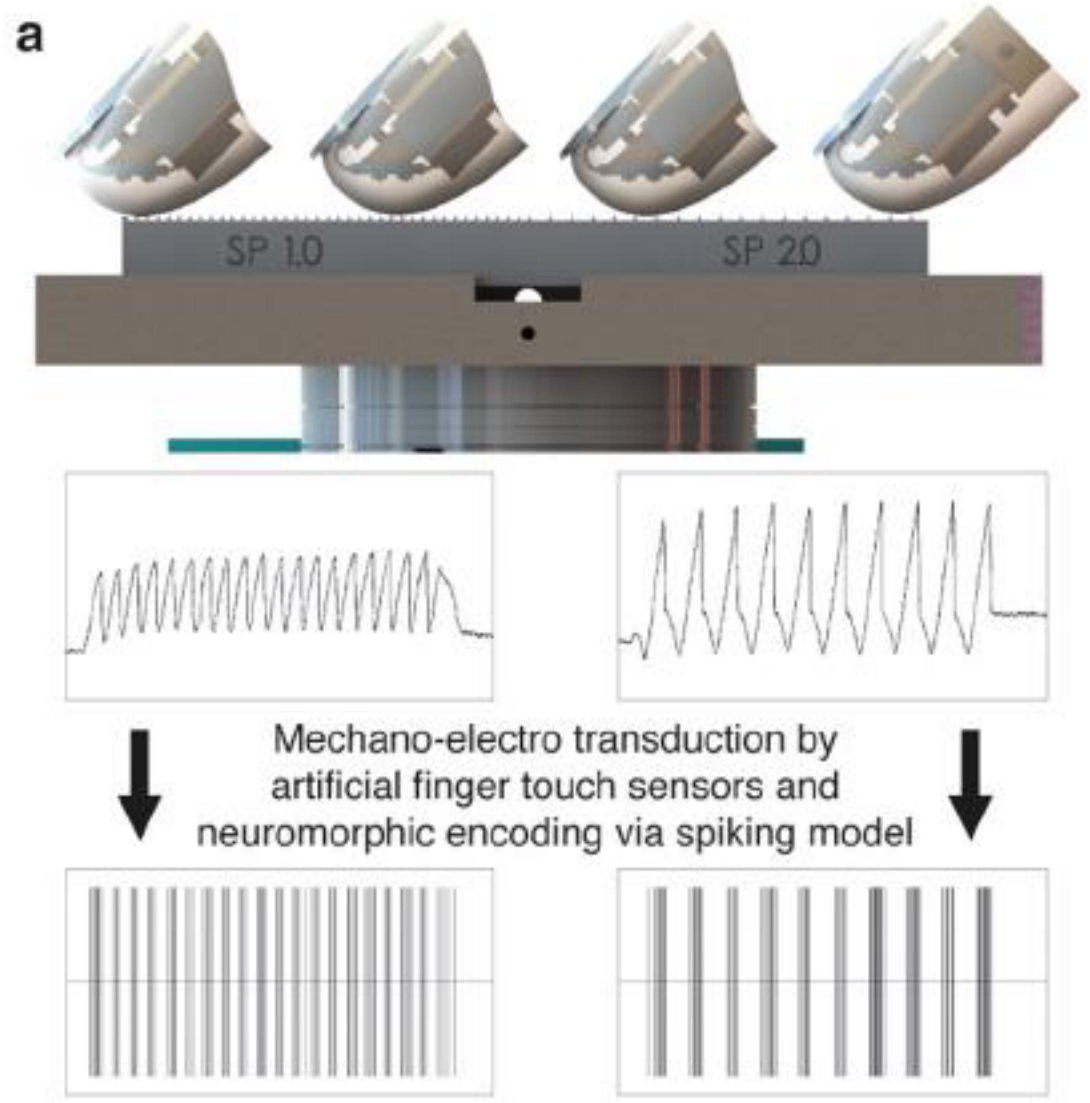

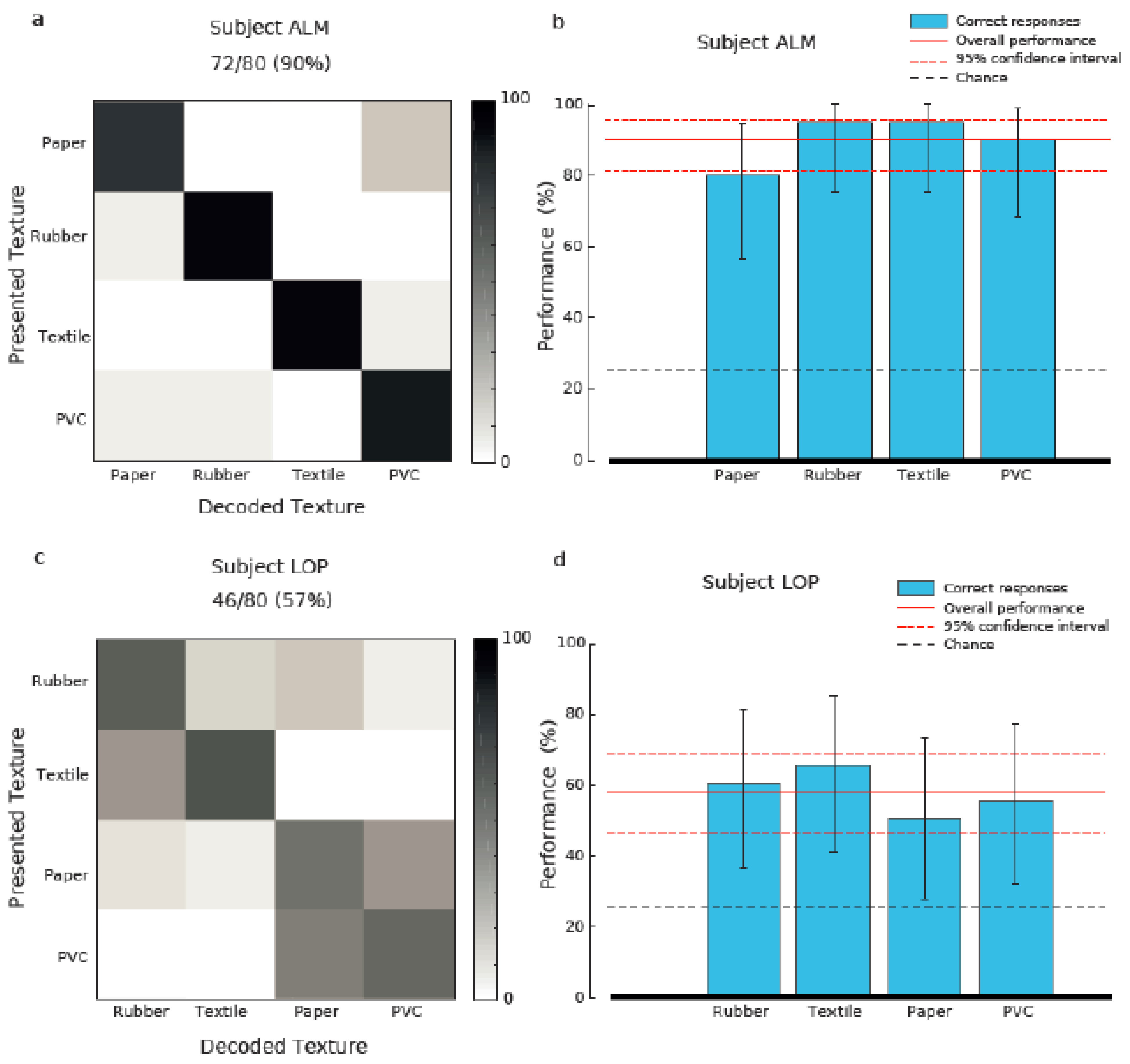

Oddo et al., eLIFE, 2016

Mazzoni et al., Sci Rep, 2019

Restoring perception of real textures

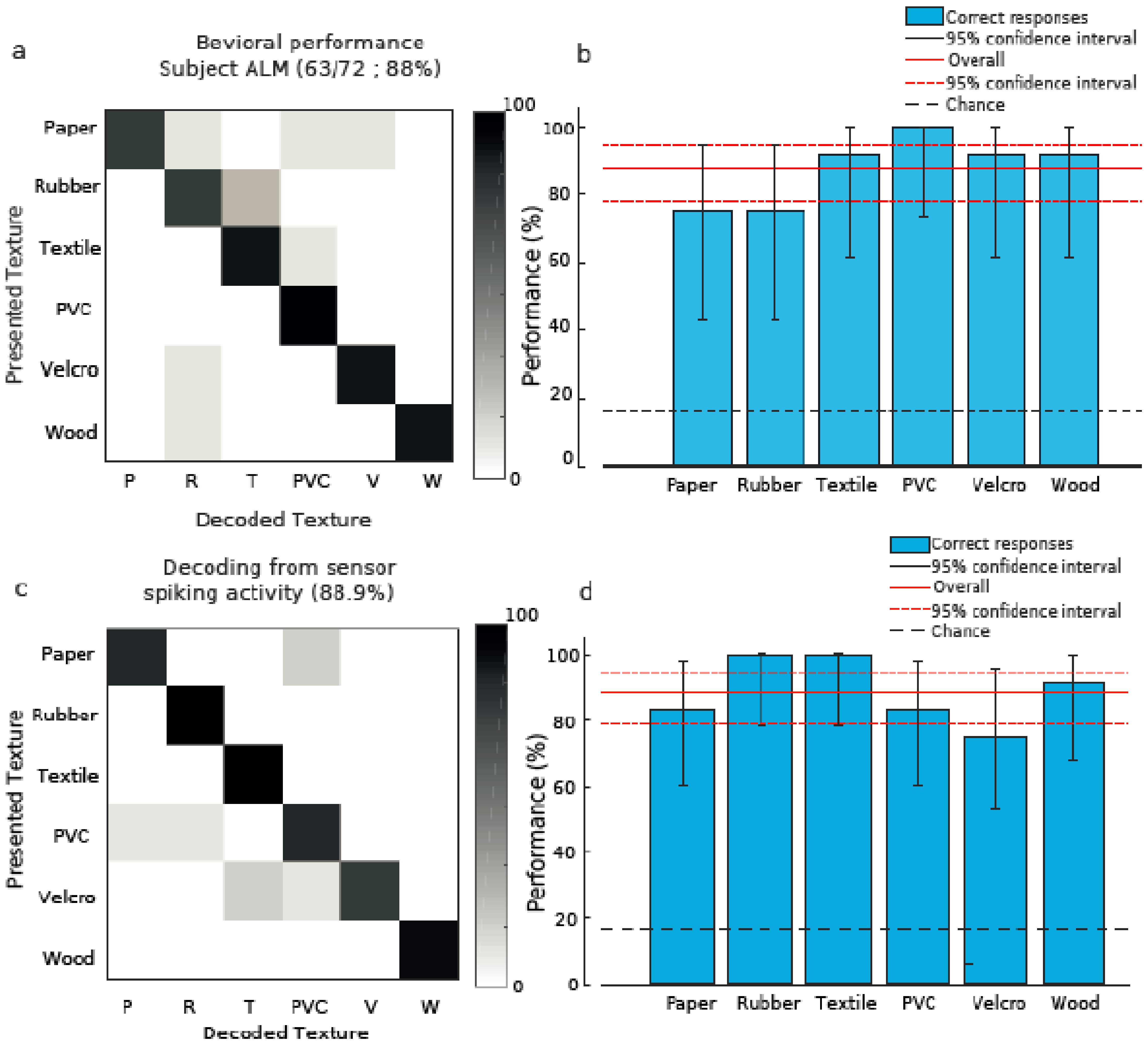

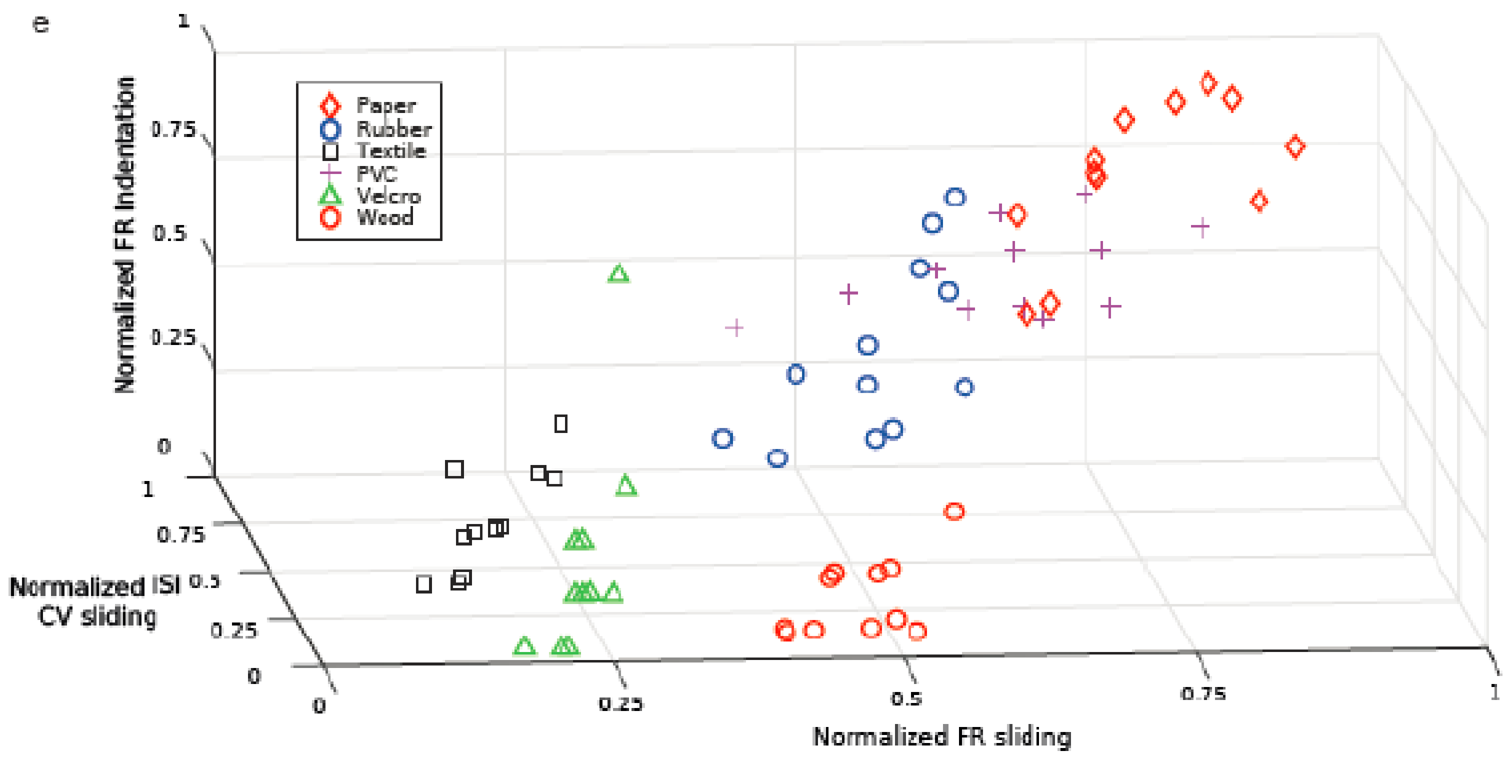

Implanted interfaces can also be used to understand basic principles

Effects of cognitive load

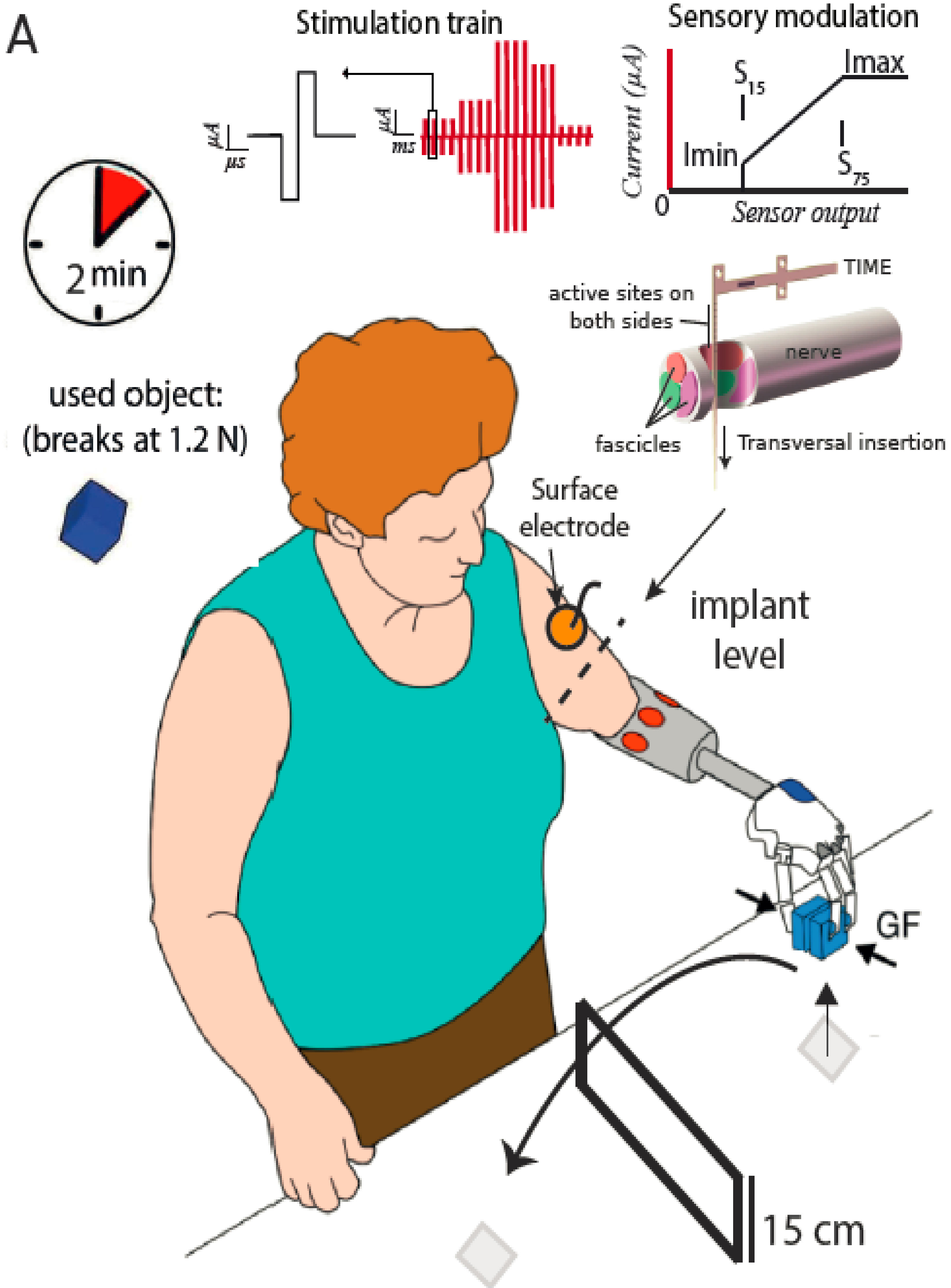

B

Induced sensations & stimulation parameters

Intraneural sensory Feedback (**IF**)

sensation type	vibration
sensation intensity	$S_{min} = 1$, $S_{max} = 8$
electrode position	proximal part of ulnar nerve above elbow
amplitude	A_{min}=200 μA, A_{max}= 300 μA
pulse-width	80 μs
frequency	50 Hz

Superficial sensory Feedback (**SF**)

sensation type	electricity
sensation intensity	$S_{min} = 1$, $S_{max} = 8$
electrode position	on the skin of the left arm
amplitude	A_{min}=100 μA, A_{max}= 500 μA
pulse-width	200 μs
frequency	50 Hz

Effects of cognitive load

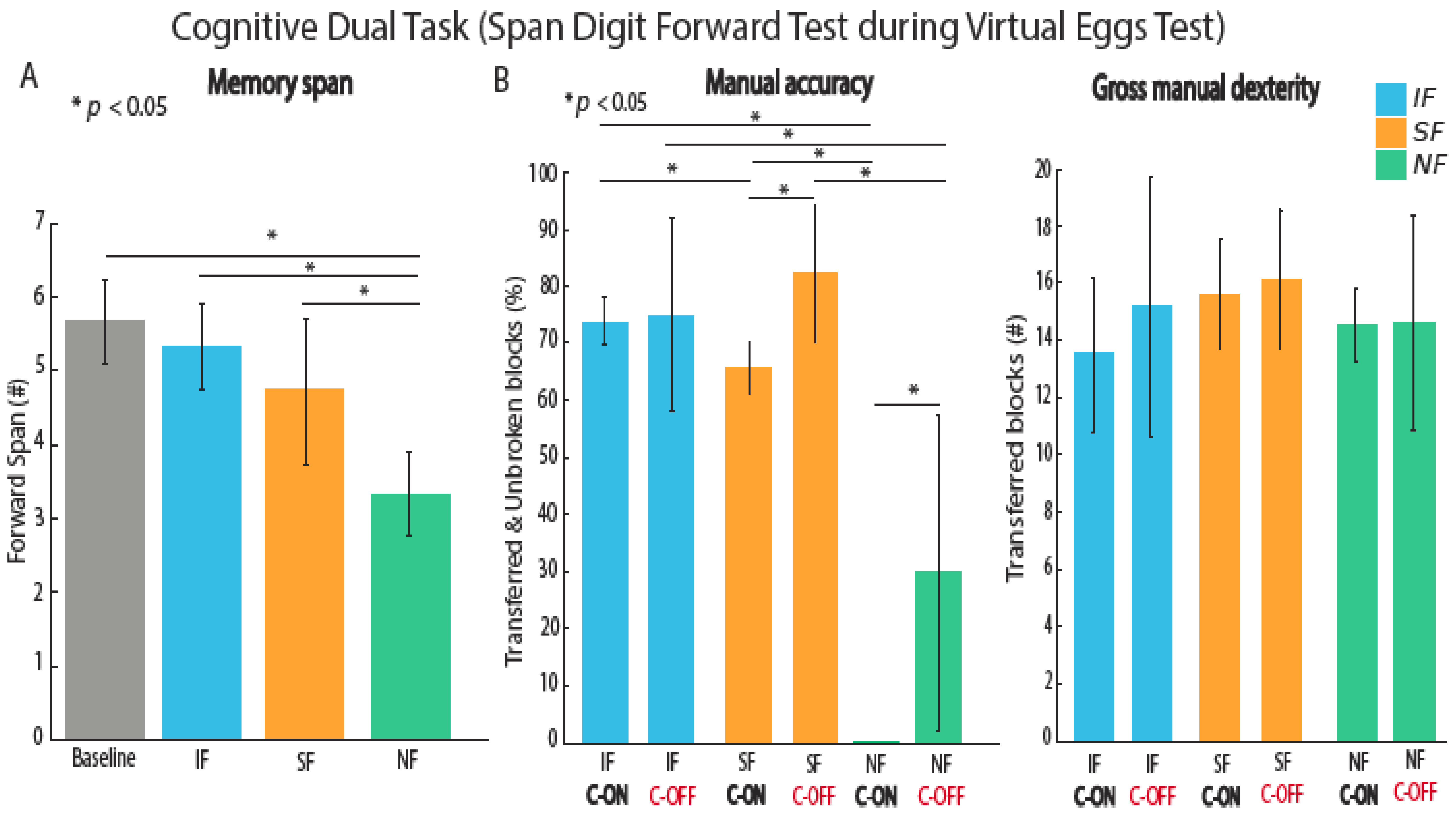

EPFL
fondation bertarelli
Sant'Anna Scuola Universitaria Superiore Pisa

Bidirectional neurocontrolled hand prostheses
"Multimodal" sensory feedback


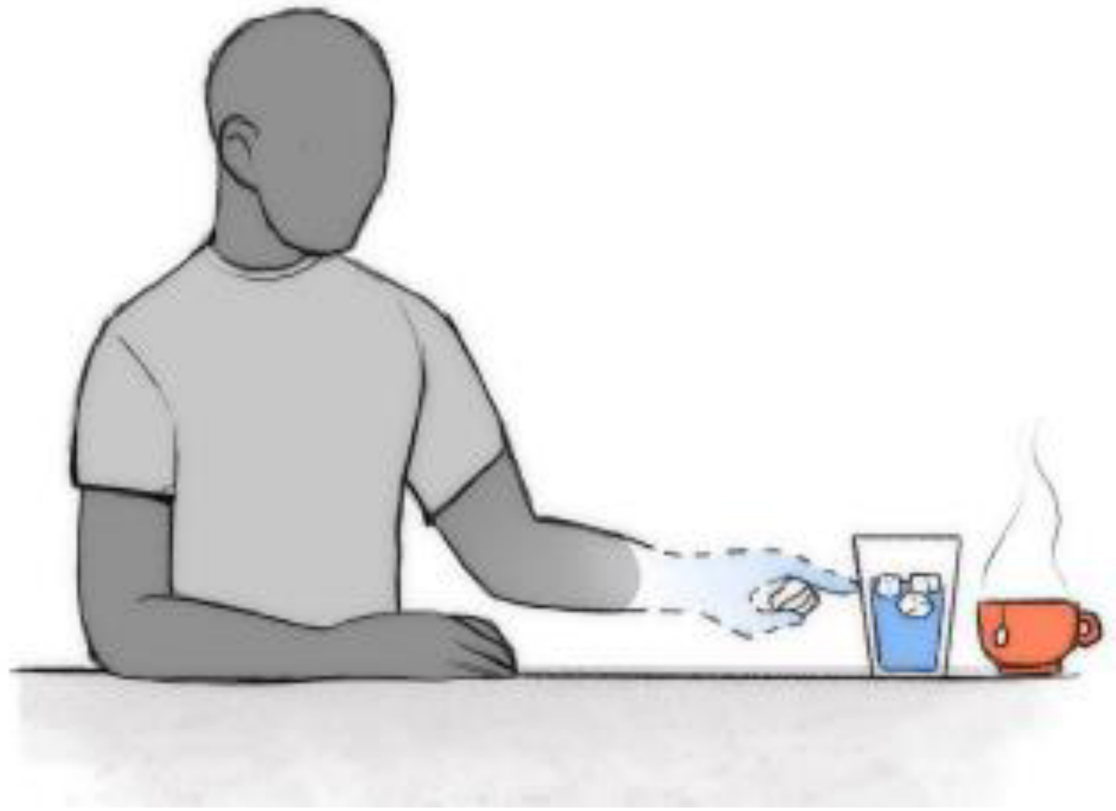

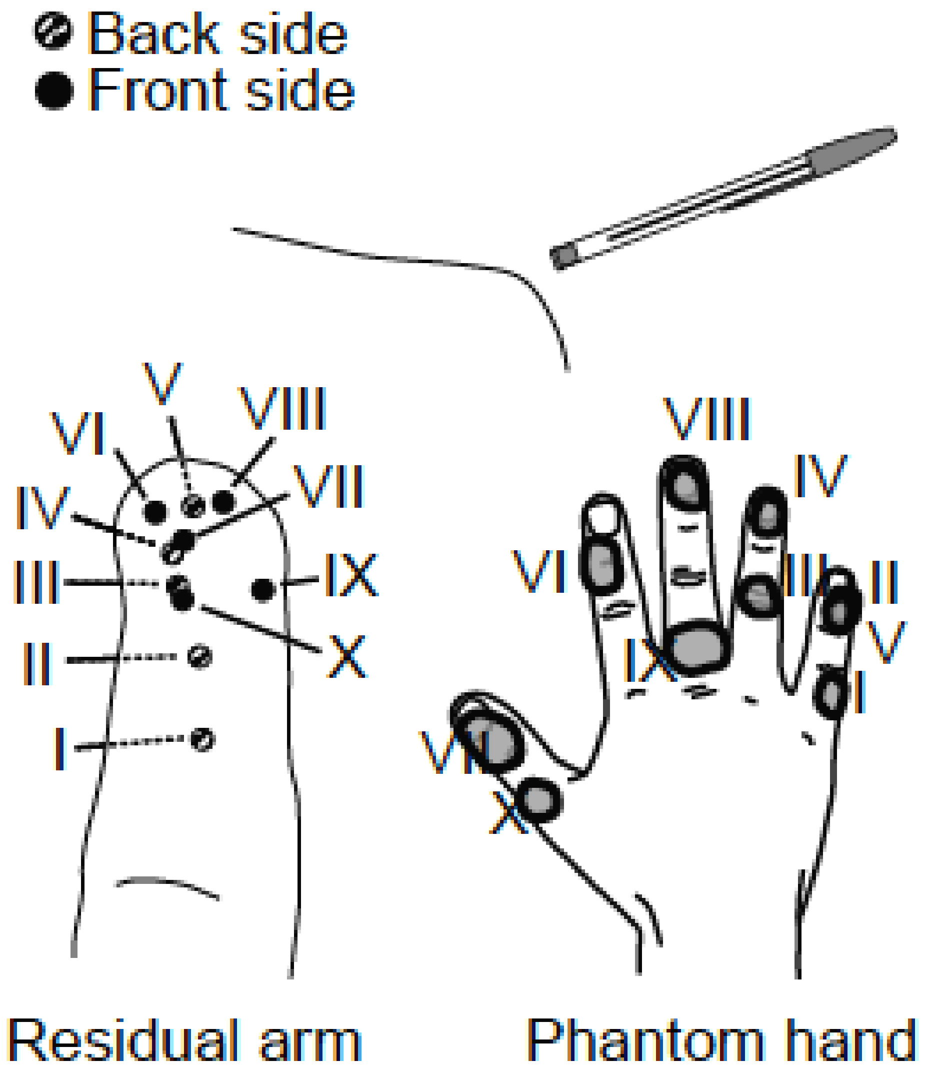

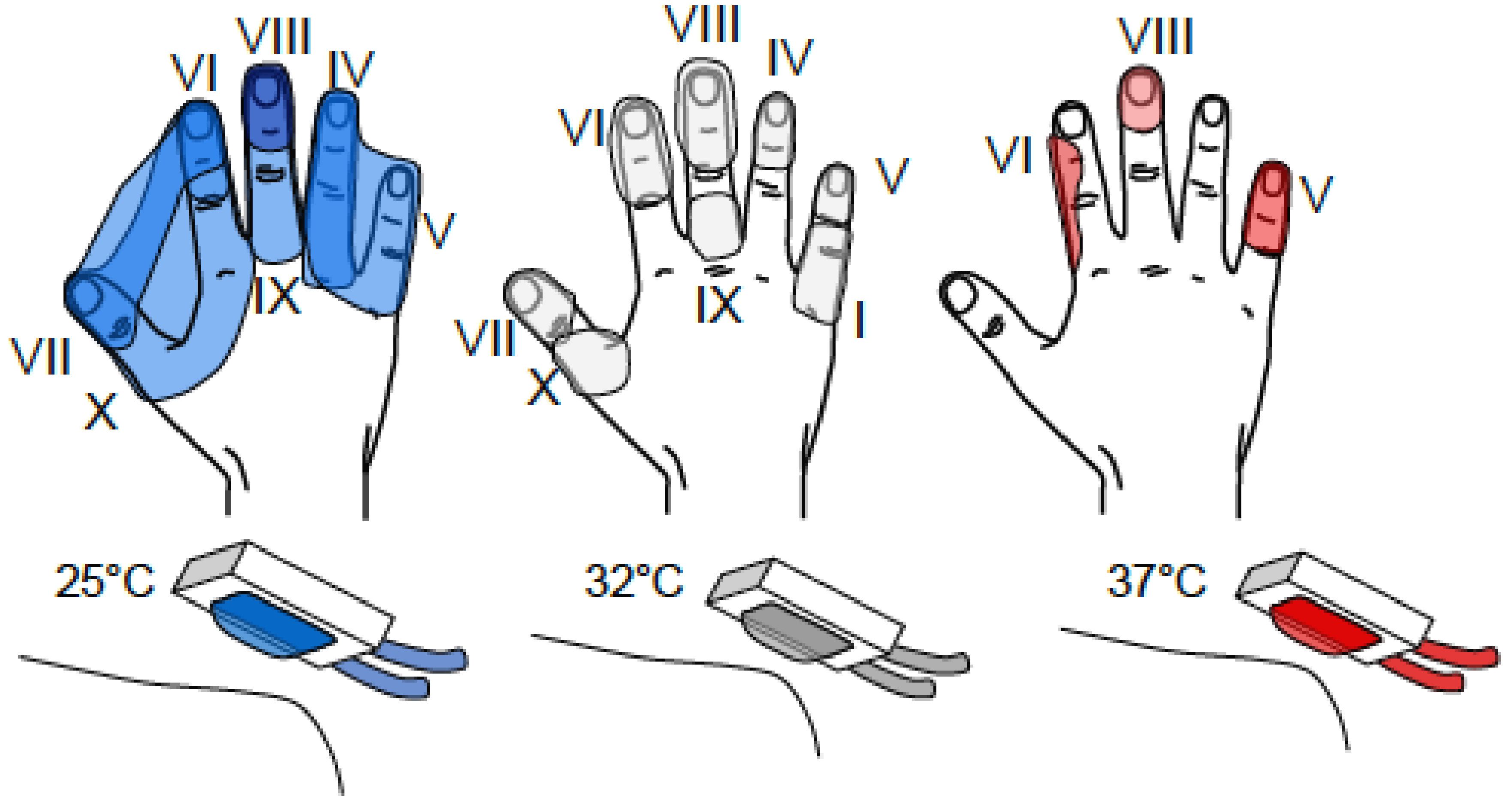

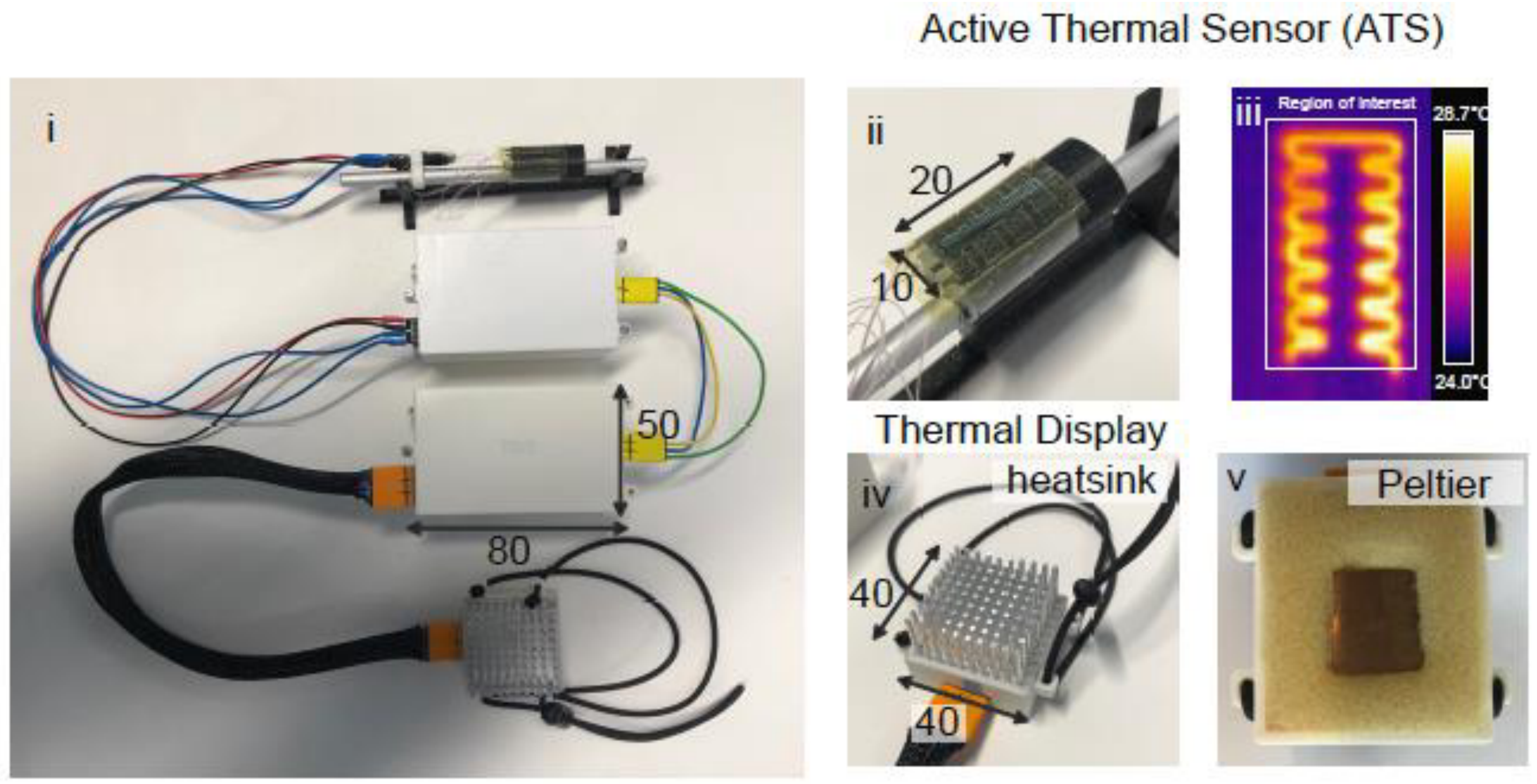

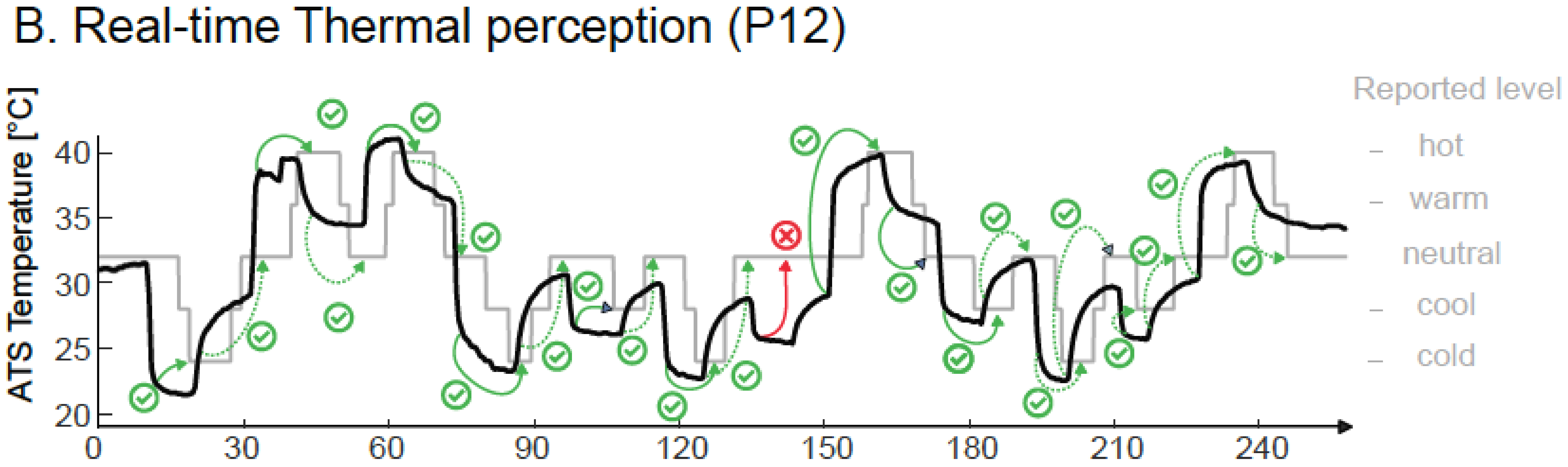

Iberite et al., Science, 2023

Bidirectional neurocontrolled hand prostheses
"Multimodal" sensory feedback

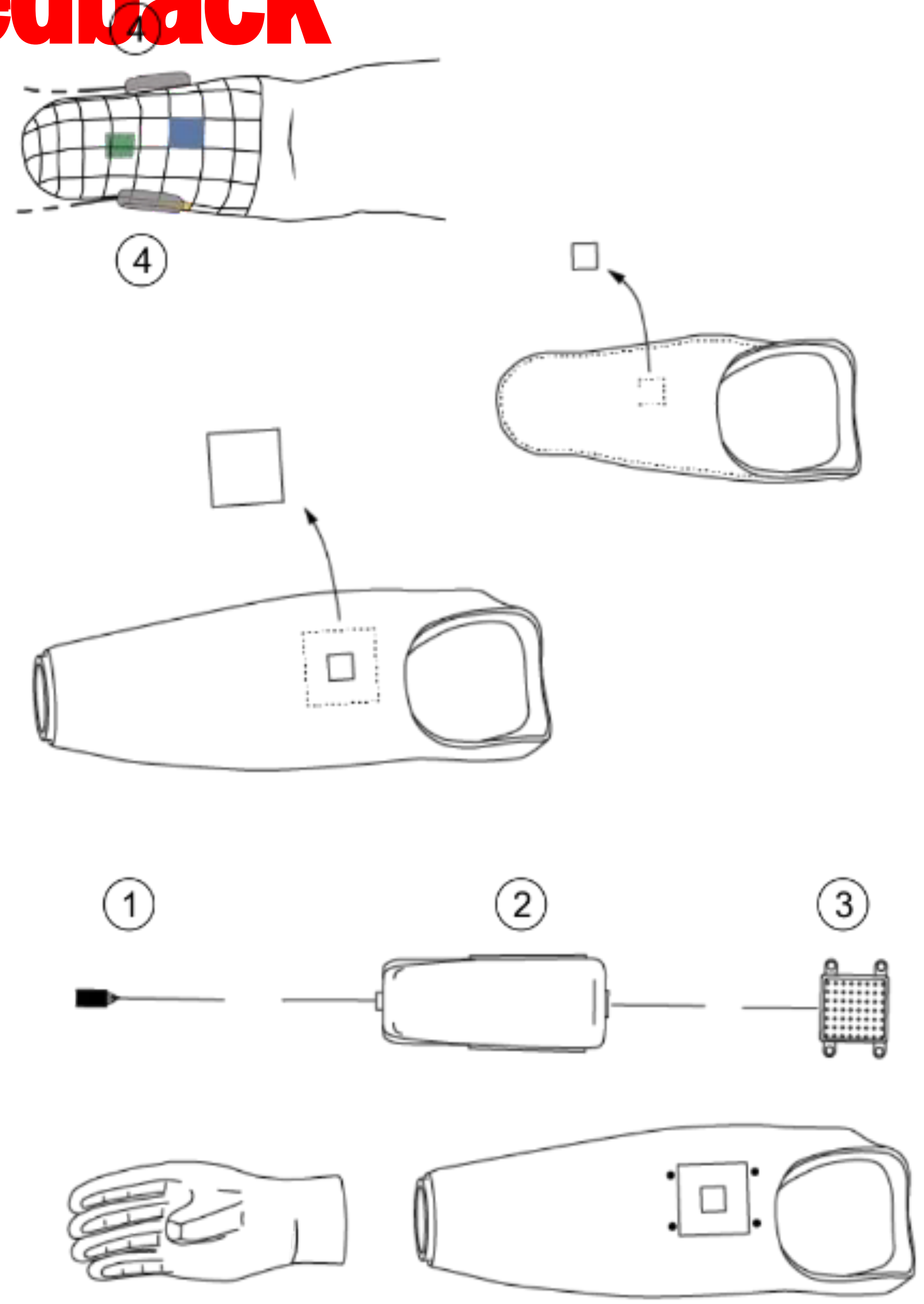

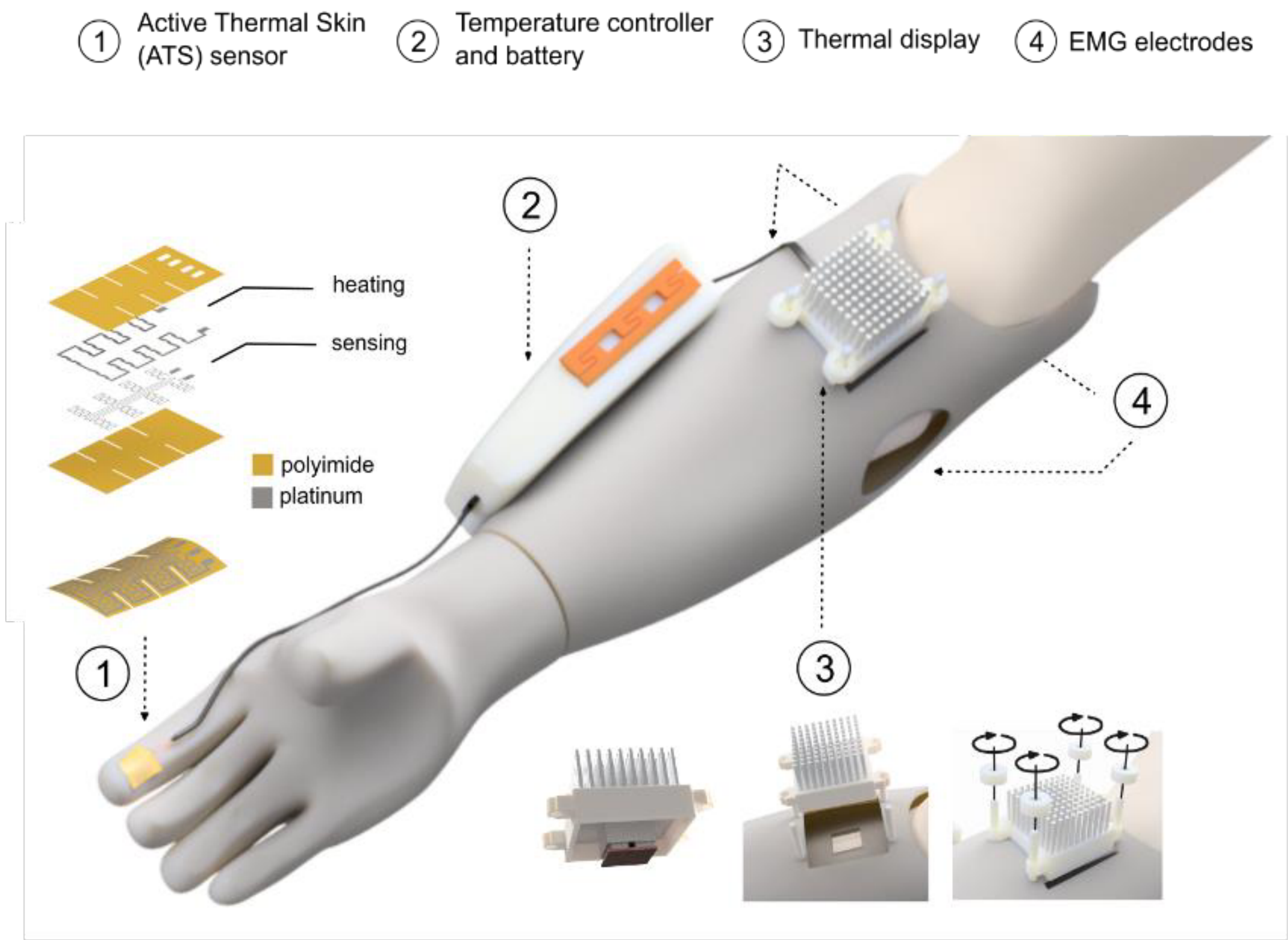

- Muheim et al., MED, 2023

EPFL

fondation bertarelli

Sant'Anna Scuola Universitaria Superiore Pisa

Bidirectional neurocontrolled hand prostheses

"Multimodal" sensory feedback



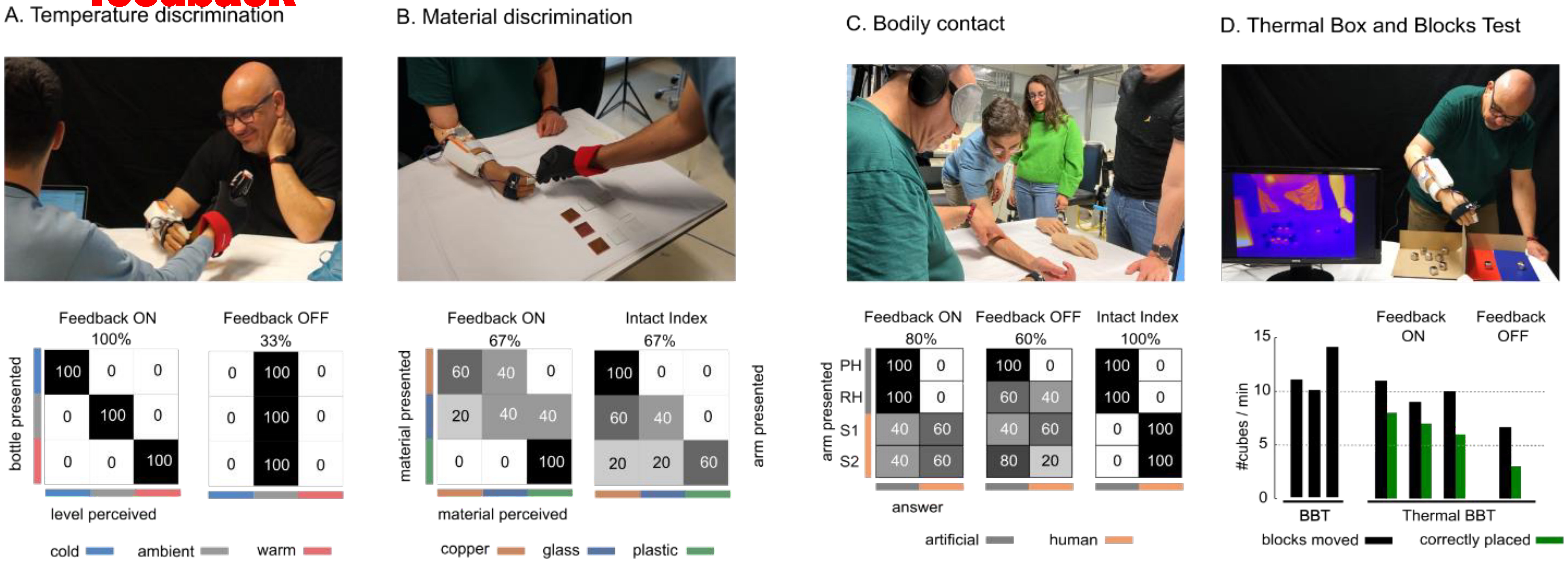

Muheim et al., MED, 2023

NEXT STEP – Going chronic at home

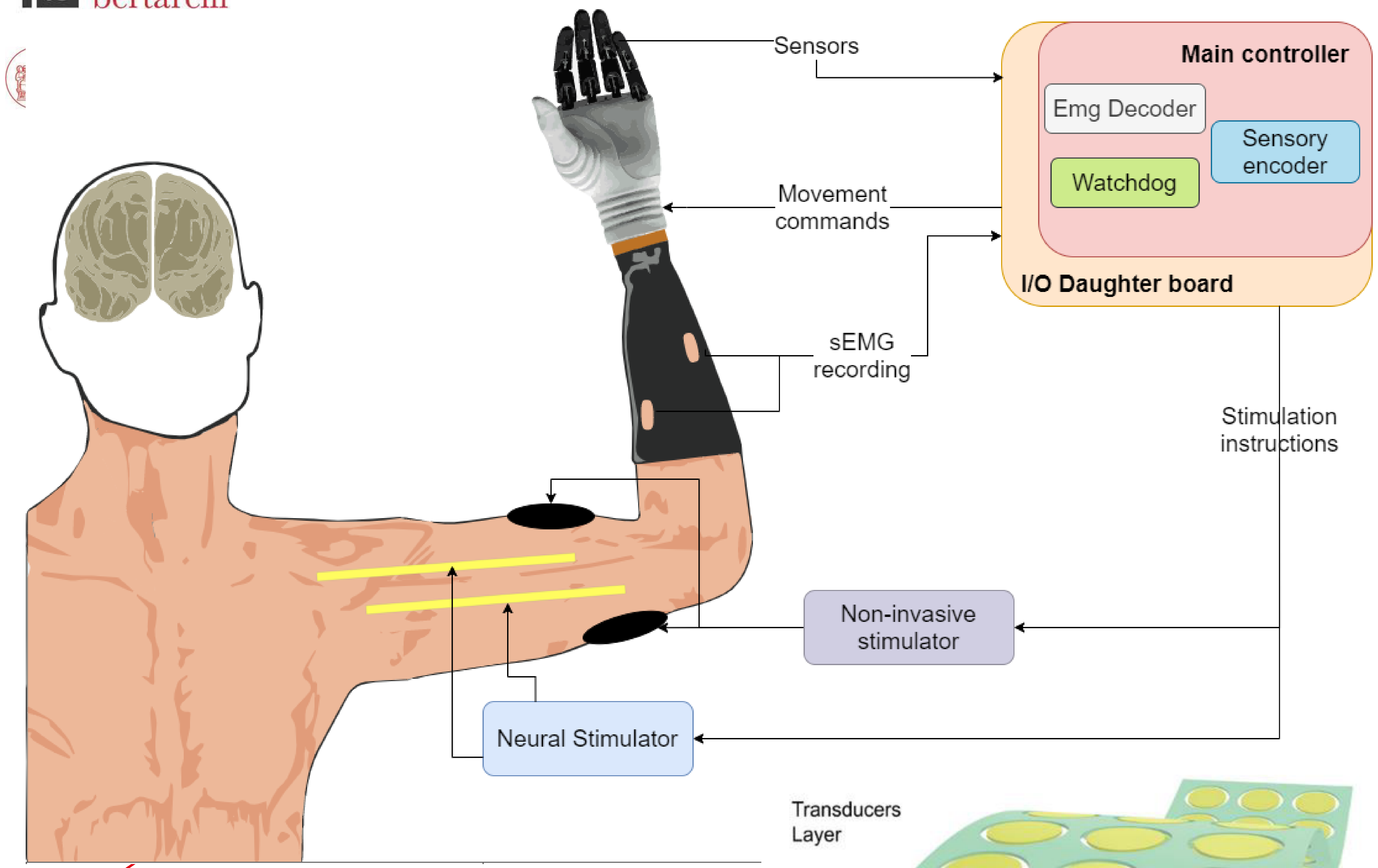

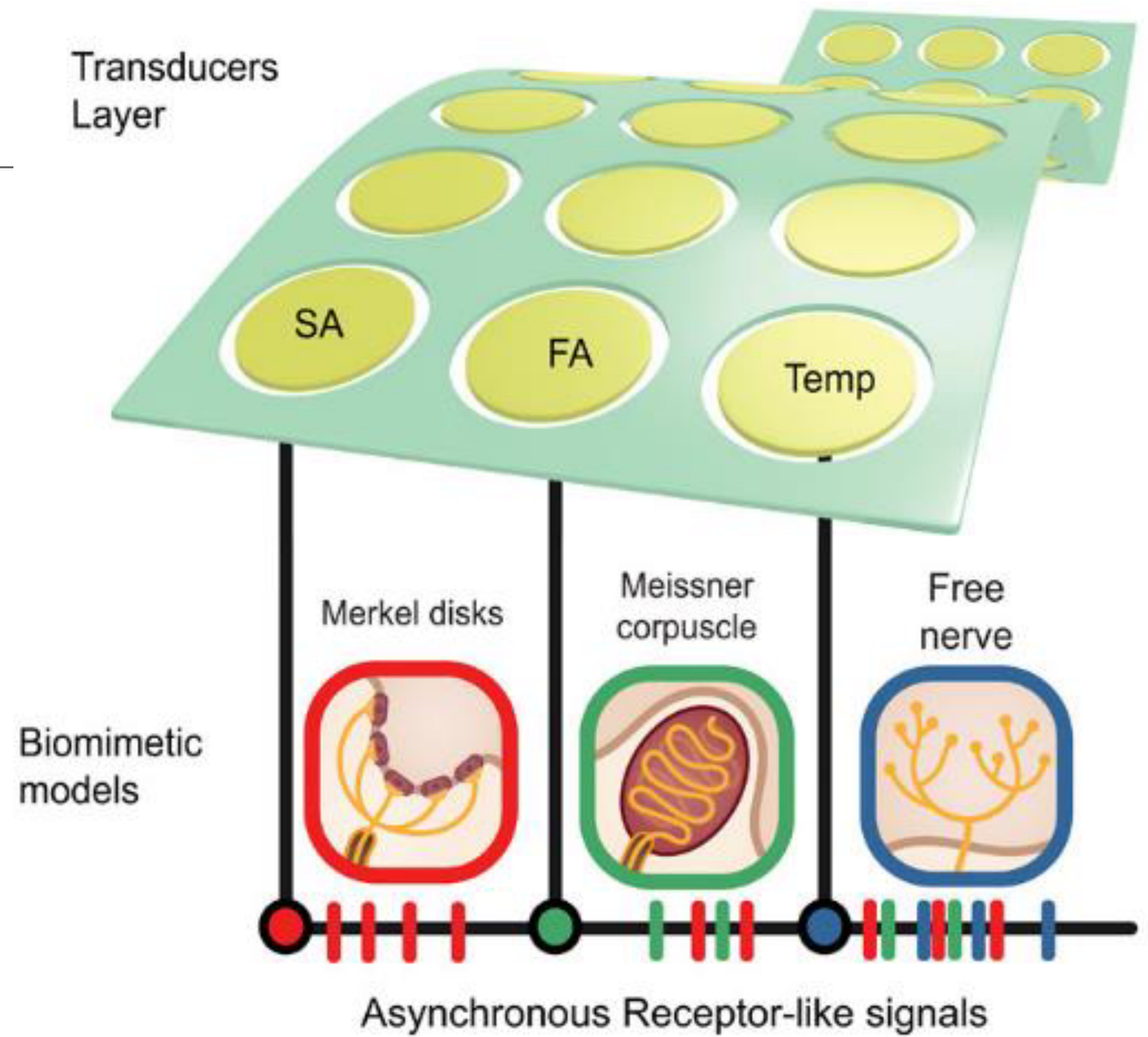

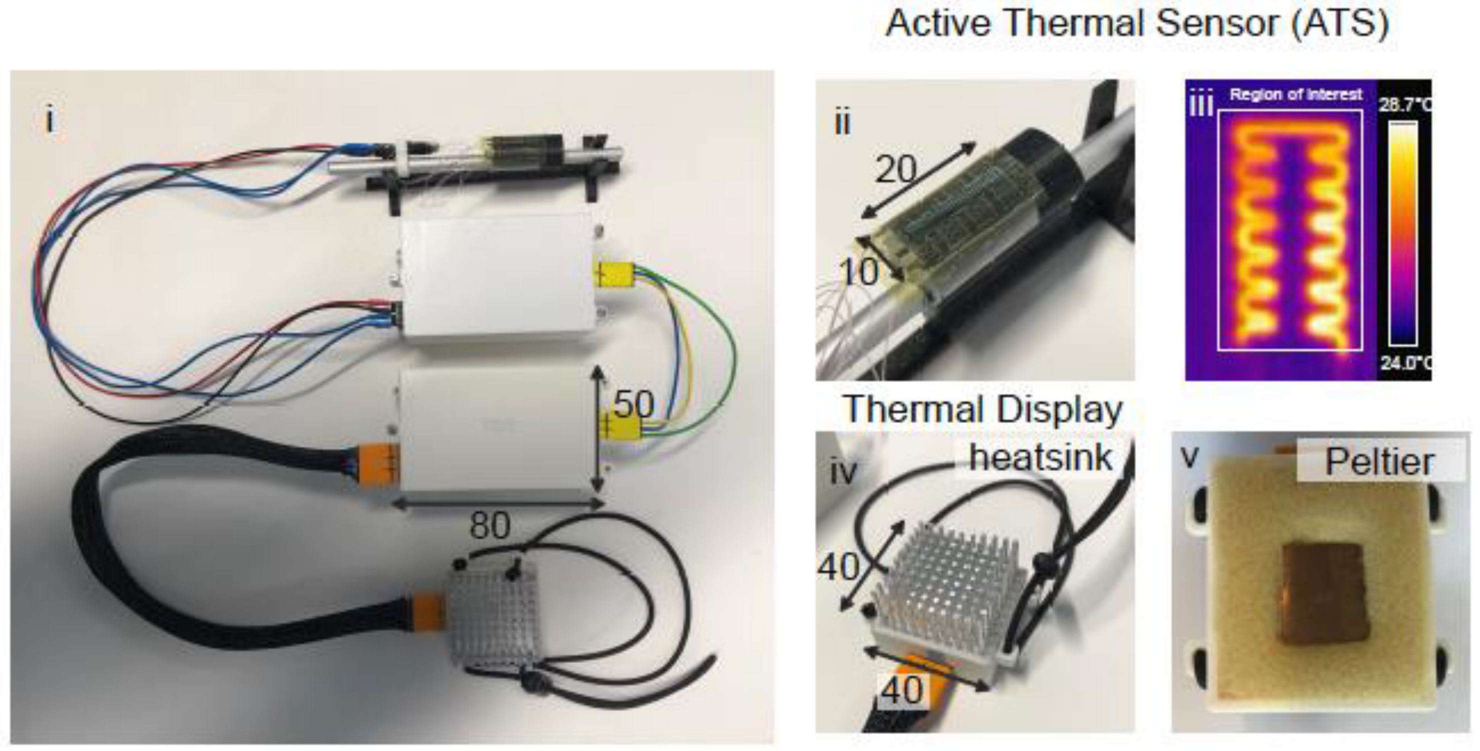

EPFL
fondation bertarelli
Sant'Anna Scuola Universitaria Superiore Pisa

Bidirectional neurocontrolled leg prostheses

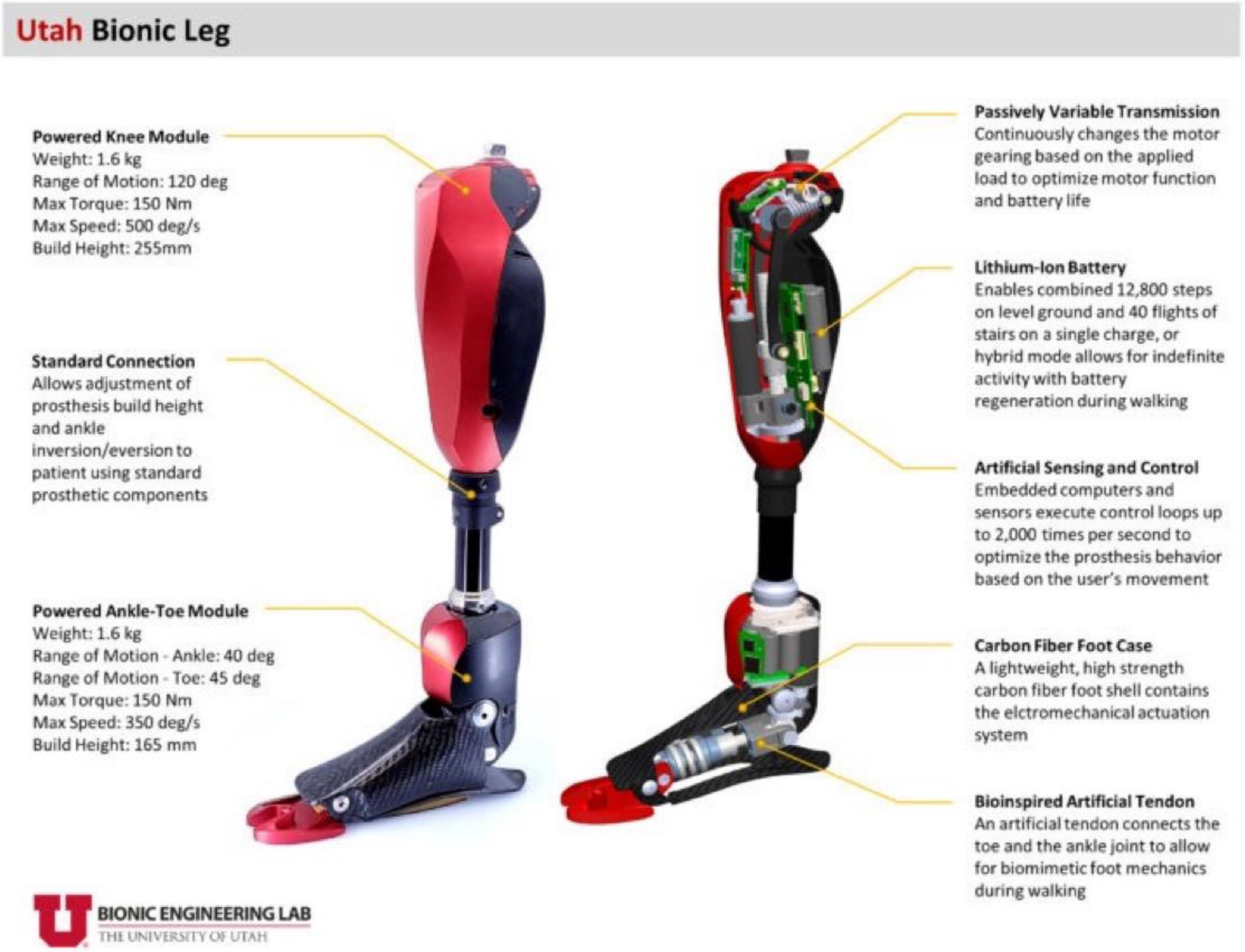

Bidirectional neurocontrolled leg prostheses

Sensory feedback

S.Micera

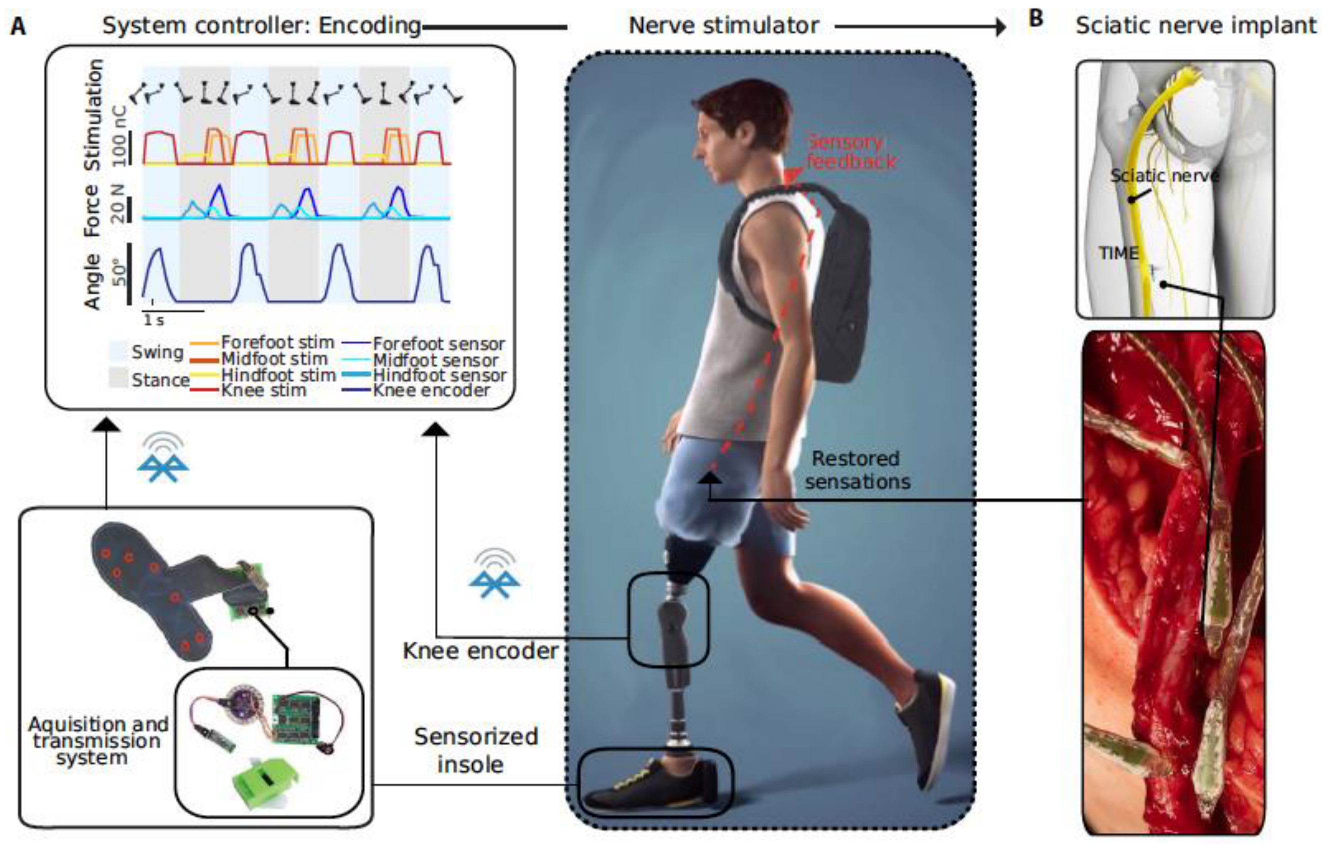

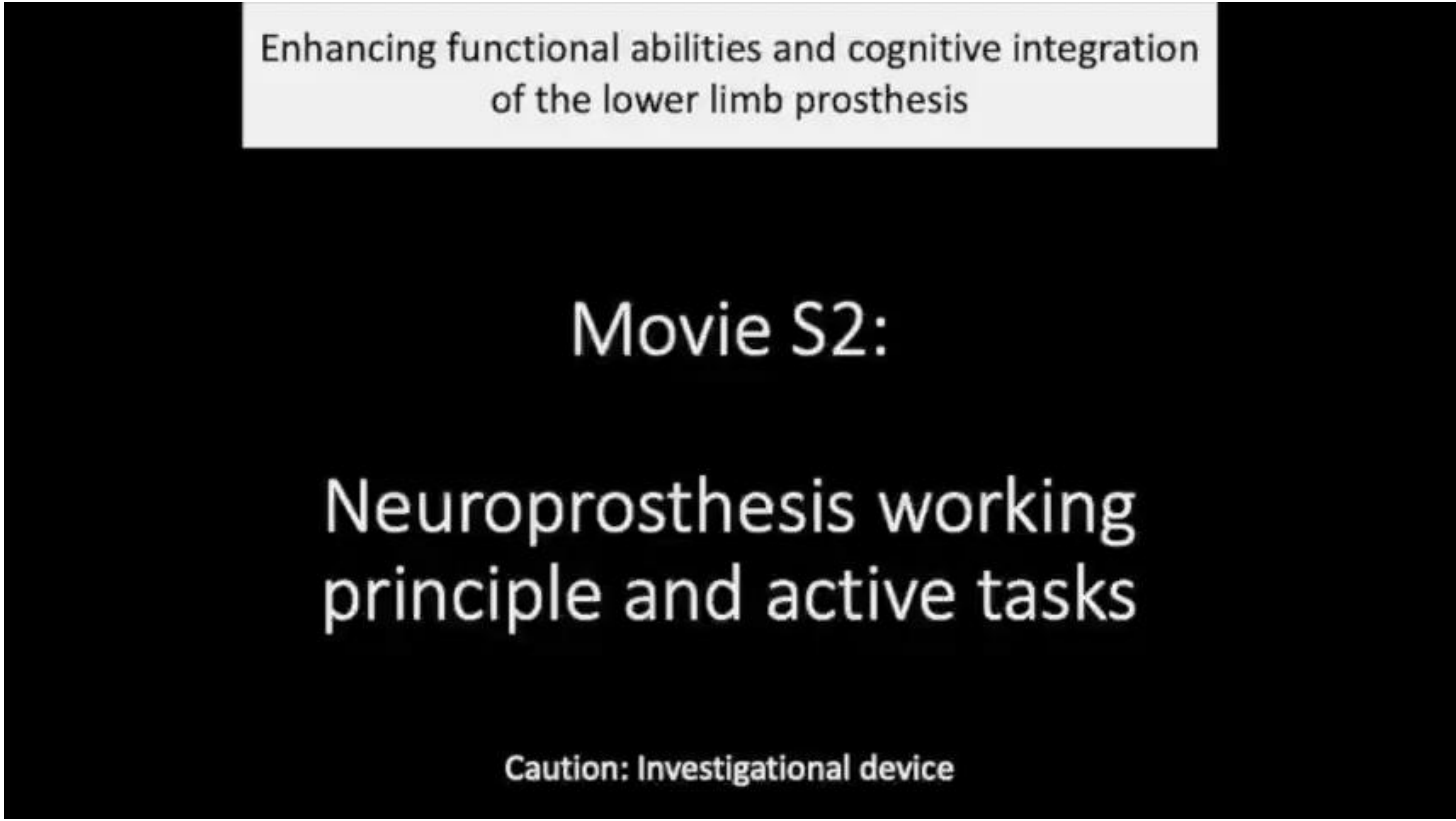

i4LIFE – Intraneural stim

EPFL
fondation bertarelli
Sant'Anna Scuola Universitaria Superiore Pisa

Bidirectional neurocontrolled leg prostheses
Sensory feedback

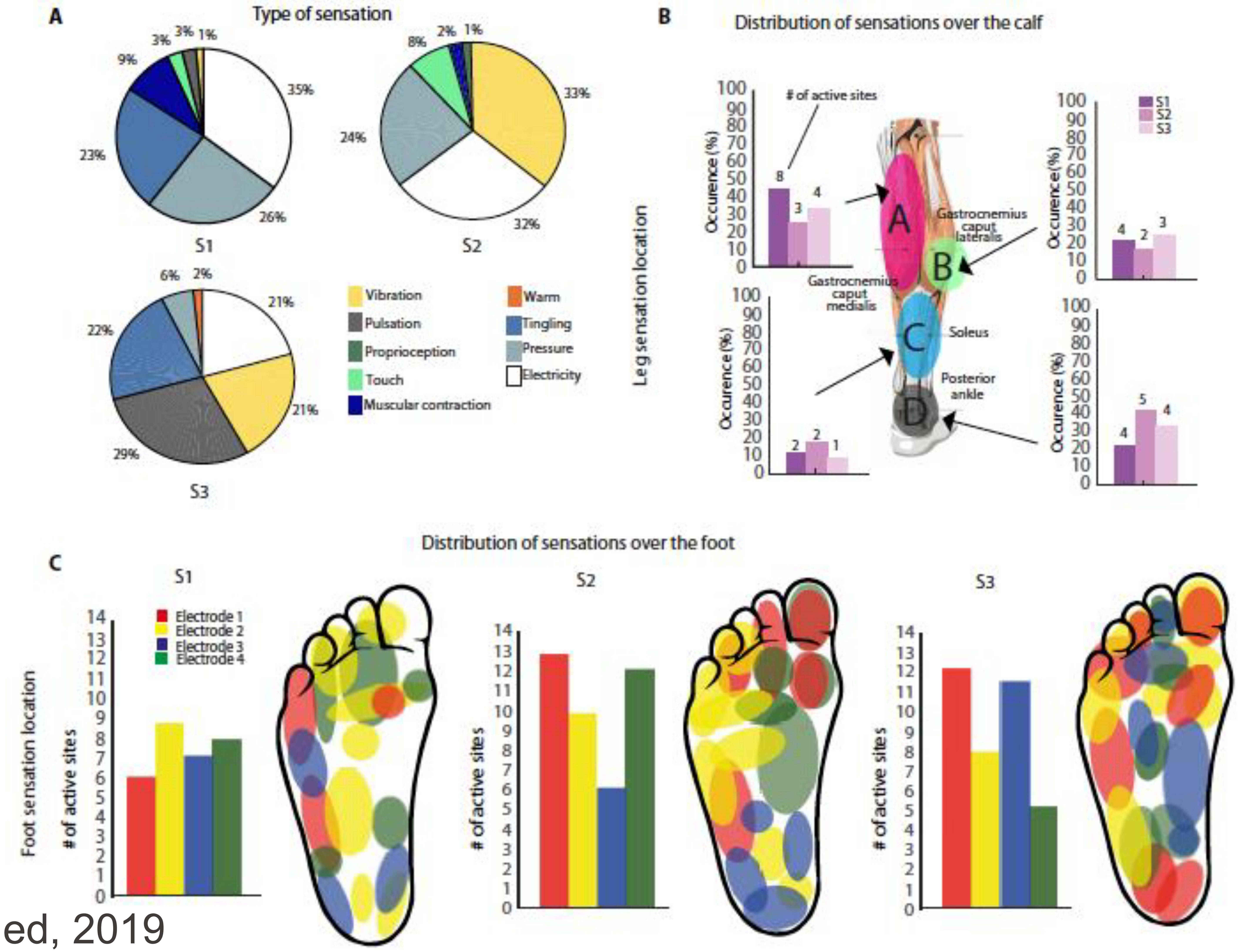

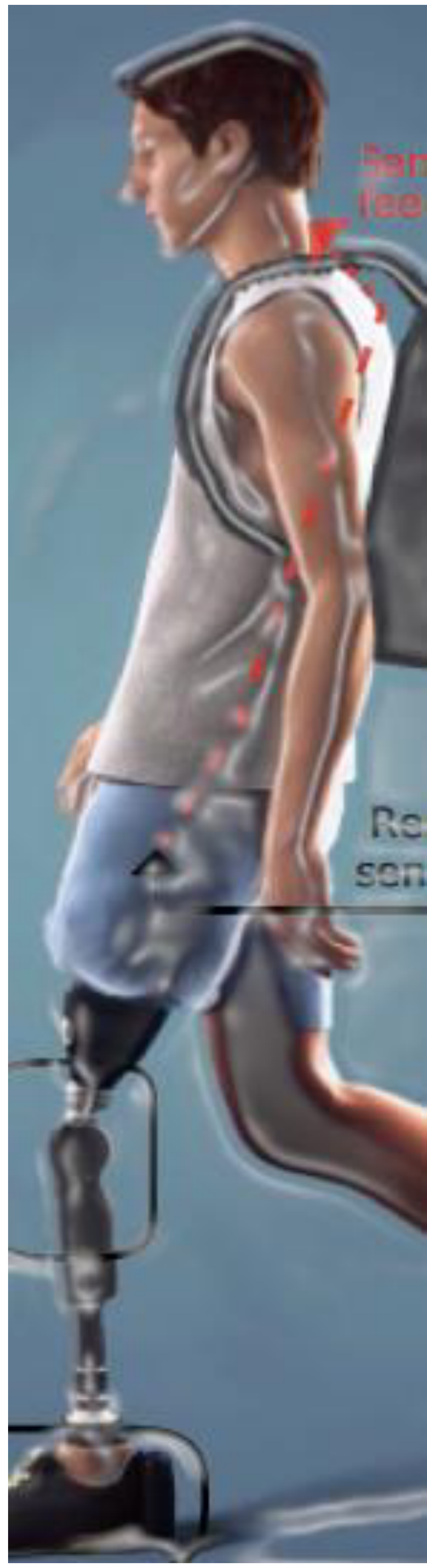

Petrini et al.,
Science Trans Med, 2019

EPFL

fondation bertarelli

Sant'Anna Scuola Universitaria Superiore Pisa

Bidirectional neurocontrolled leg prostheses

Sensory feedback

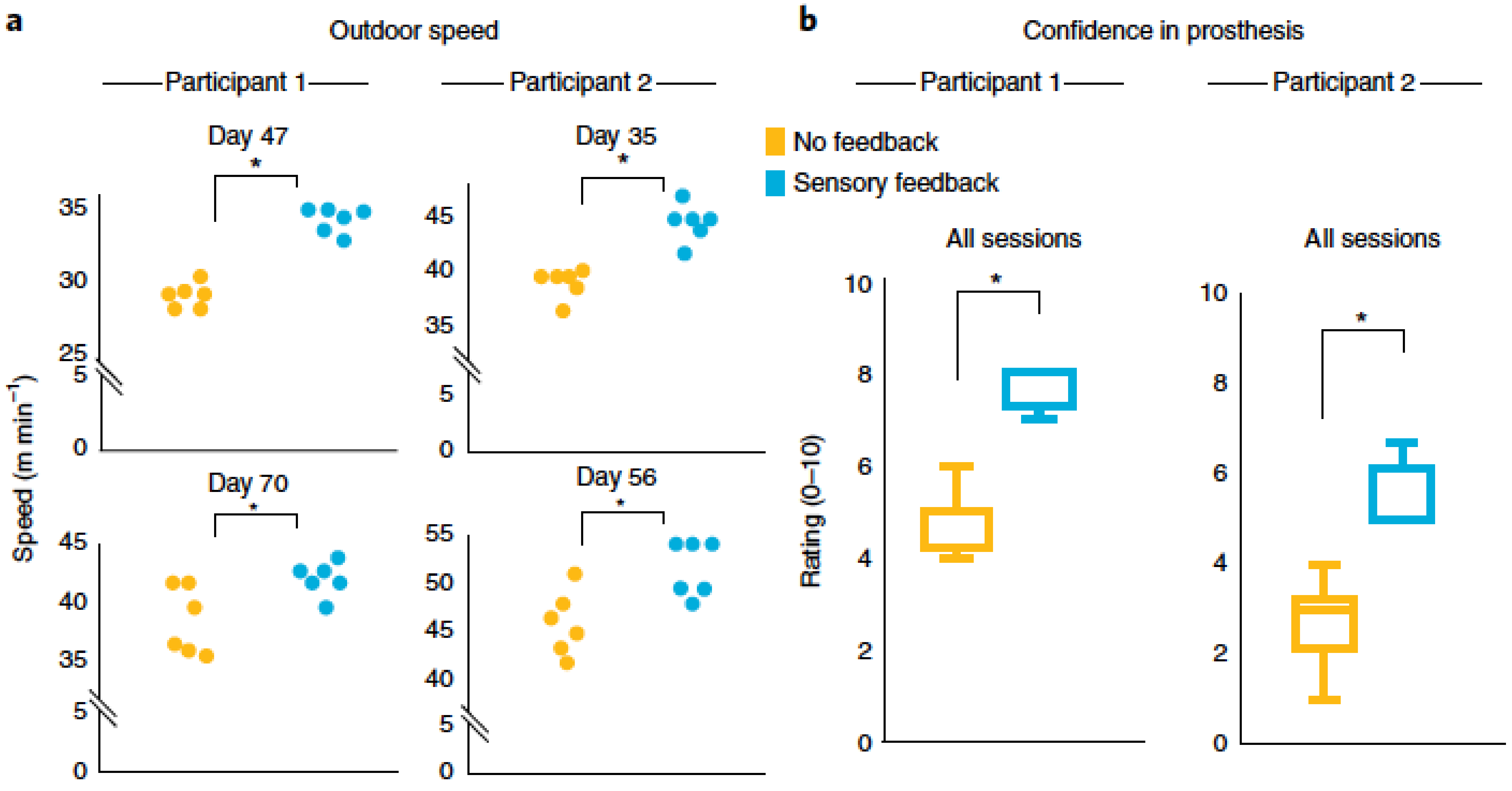

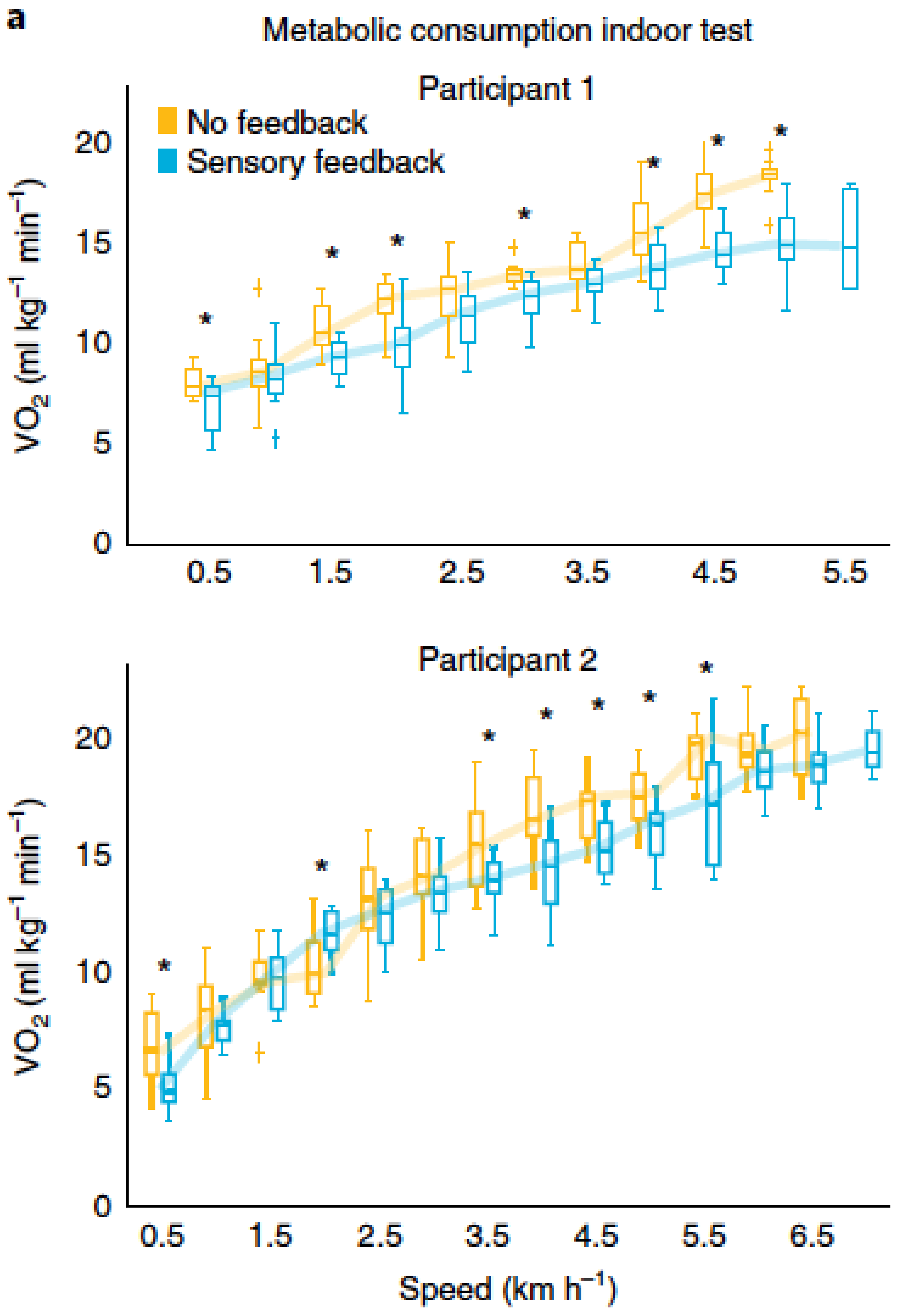

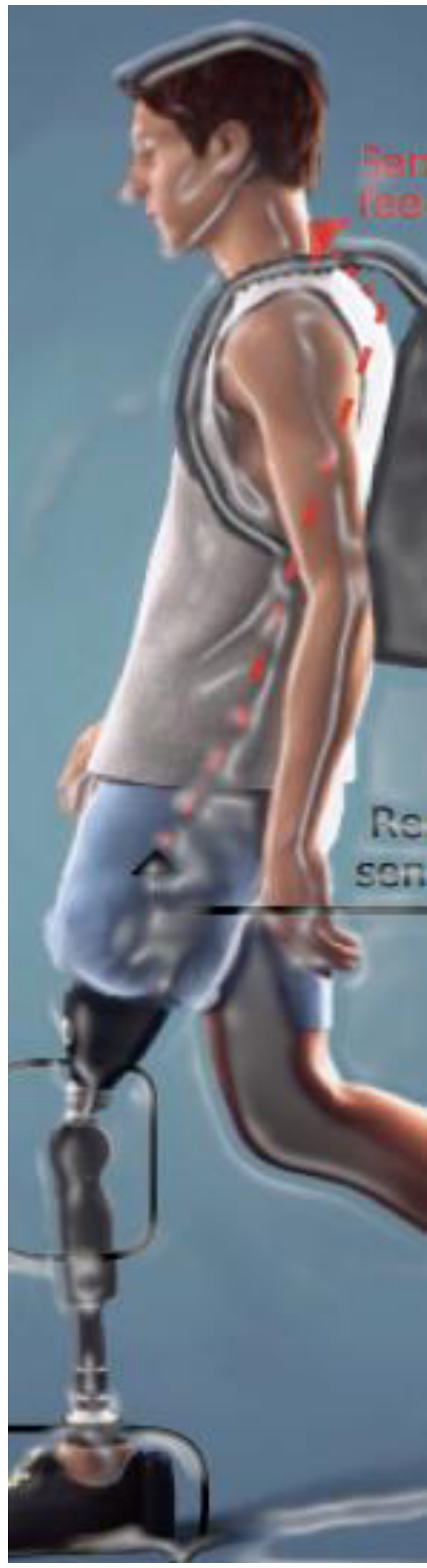

S.Micera

Walking speed and self-reported confidence increased while mental and physical fatigue decreased for both participants

Participants exhibited reduced phantom limb pain with neural sensory feedback.

Petrini et al., Nature Medicine, 2019

Bidirectional neurocontrolled leg prostheses

Sensory feedback

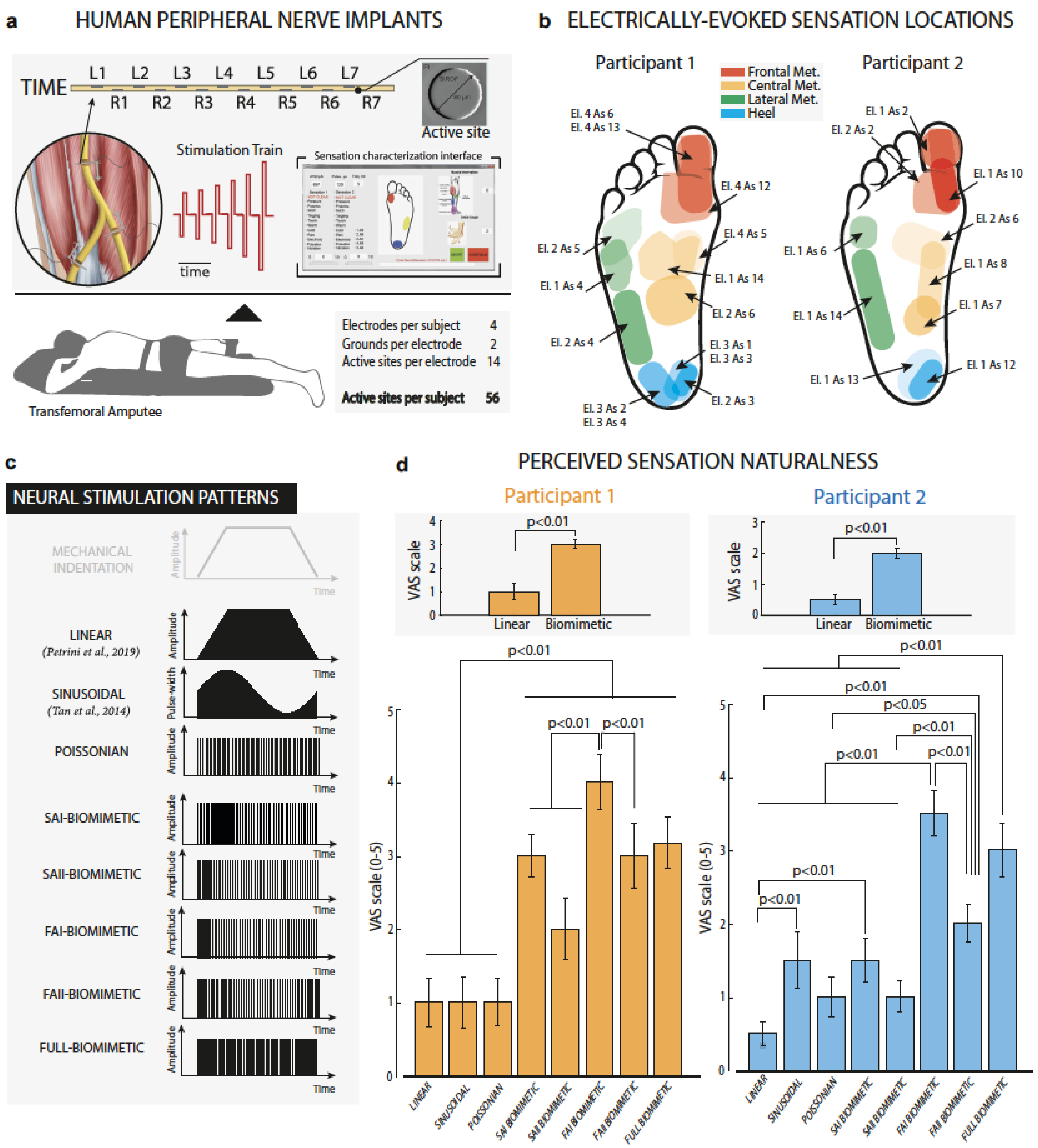

...This was probably caused by the different composition of the fibers activated by the electrode channels in the different foot regions.

...We hypothesized that not only the proportion of SA and FA fibers is relevant but also their role in encoding touch information in that specific region.

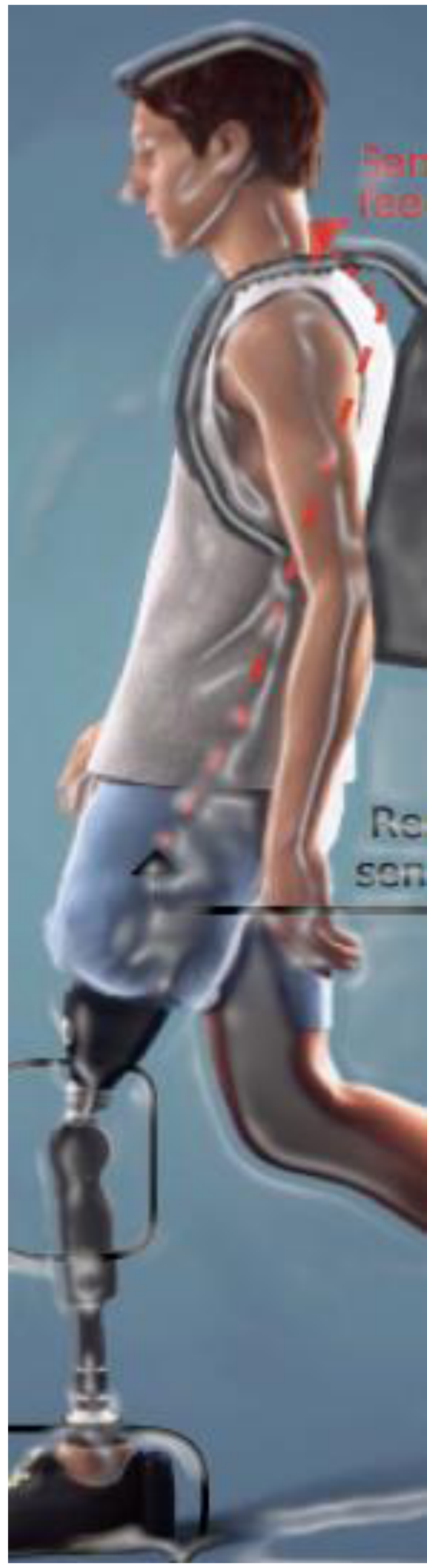

Valle et al., Nature Comm, 2024

S.Micera

EPFL
fondation bertarelli
Sant'Anna Scuola Universitaria Superiore Pisa

Bidirectional neurocontrolled leg prostheses
Sensory feedback

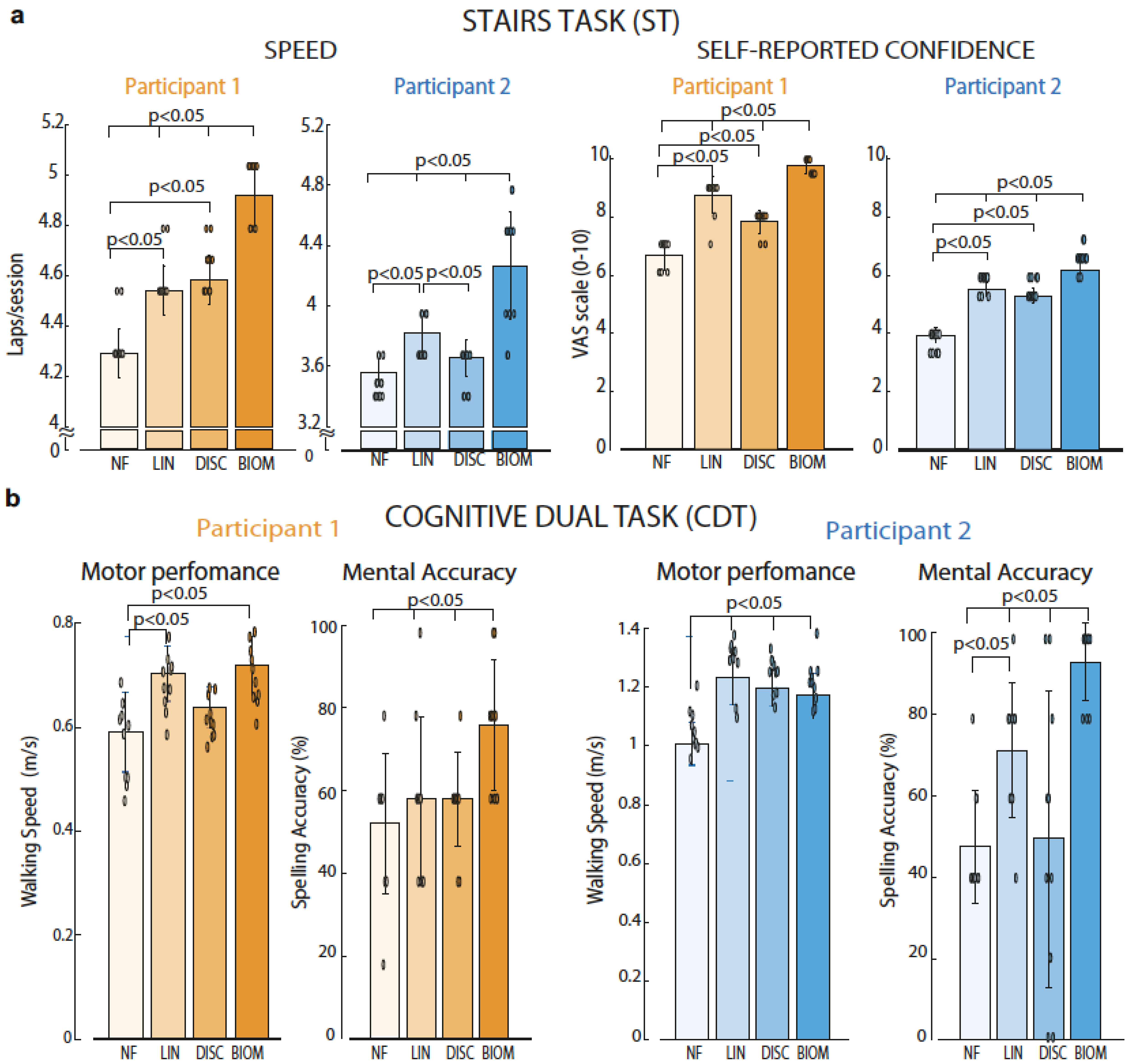

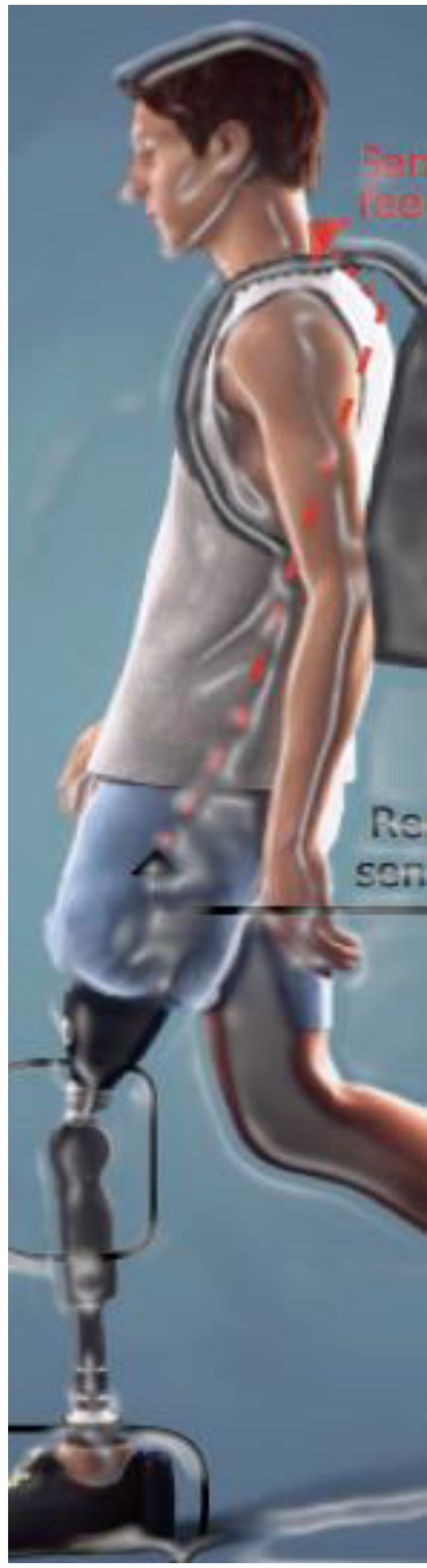

Valle et al., Nature Comm, 2024

Agonist-antagonist myoneural interface

- As a methodology of improving efferent (neural pathways that relay commands from the central nervous system to a muscle or other end organ) prosthetic control and providing afferent proprioceptive sensation, we present an agonist-antagonist myoneural interface (AMI)
- An AMI is made up of an agonist and an antagonist muscle tendon connected mechanically in series: When the agonist contracts, the antagonist is stretched and vice versa
- The purpose of an AMI is to control and interpret proprioceptive feedback from a bionic joint.

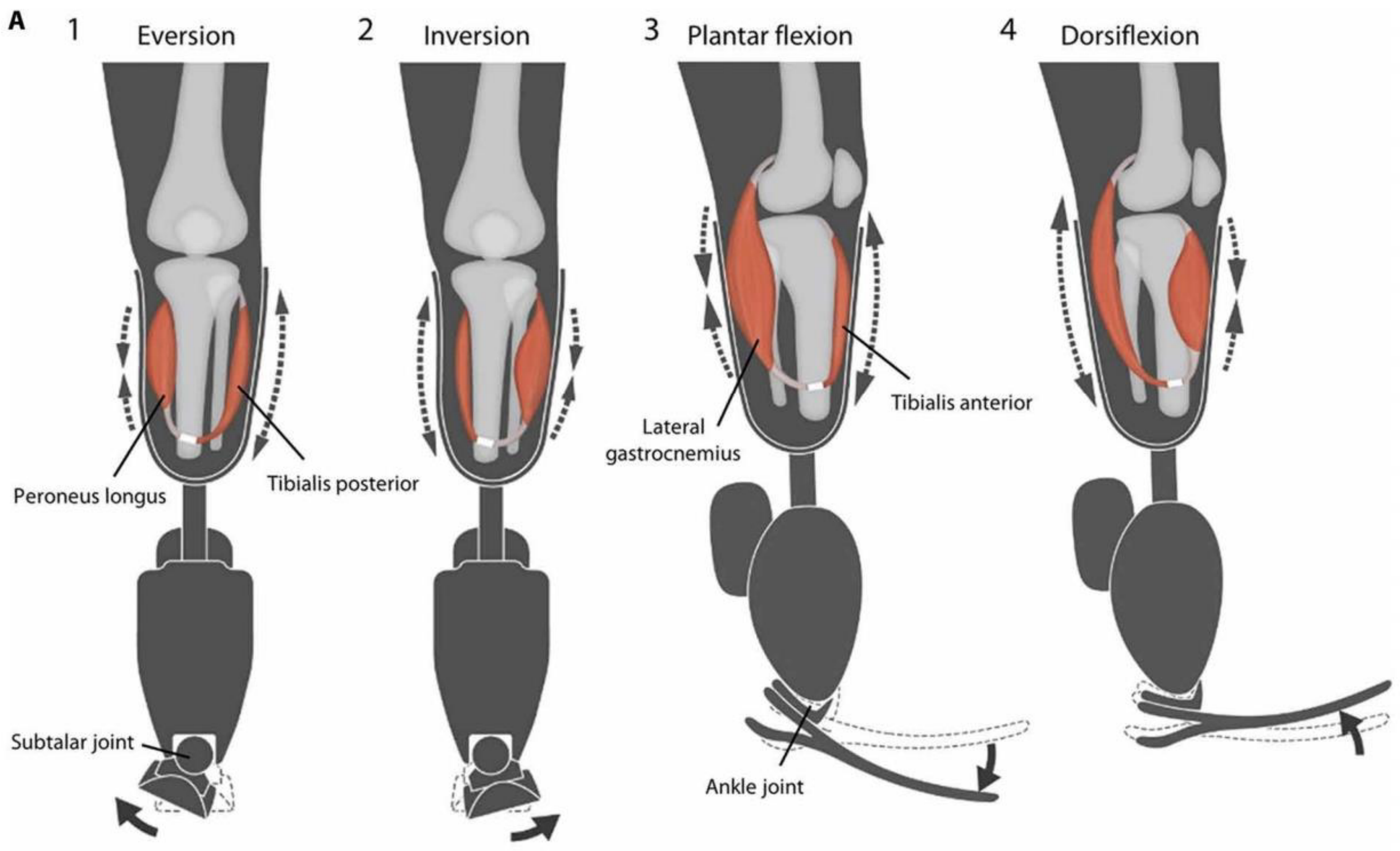

Clites et al., Science Trans Med, 2018

Agonist-antagonist myoneural interface – Closed-loop torque control

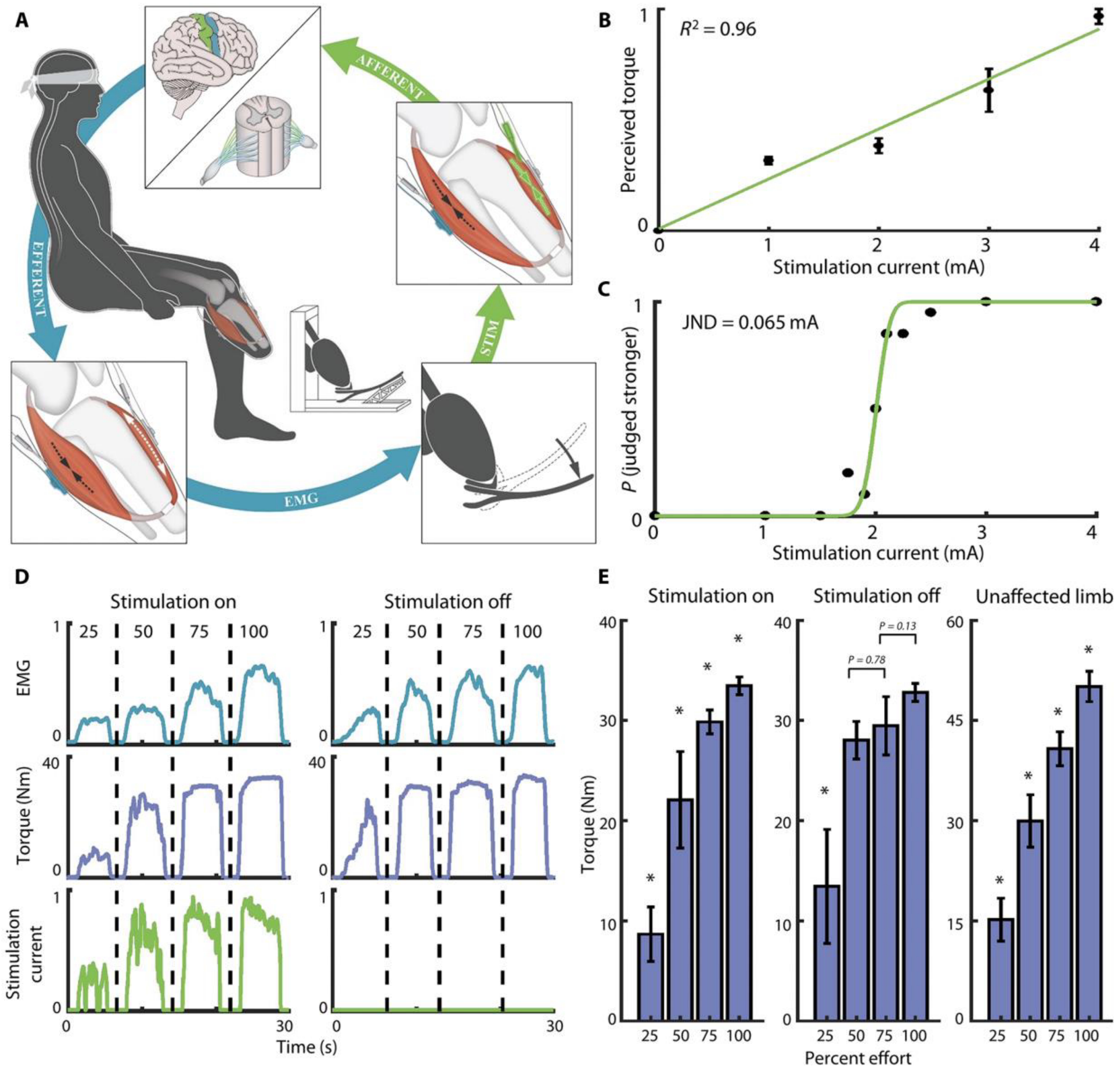

- (A) Schematic of the prosthesis-in-the-loop control architecture, in which afferent feedback of prosthetic joint torque is provided via FES of the antagonist muscle. The patient perceives this stimulation as a natural sensation of ankle torque
- (B) Magnitude estimation of perceived dorsiflexion torque as a function of stimulation current delivered to the tibialis anterior
- (C) Discrimination performance as a function of differences in stimulation current
- (D) Representative sample traces of lateral gastrocnemius EMG (blue), torque (purple), and stimulation current (green) during closed-loop torque control trials for the "stimulation on" (n = 79 total trials) and "stimulation off" (n = 79 total trials) cases
- (E) Summary data for closed-loop torque control trials in each of the stimulation on (n = 79 trials), stimulation off (n = 79 trials), and "unaffected limb" (n = 80 trials) cases

Clites et al., Science Trans Med, 2018

Human touch system

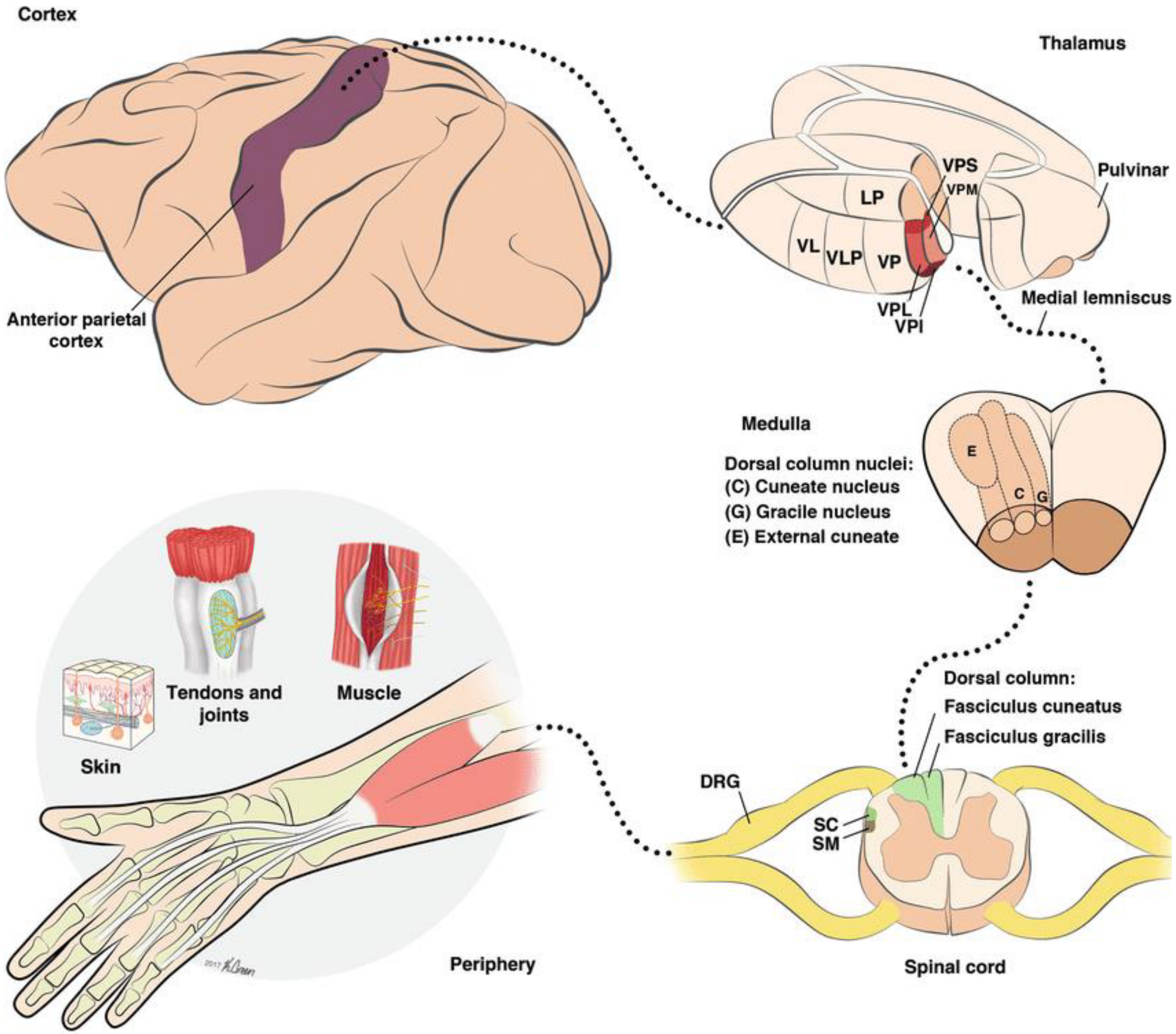

Spinal cord stimulation

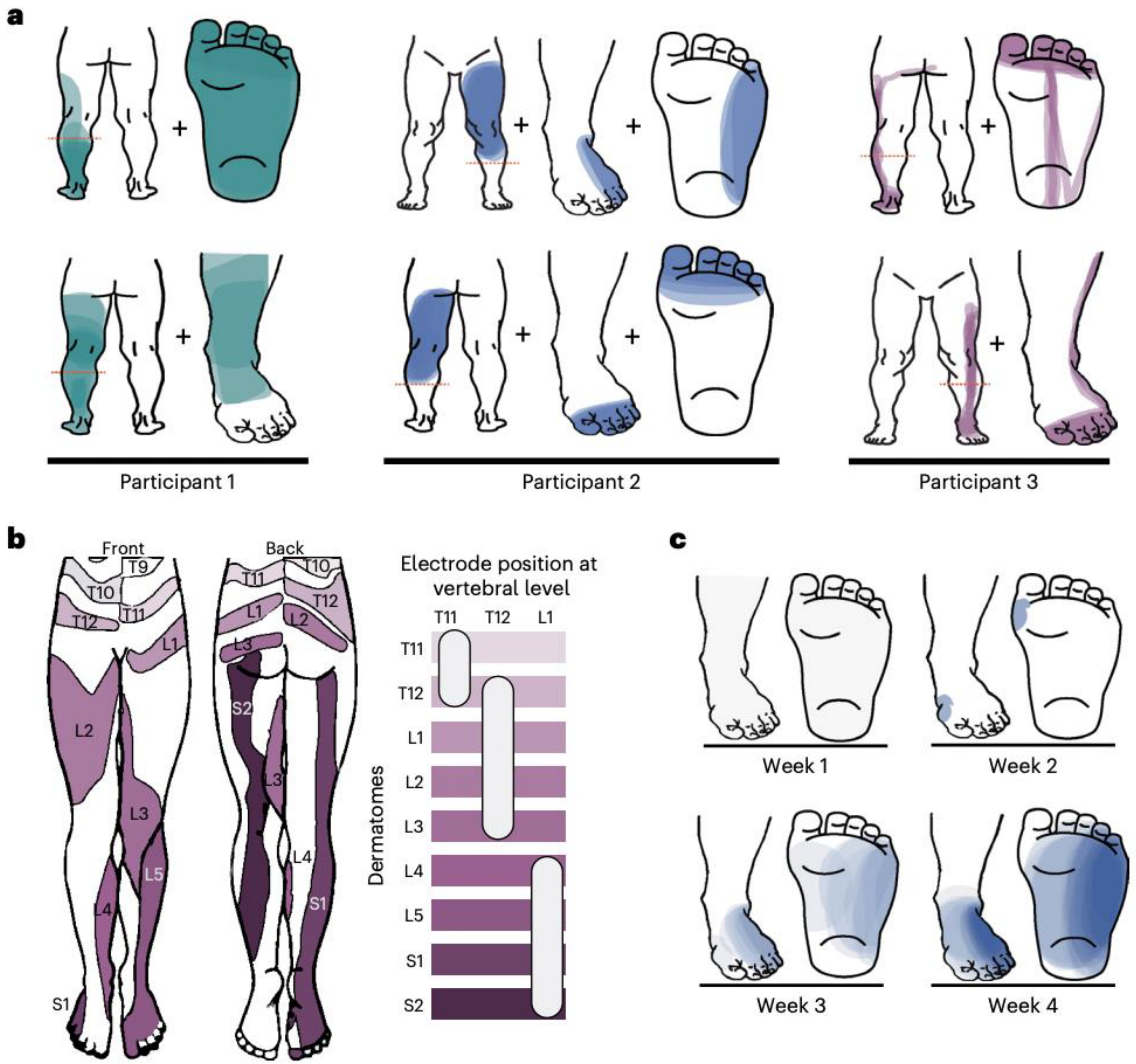

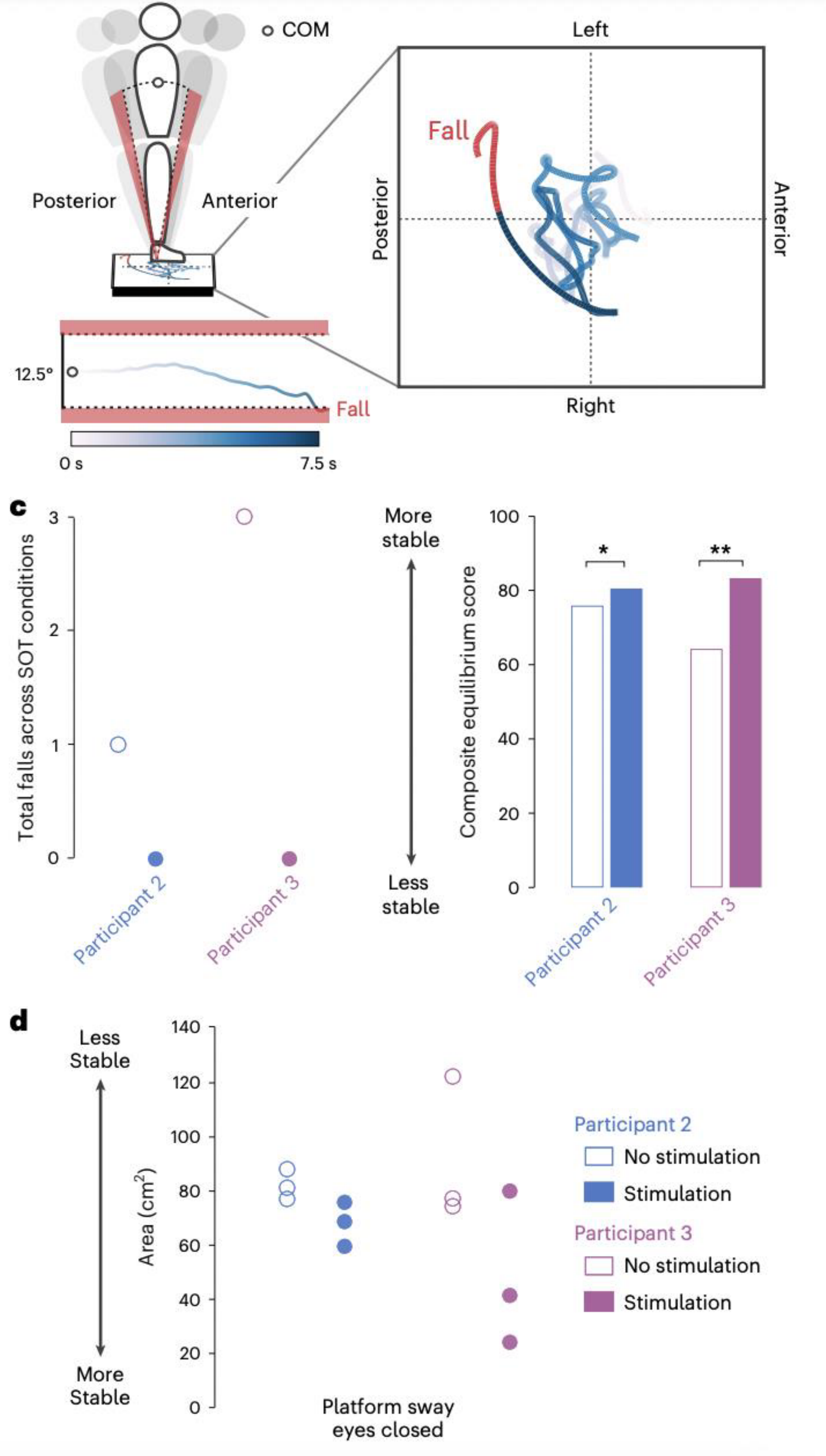

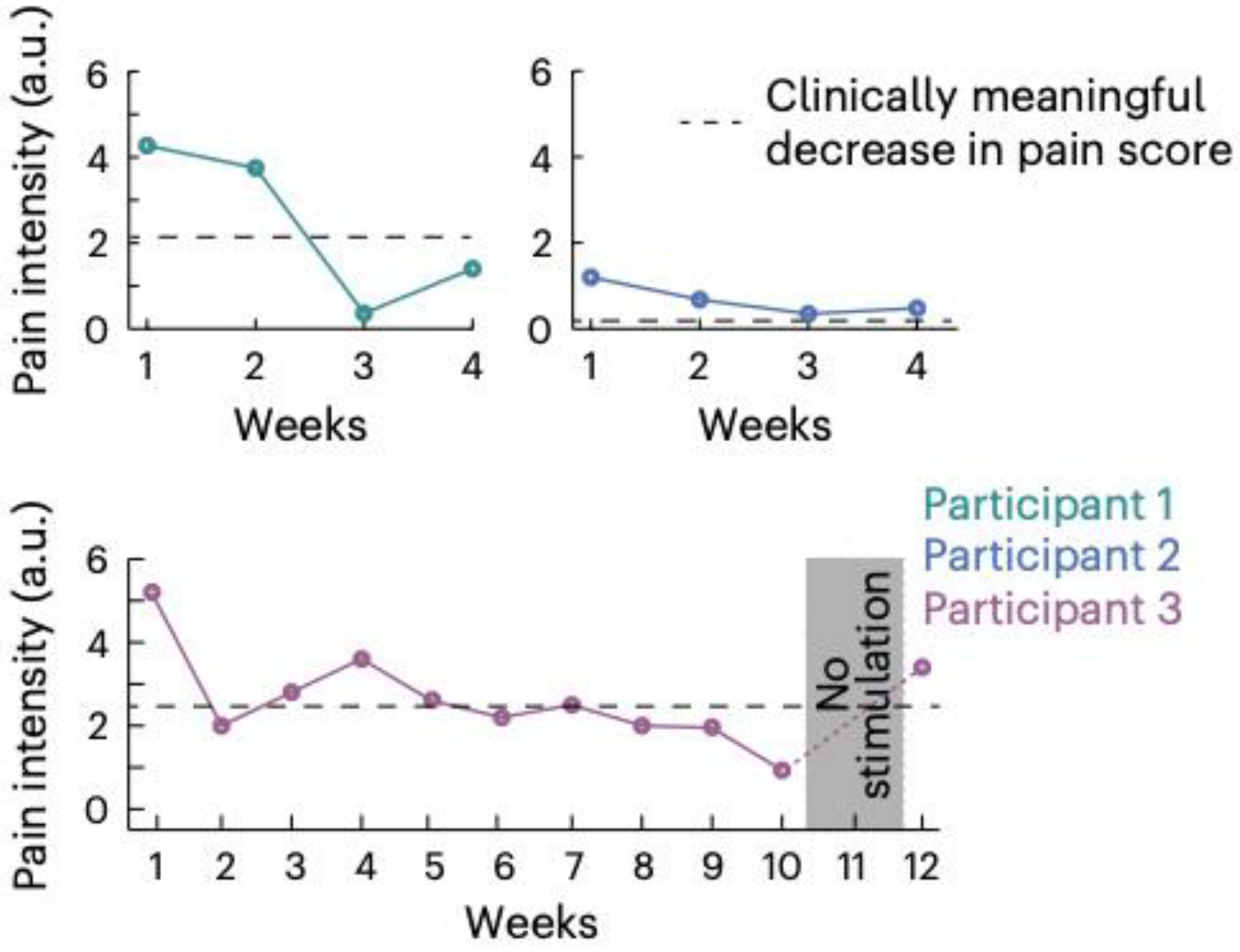

Performance good (maybe a bit less than PNS stimulation) BUT with a clinically accepted surgical procedure

Stimulation of the cuneate for sensory feedback

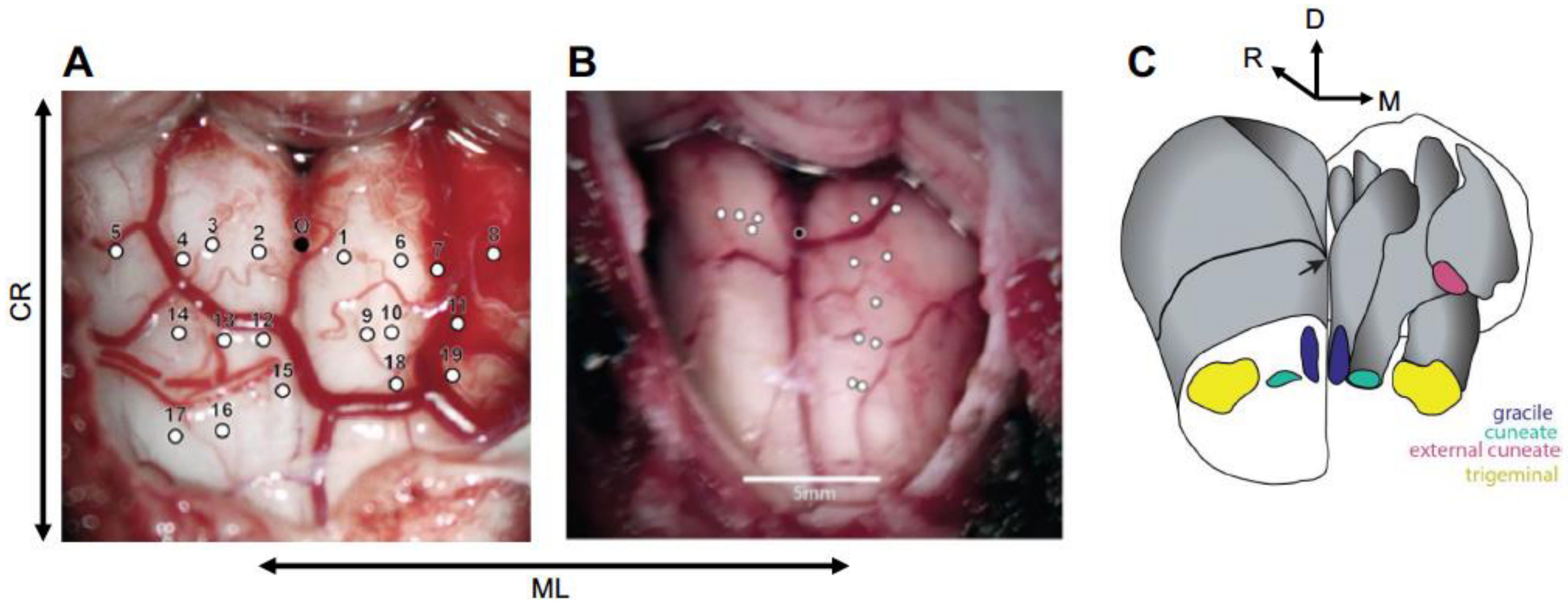

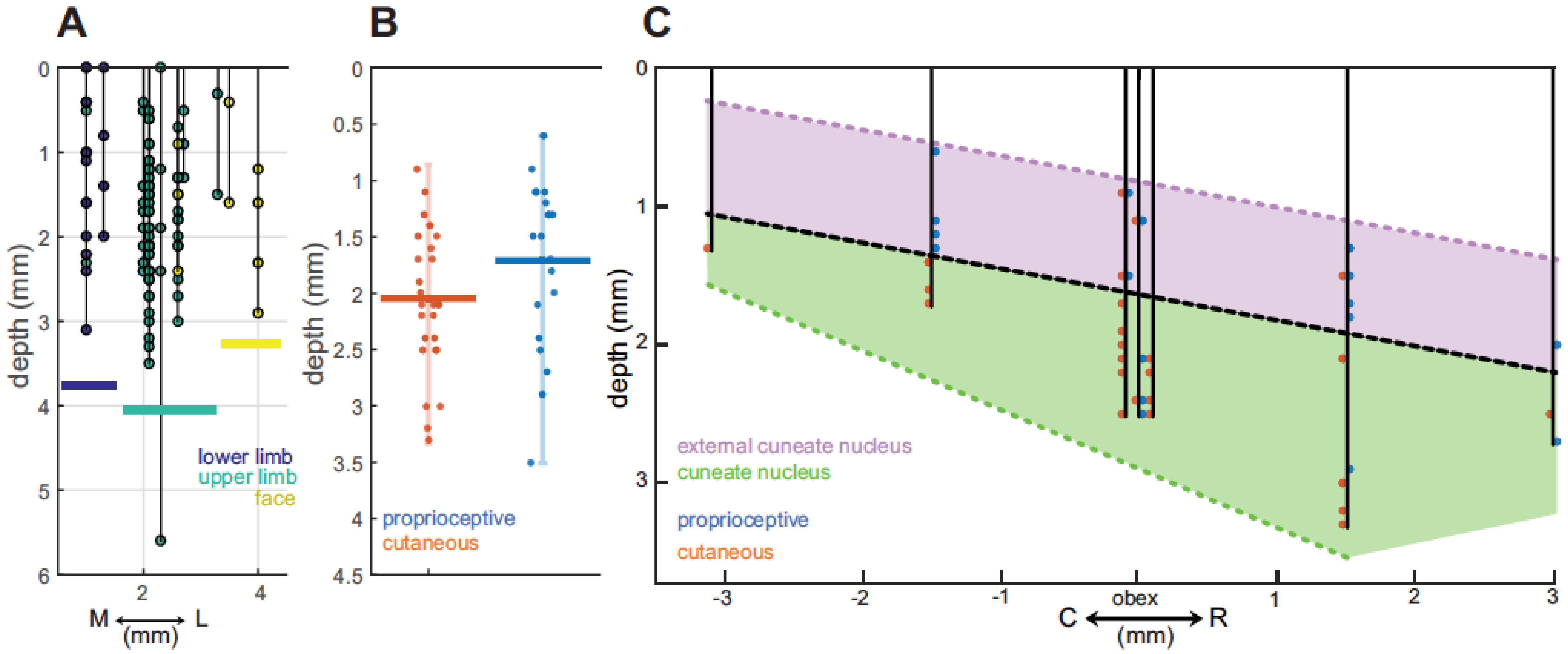

Stimulation of the cuneate for sensory feedback

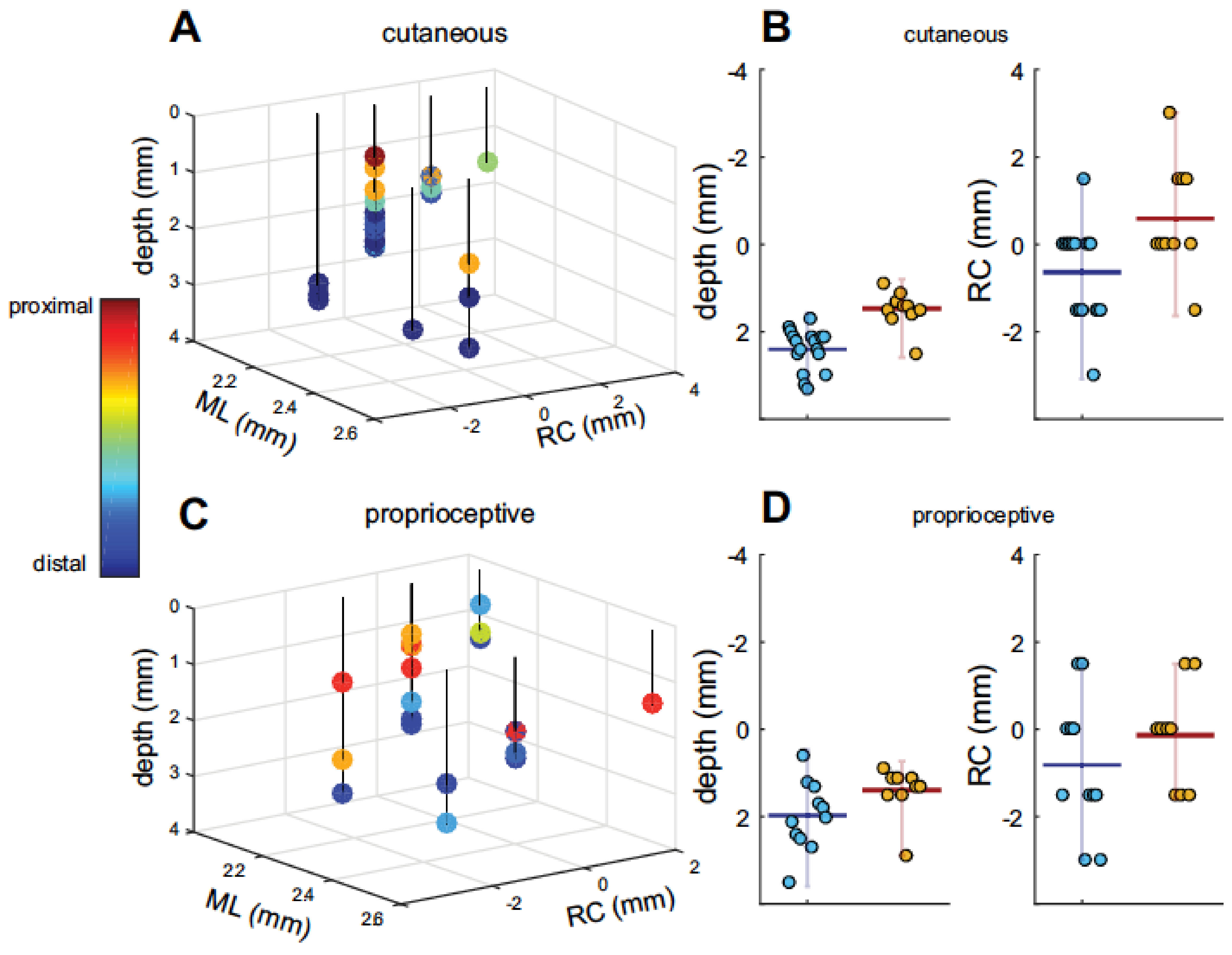

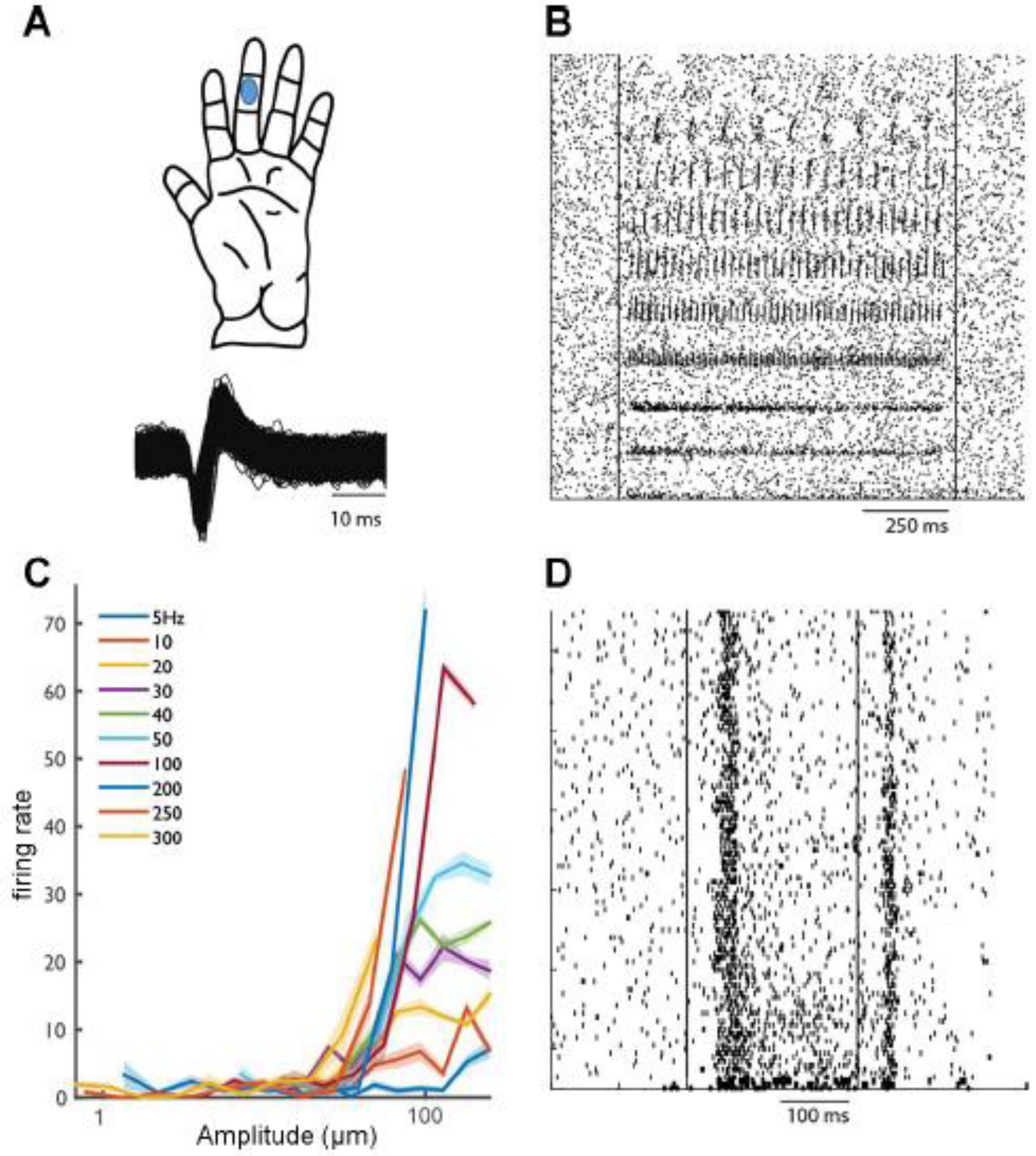

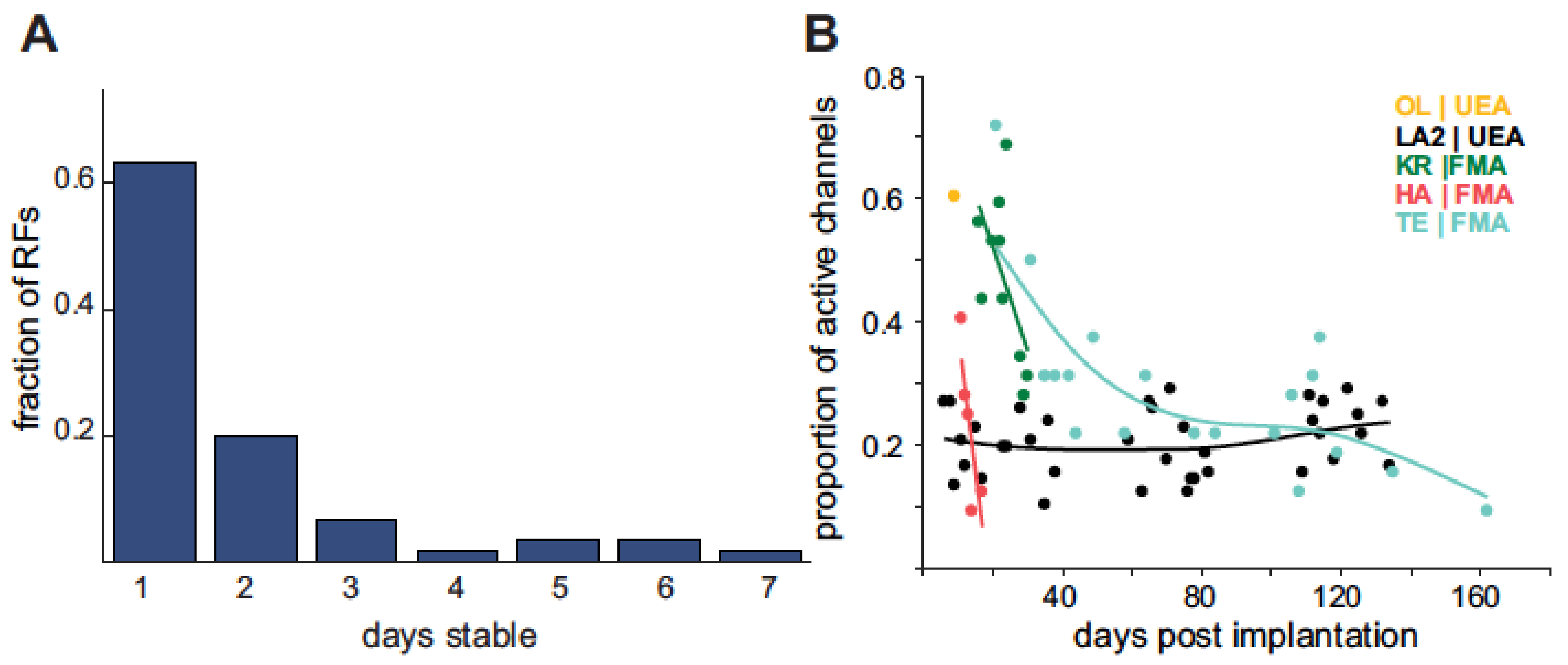

Brain-to-machine-to-brain interface

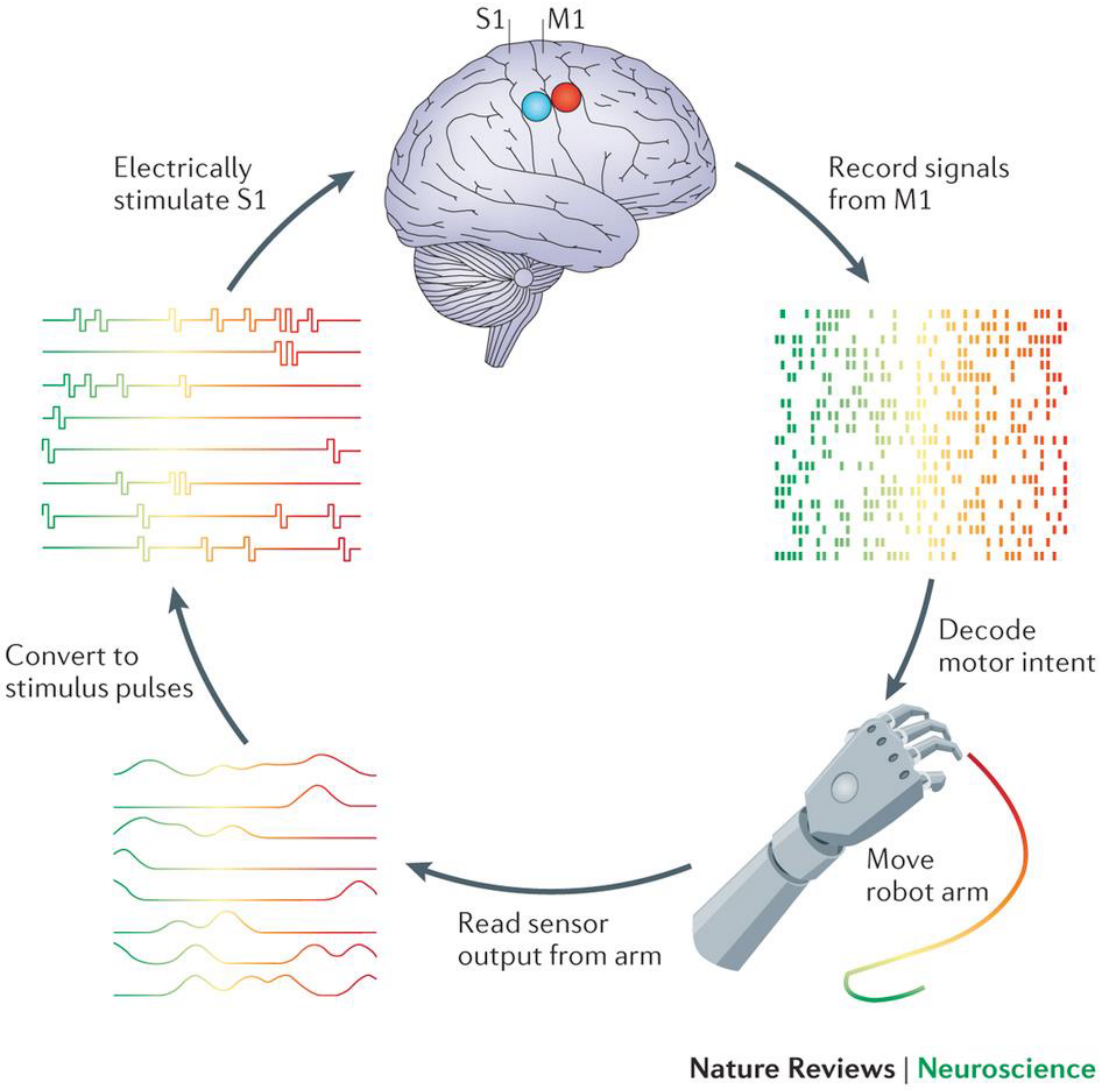

Brain-to-machine-to-brain interface

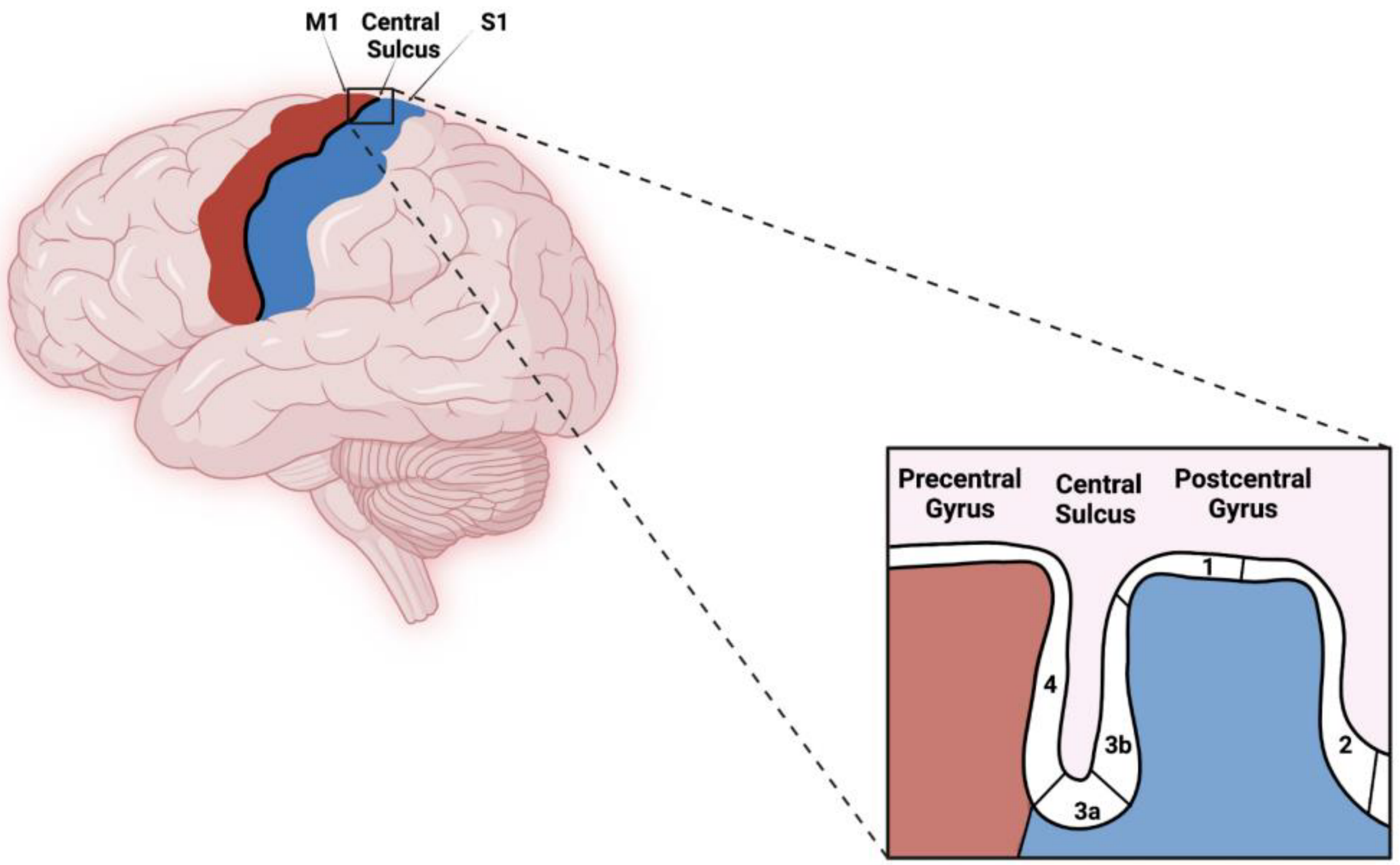

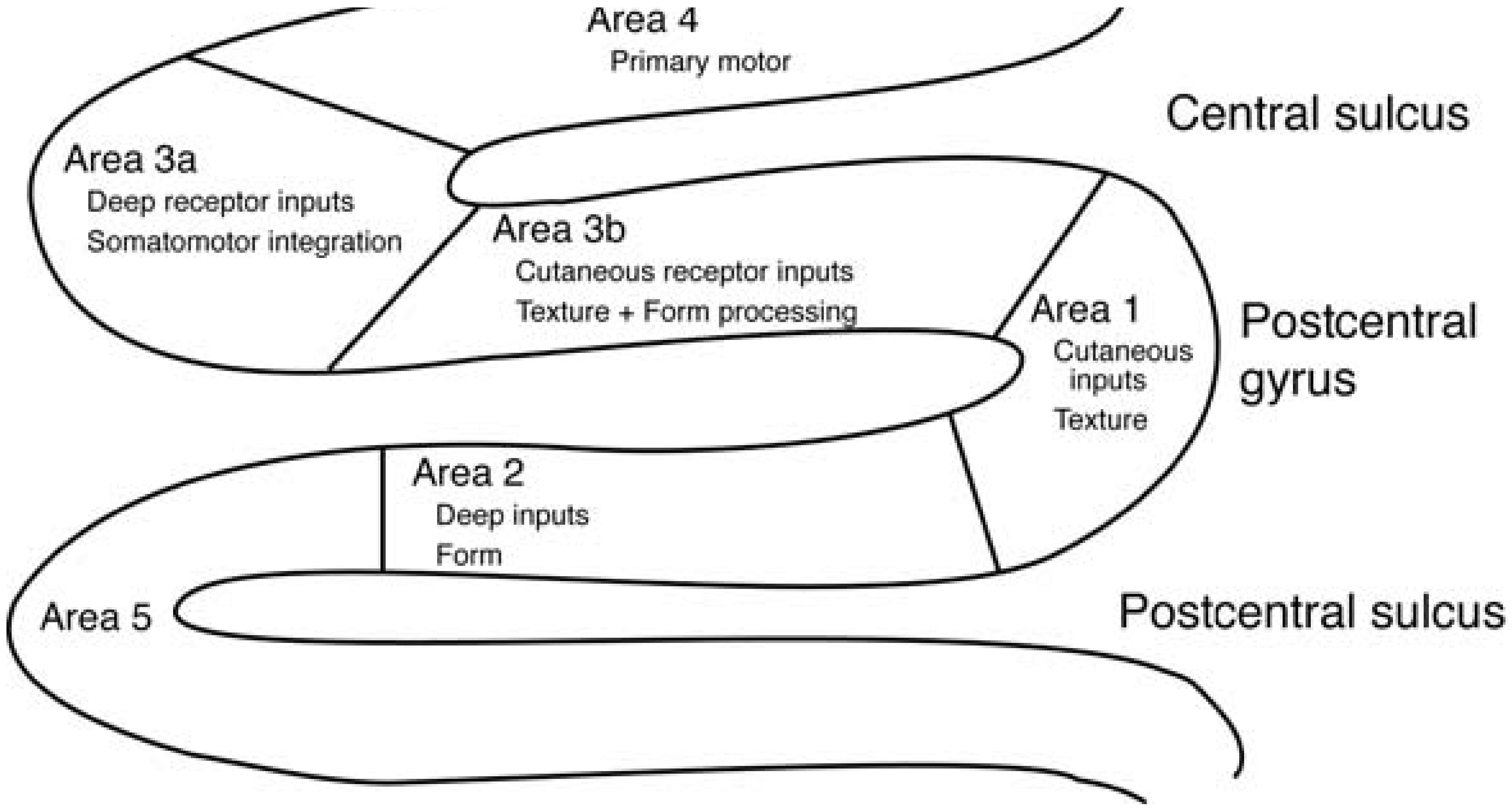

The somatosensory homunculus comprises four body maps, one each in Brodmann areas 3a, 3b, 1 and 2, which exhibit proprioceptive responses (area 3a), cutaneous responses (areas 3b and 1) or both (area 2).

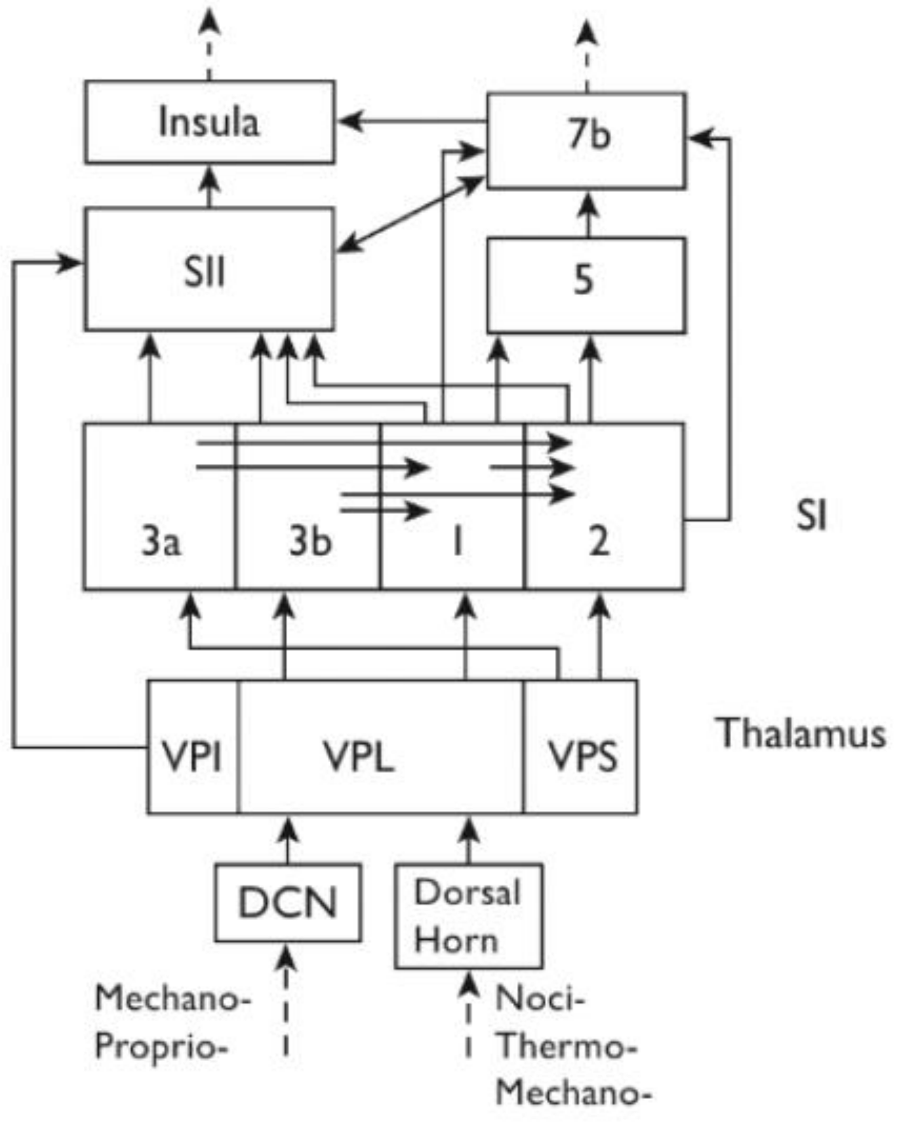

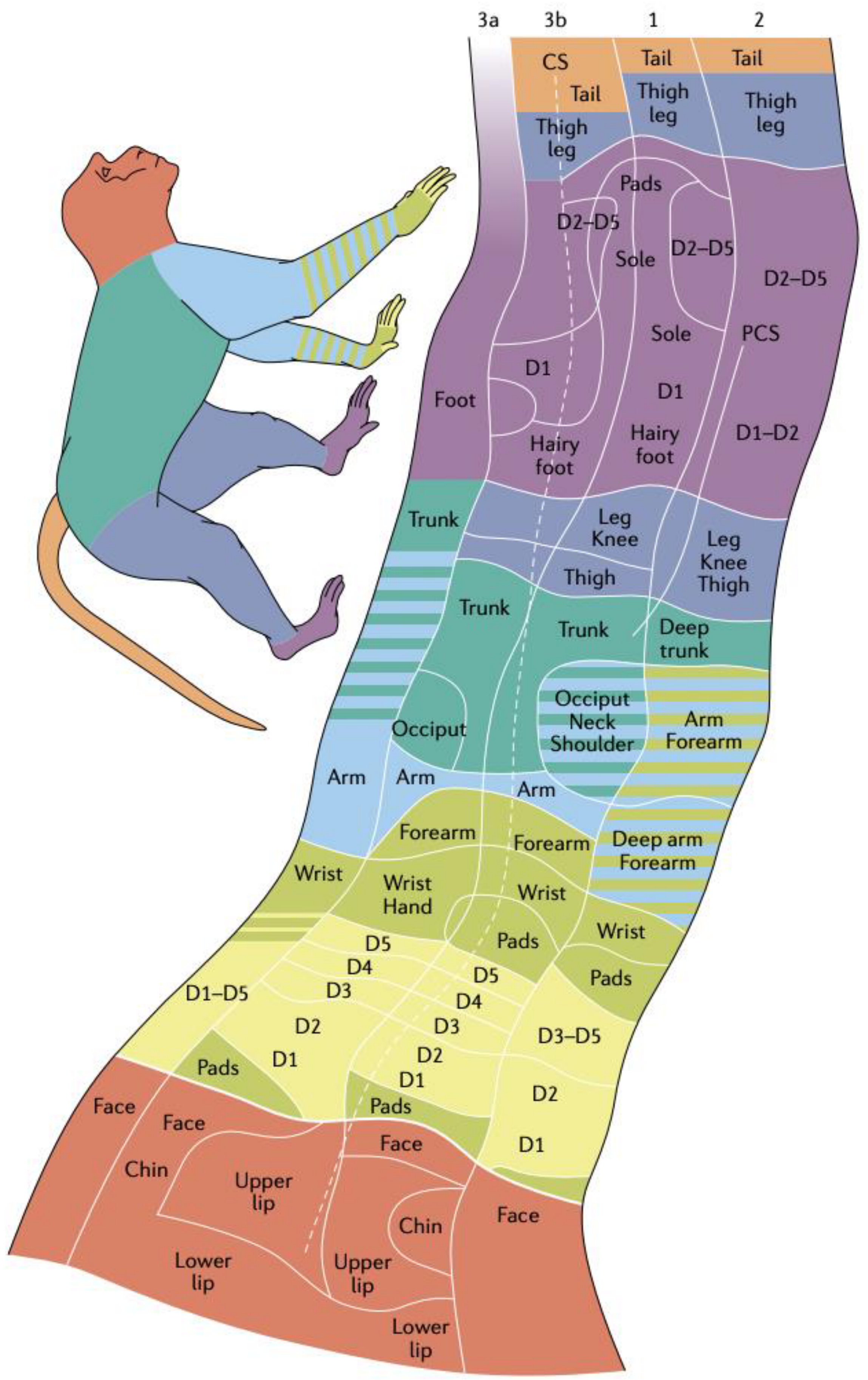

Sobinov and Bensmaia
Nat Rev Neuro, 2021

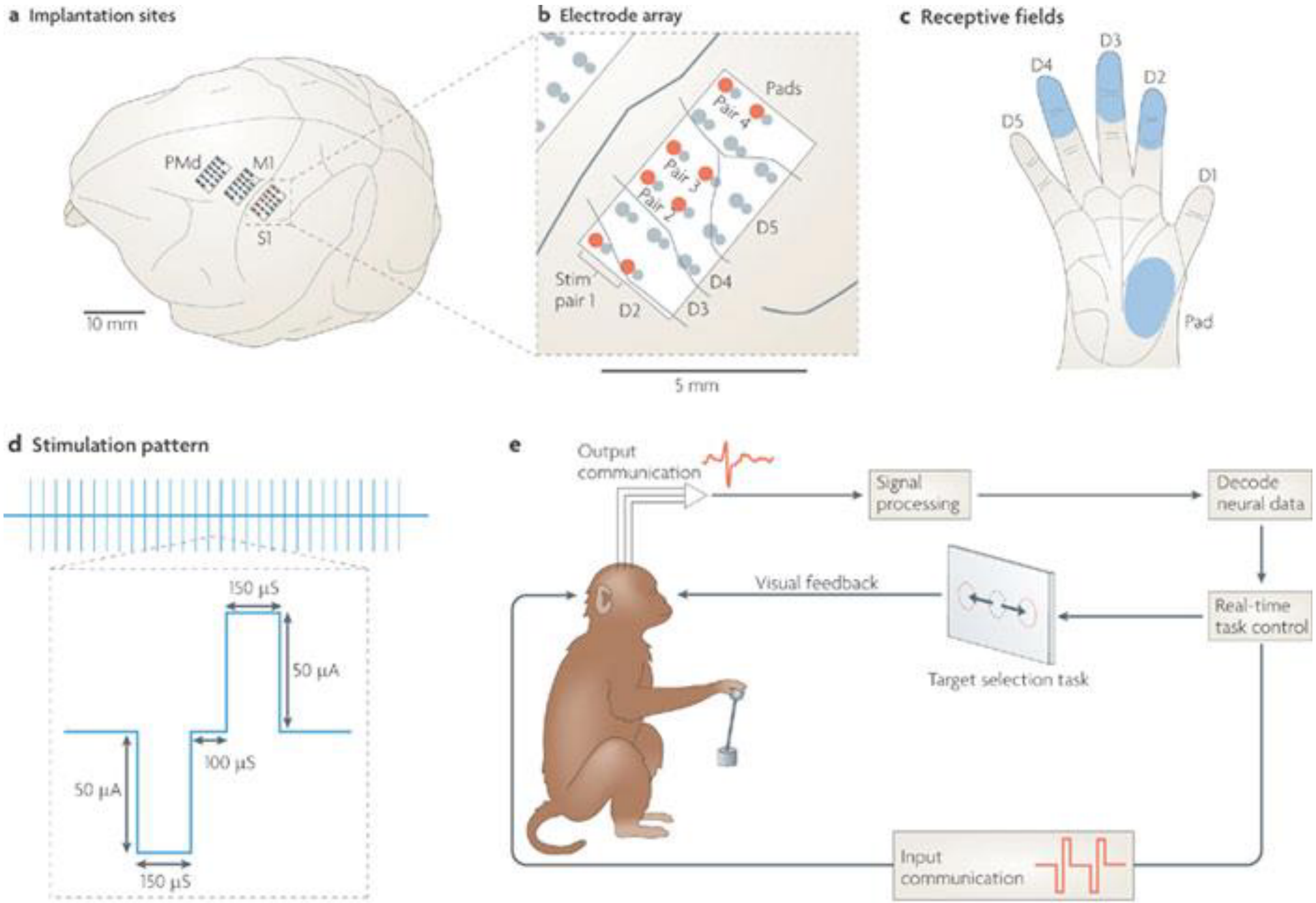

Nature Reviews | Neuroscience

Intracortical sensory feedback

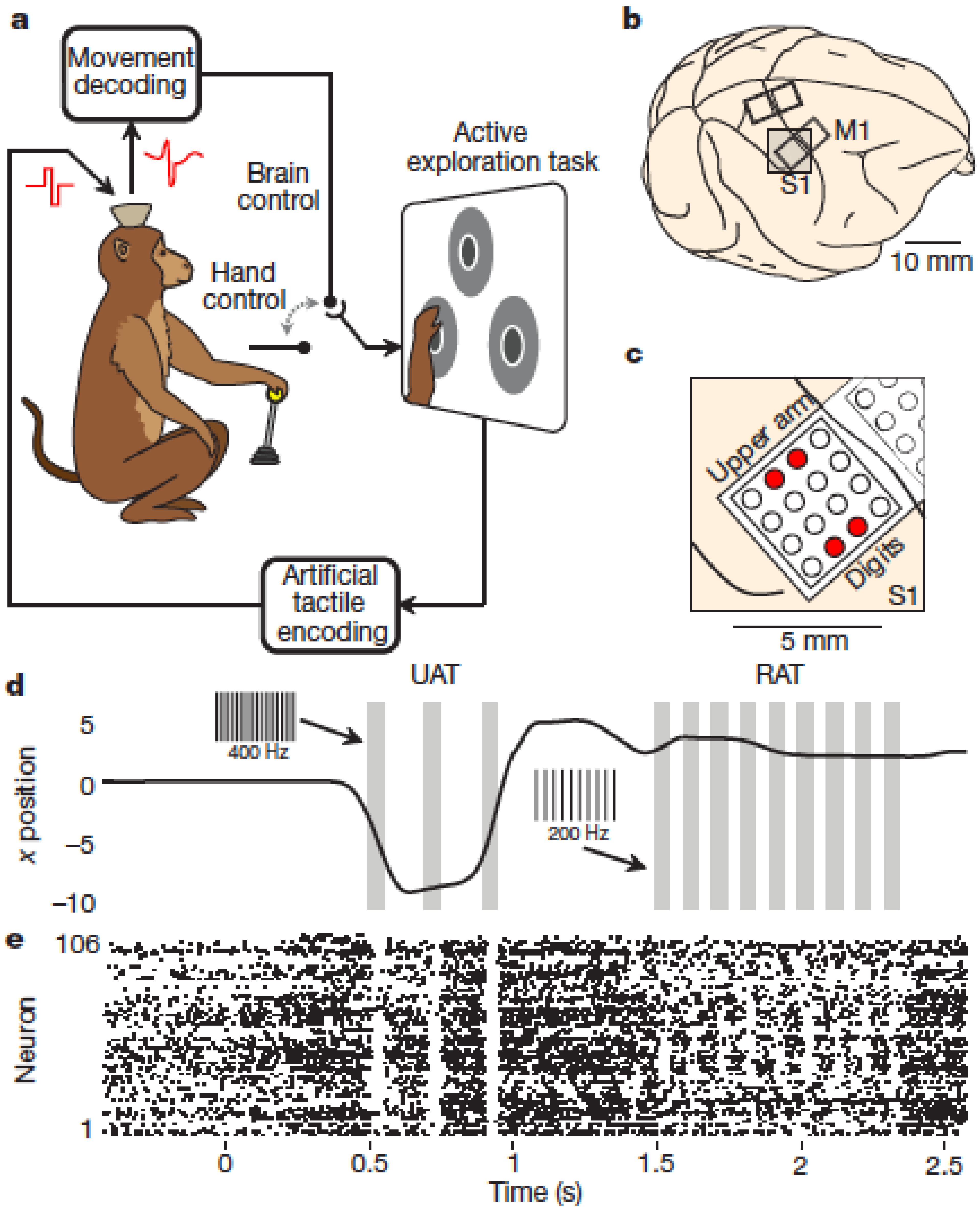

Intracortical sensory feedback is possible but the performance are still limited

O'Doherty et al., 2011

Brain-to-machine-to-brain interface in a quadriplegic subject

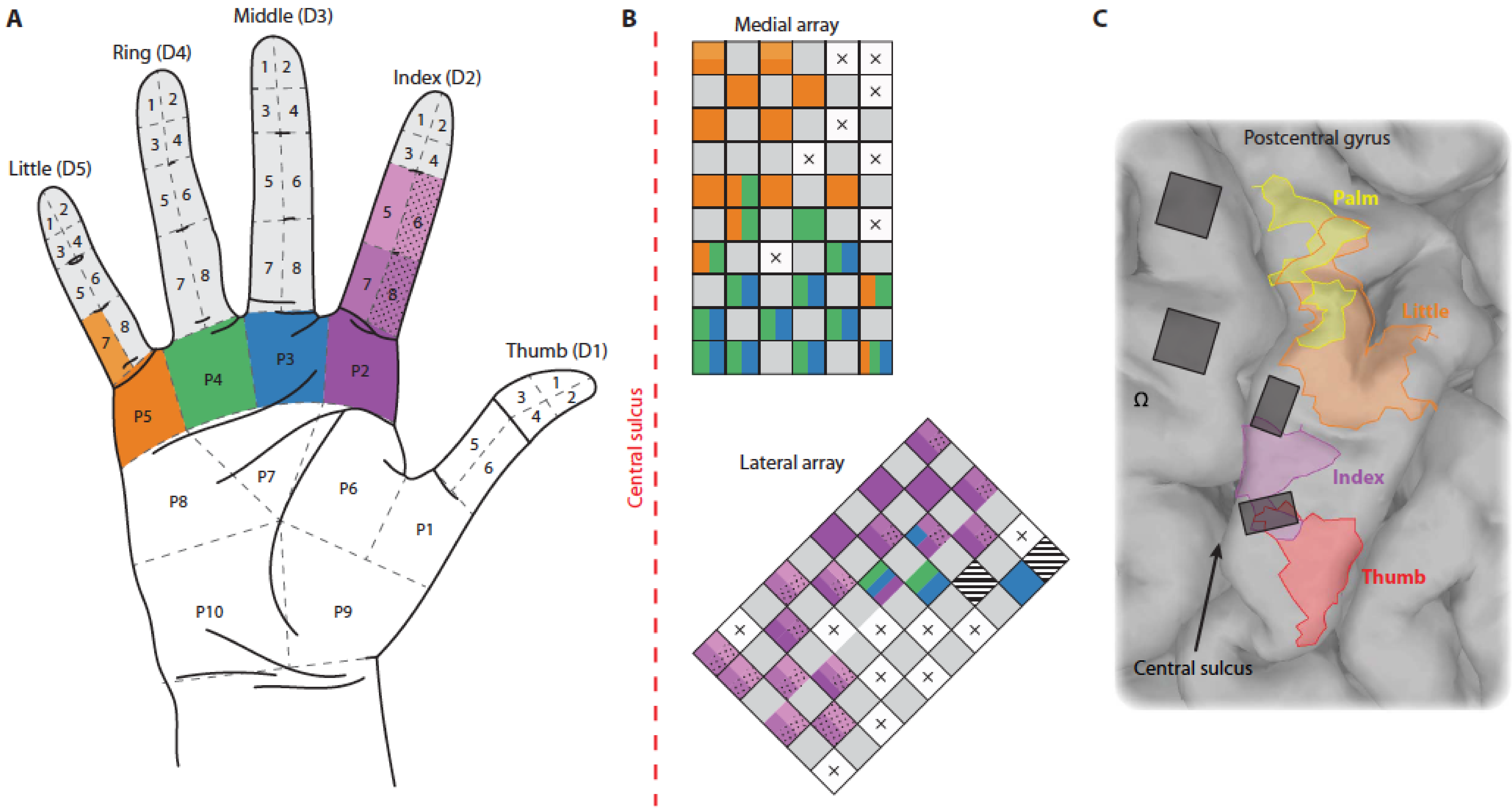

Brain-to-machine-to-brain interface in a quadriplegic subject

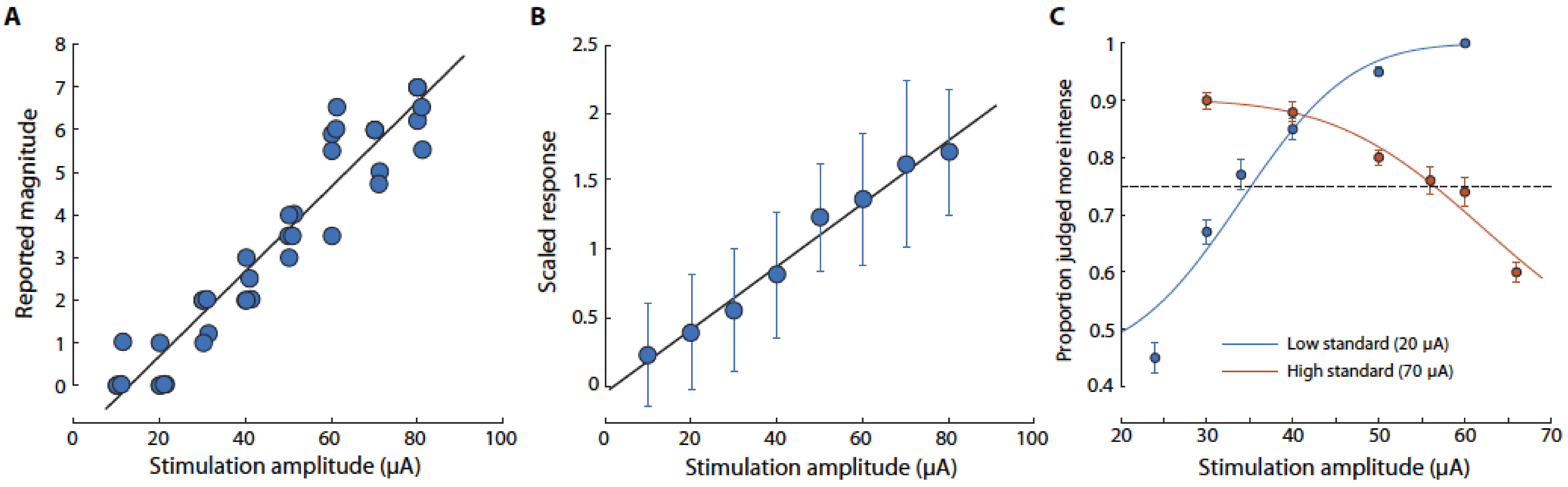

Table 2. Accuracy of prosthetic finger discrimination. The percentage of times that sensations were reported to originate from a specific finger (columns) when each prosthetic finger was touched (rows).

	Reported D2	Reported D3	Reported D4	Reported D5
Actual D2	96.9 ± 7.2%	1.5 ± 5.3%	1.5 ± 5.3%	0%
Actual D3	0%	73.5 ± 18.1%	21.9 ± 18.4%	0%
Actual D4	0%	18.5 ± 22.8%	73.1 ± 24.6%	6.5 ± 16.8%
Actual D5	0%	3.1 ± 7.2%	3.1 ± 10.7%	93.9 ± 12.1%

Brain-to-machine-to-brain interface in a quadriplegic subject

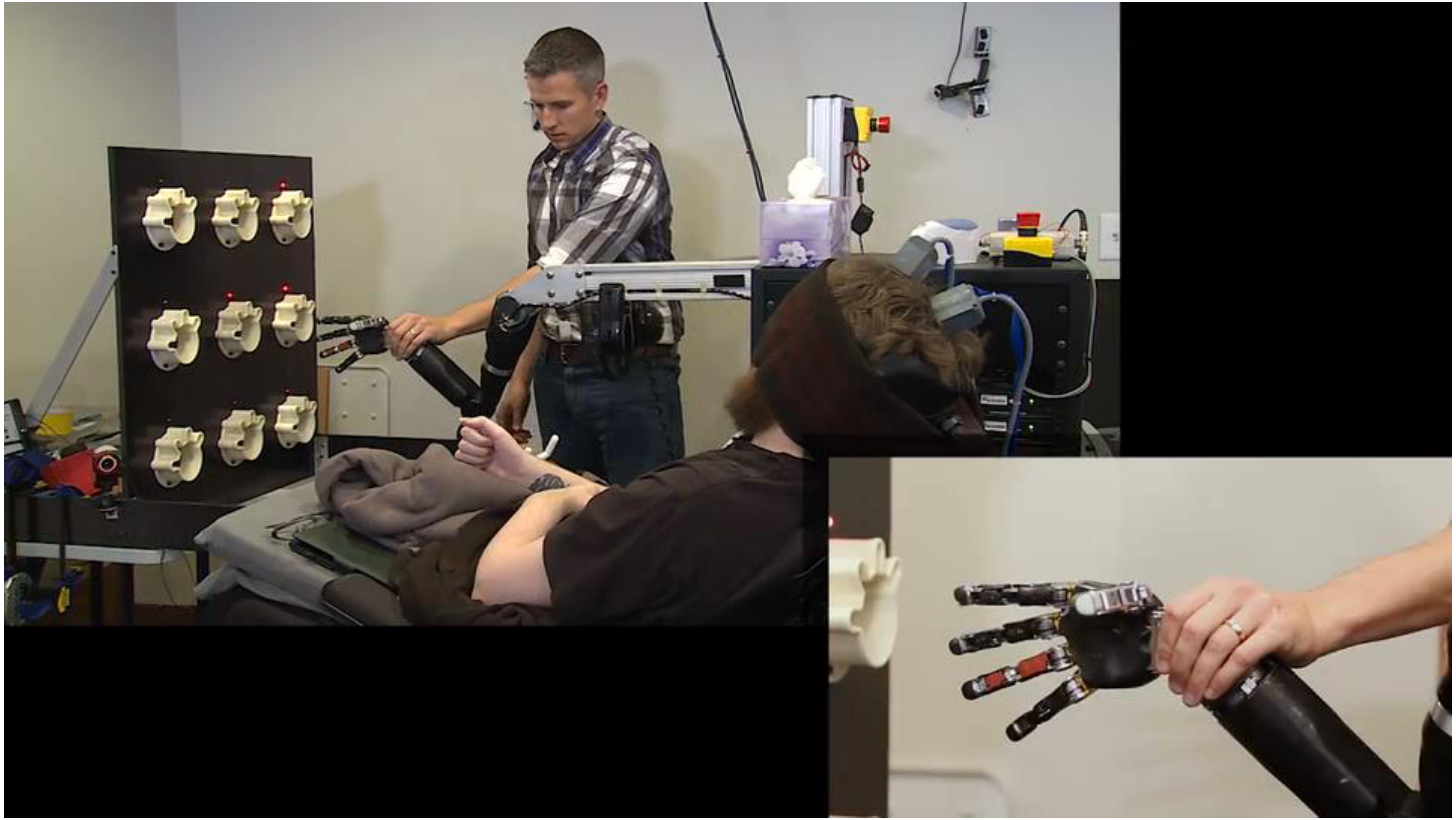

Closed-loop BMI

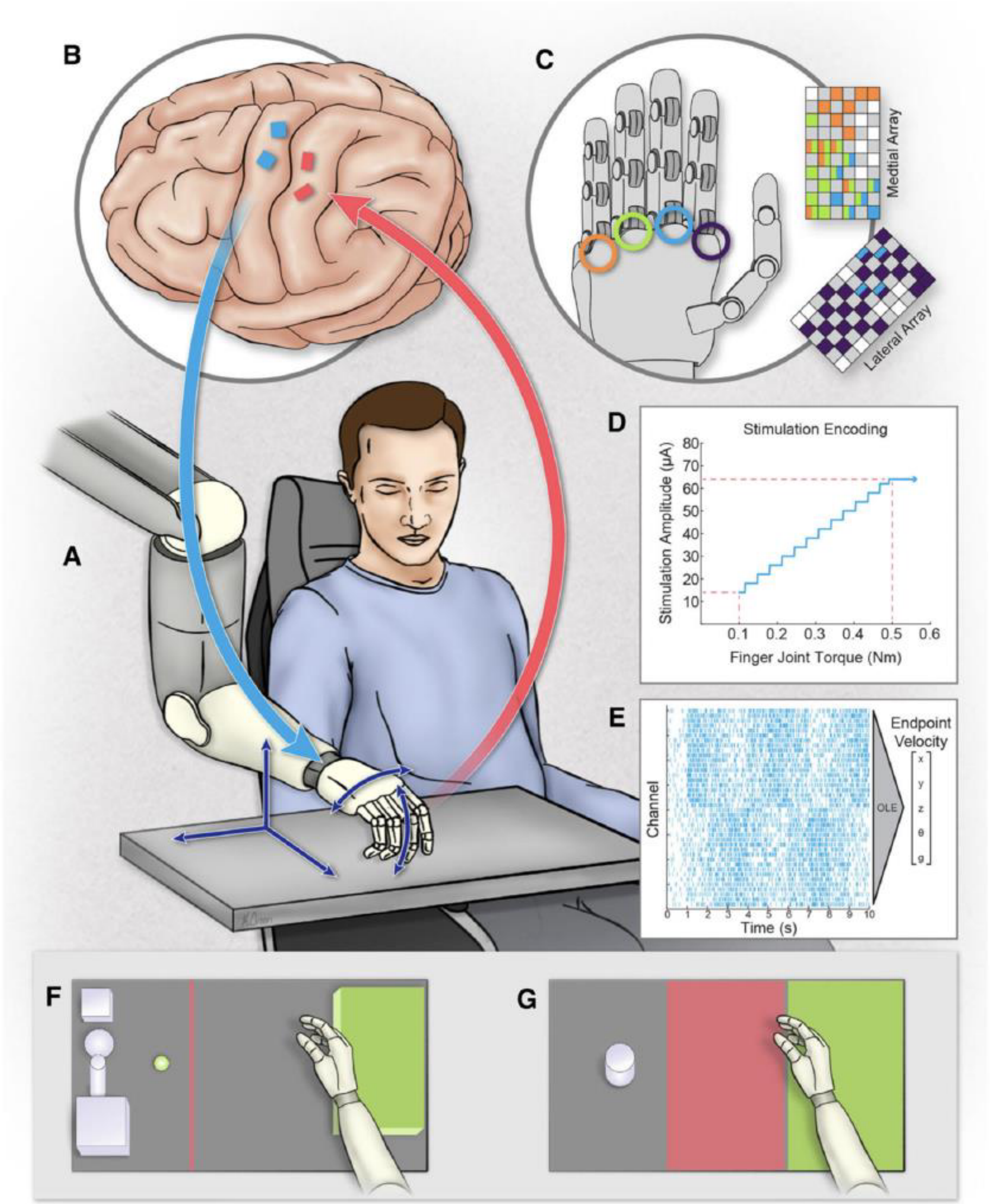

Article

https://doi.org/10.1038/s41467-023-43140-2

Microstimulation of human somatosensory cortex evokes task-dependent, spatially patterned responses in motor cortex

Received: 30 September 2022

Accepted: 1 November 2023

Published online: 10 November 2023

Check for updates

Natalya D. Shelchkova[1,13], John E. Downey[2,13], Charles M. Greenspon[2,13], Elizaveta V. Okorokova[1], Anton R. Sobinov[2], Ceci Verbaarschot[3,4], Qinpu He[1], Caleb Sponheim[1], Ariana F. Tortolani[1], Dalton D. Moore[1], Matthew T. Kaufman[1,2,5], Ray C. Lee[6], David Satzer[7], Jorge Gonzalez-Martinez[8], Peter C. Warnke[5,7], Lee E. Miller[9], Michael L. Boninger[3,10,11], Robert A. Gaunt[3,10,11,12], Jennifer L. Collinger[3,10,11,12], Nicholas G. Hatsopoulos[1,2,5] & Sliman J. Bensmaia[1,2,5]

Flesher et al., Science, 2021

Closed-loop BMI

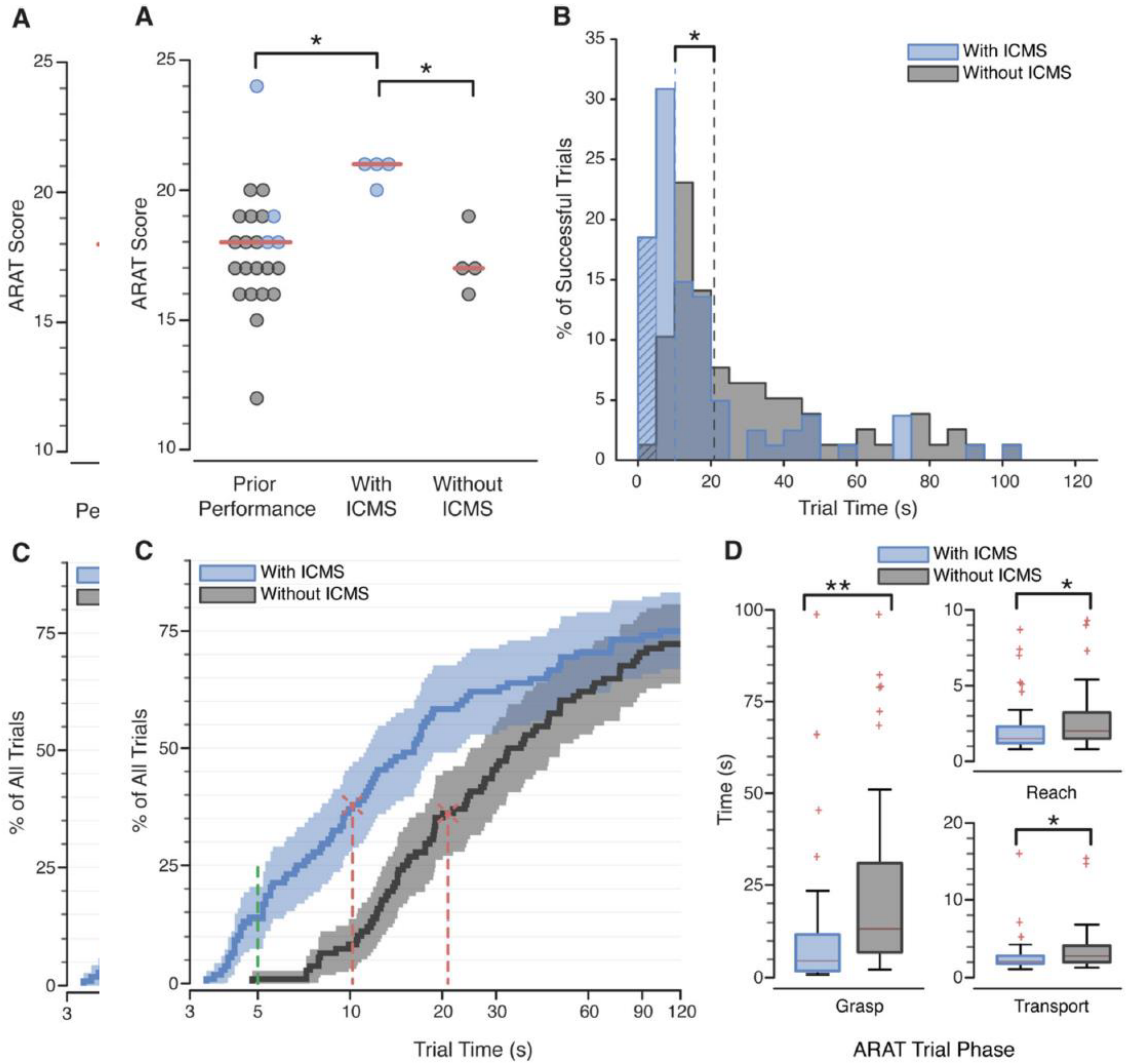

Closed-loop feedback BMI shows a significant improvement in motor performance

Flesher et al., Science, 2021

Biomimetic cortical stimulation

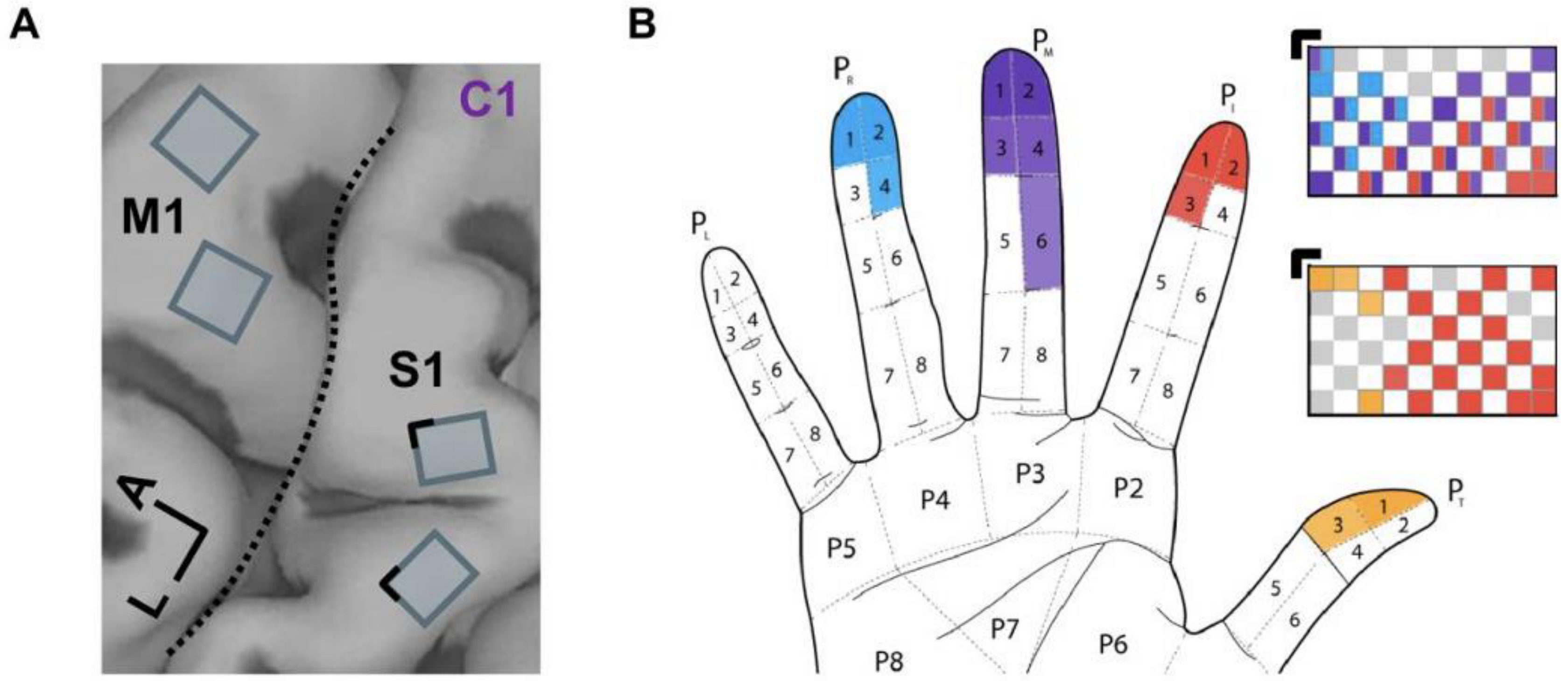

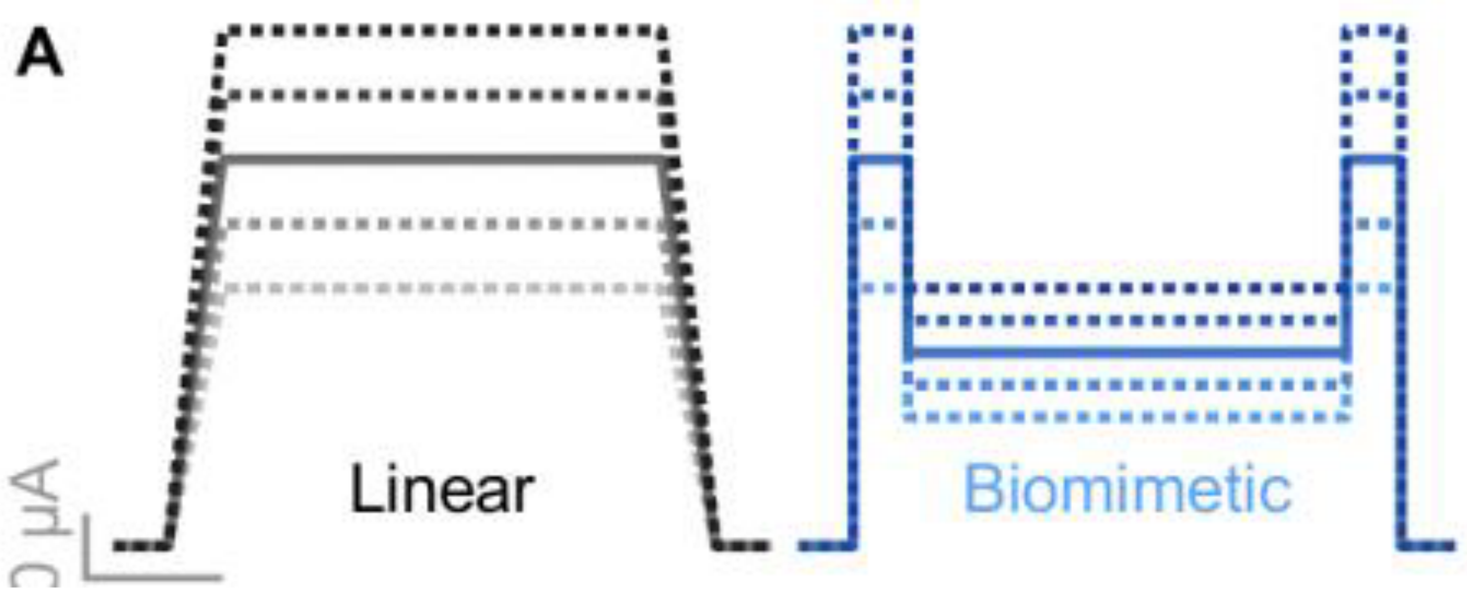

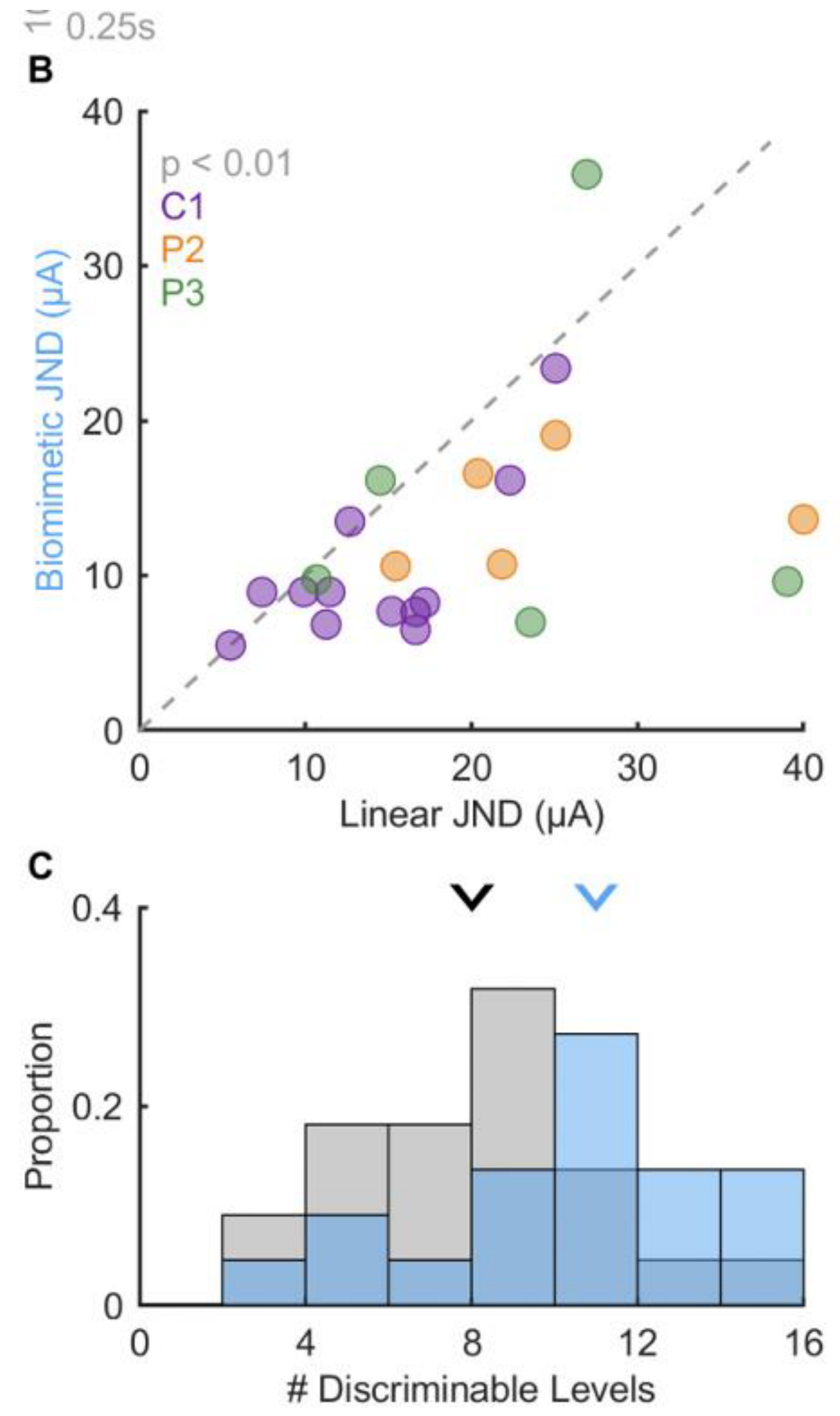

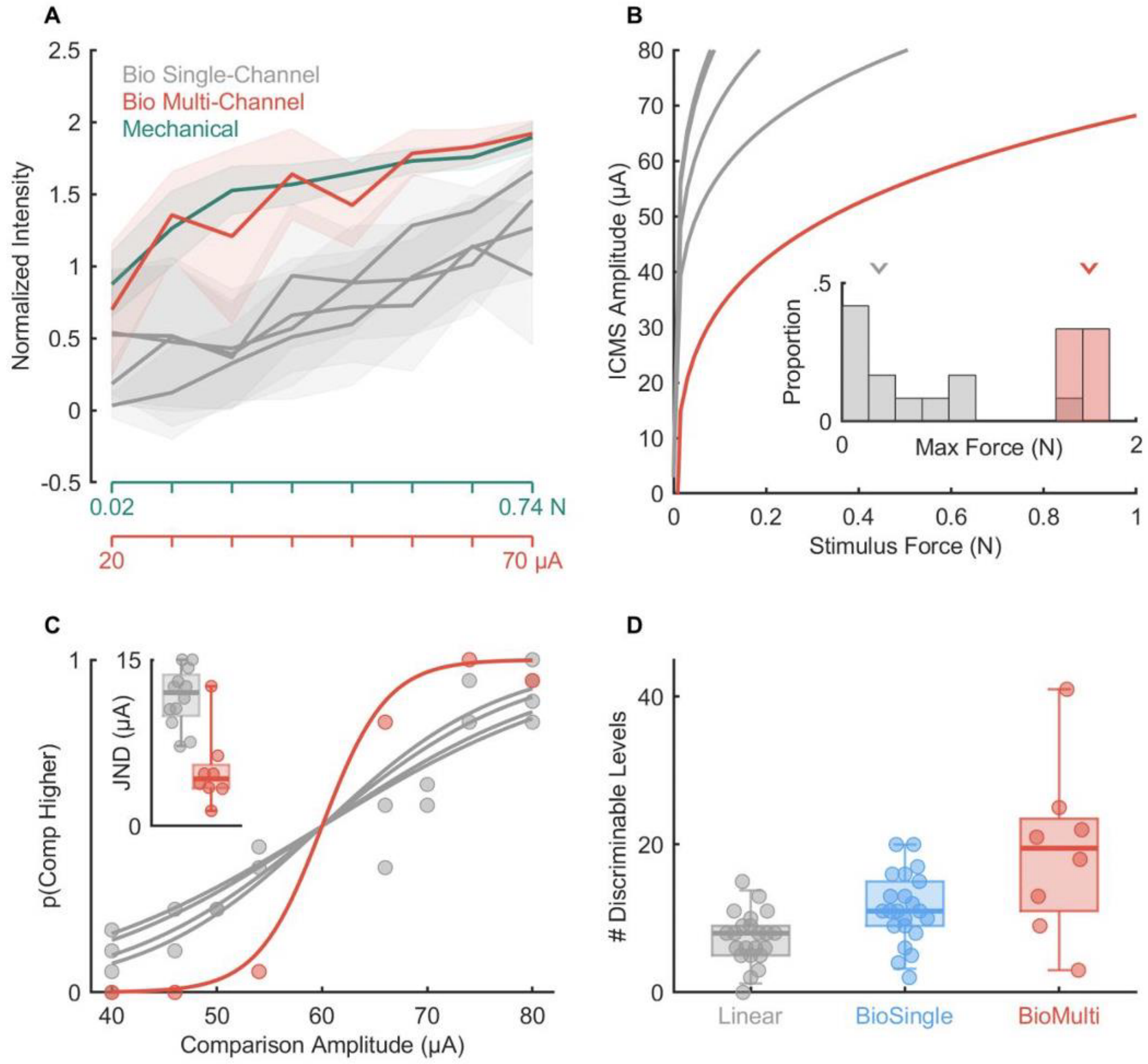

Greenspon et al., under review

Biomimetic cortical stimulation

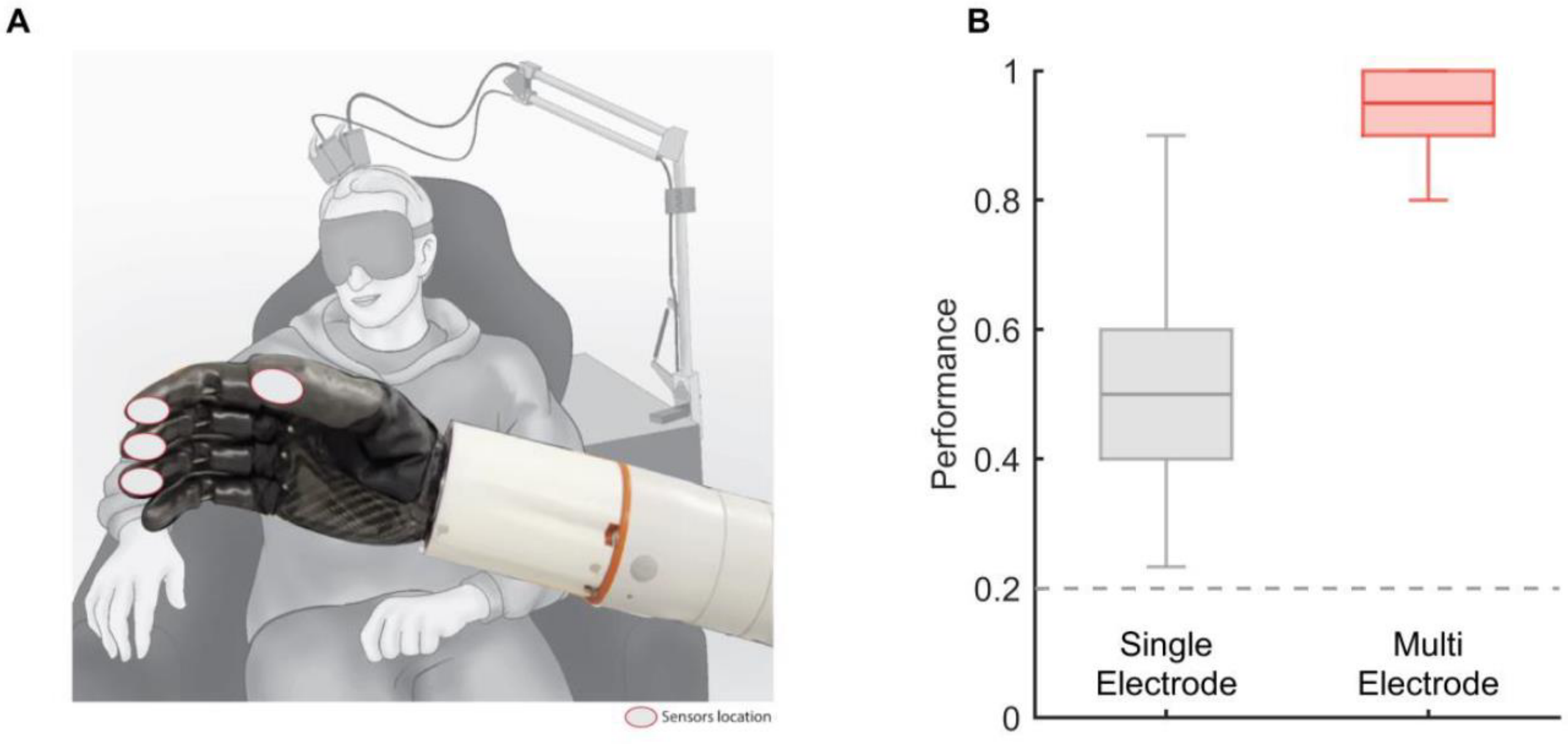

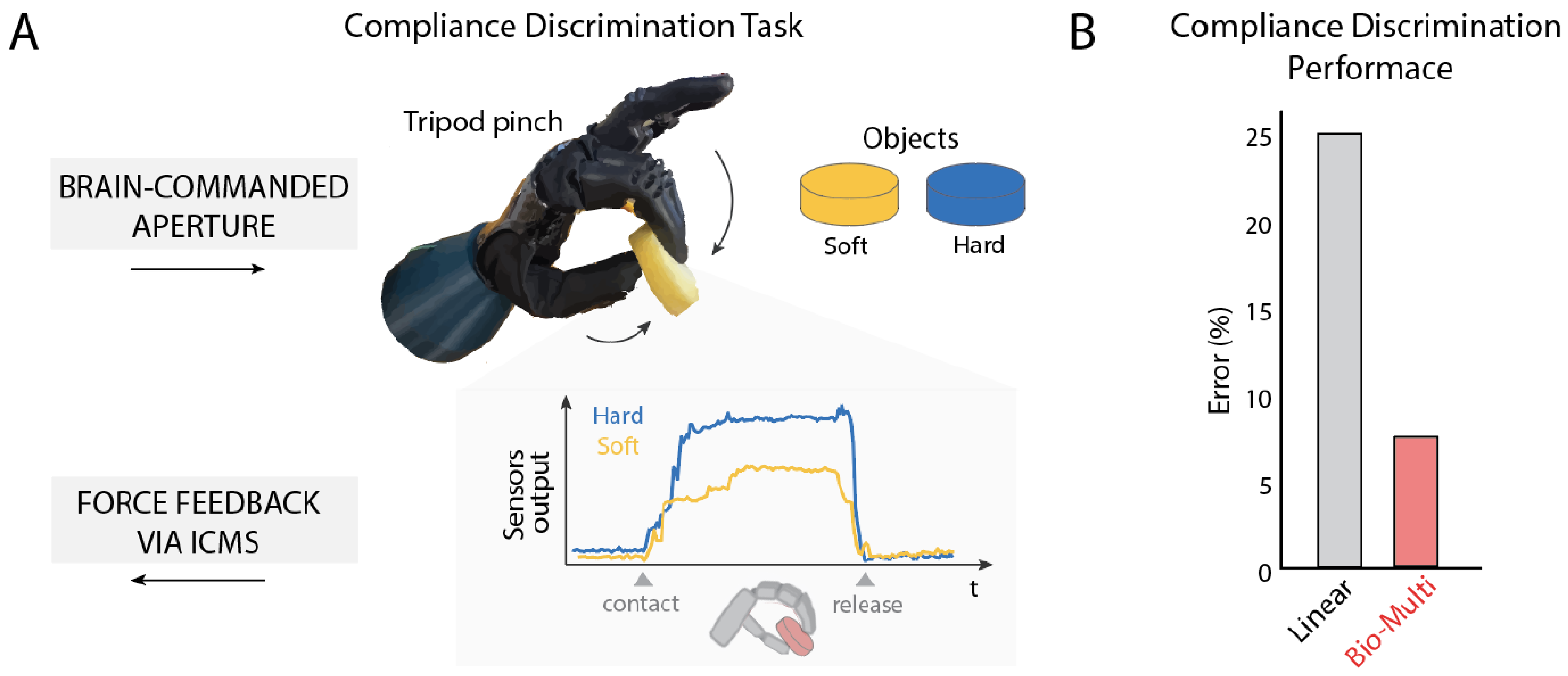

Greenspon et al., under review

Muscular control of artificial limbs

Hand prosthesis – Proportional control

- N antagonist muscles are used to control 1 degree of freedom of the prosthesis (hand opening/closing). Often biceps/triceps or wrist extension/flexion
- An increased number of required movements makes very difficult to use this approach

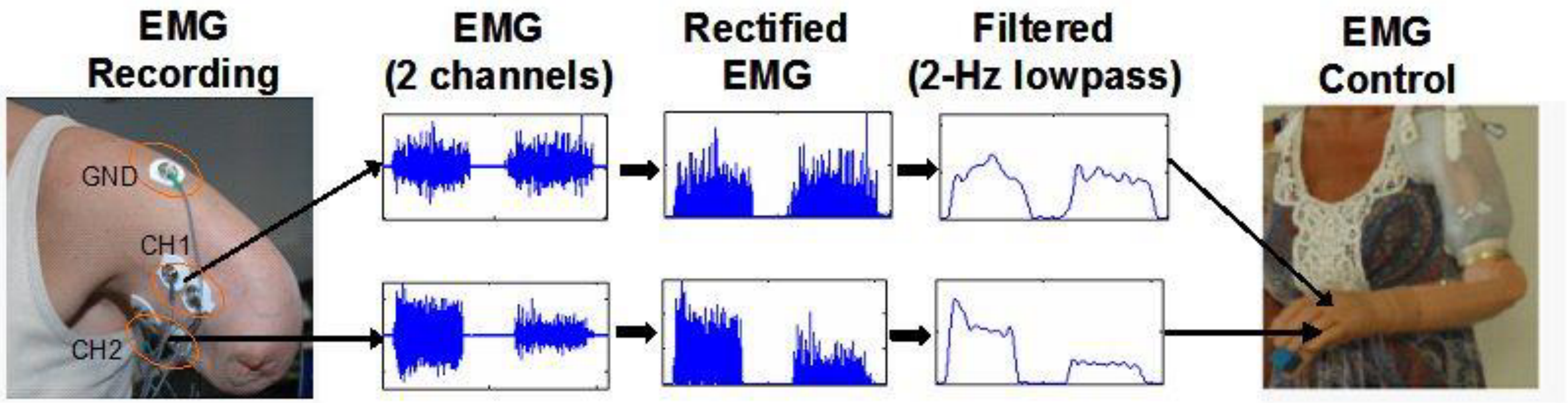

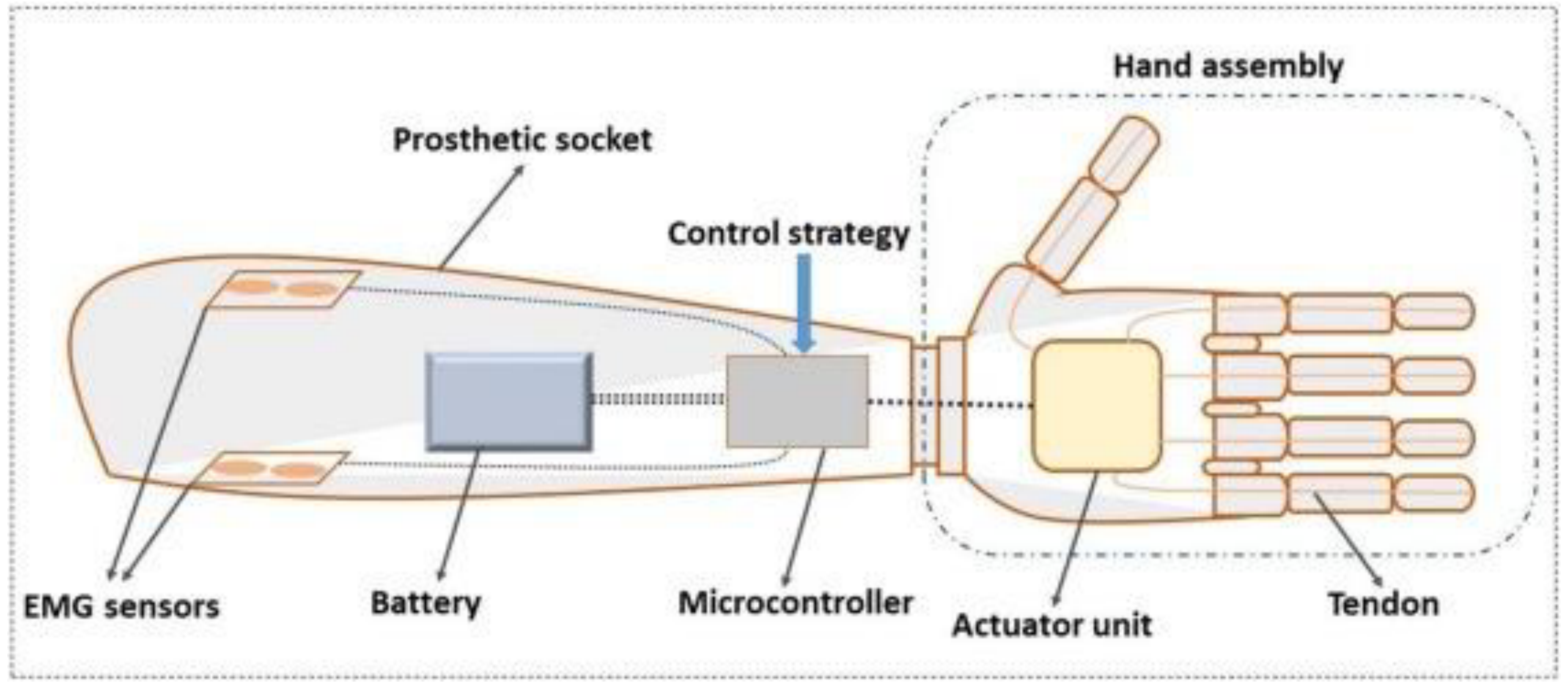

Hand prosthesis – Pattern recognition

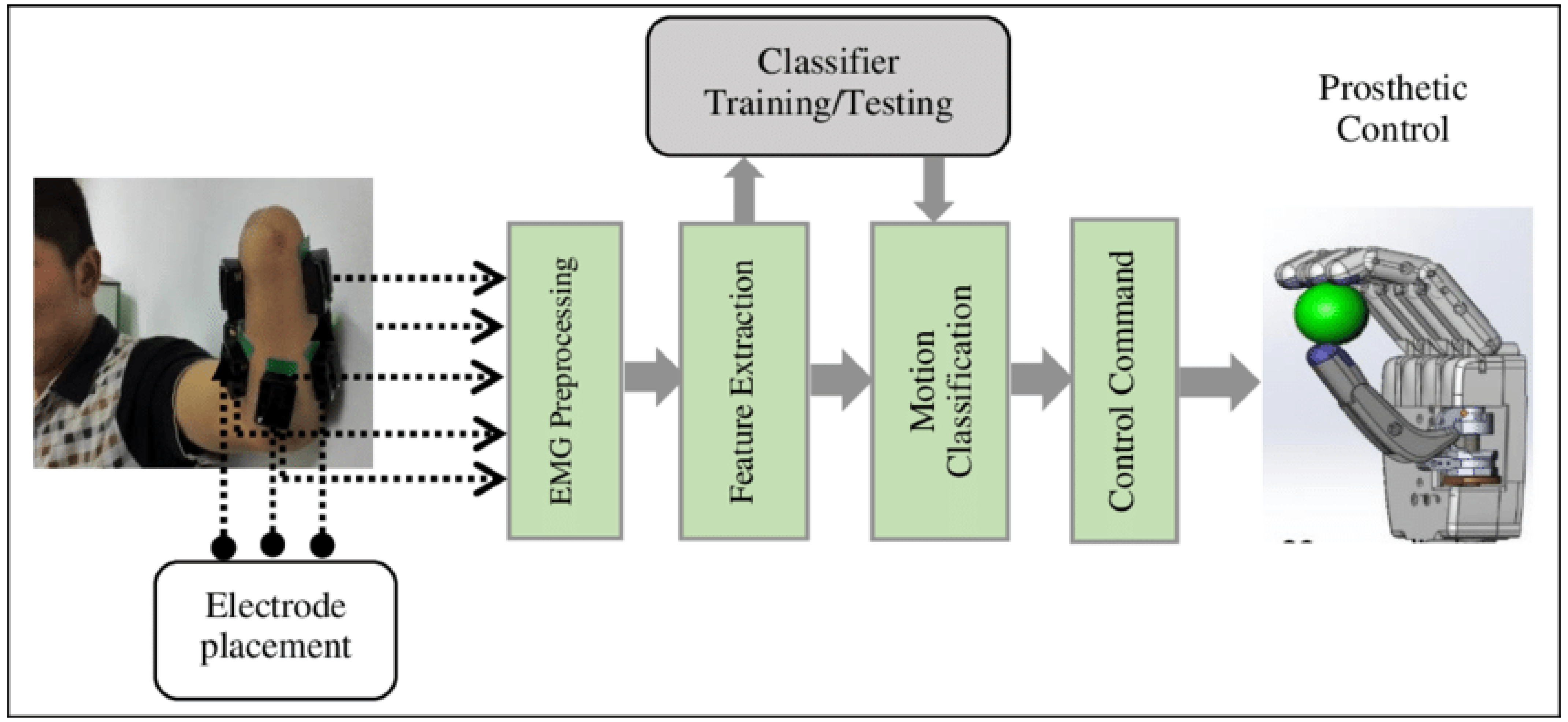

- In this case, the muscles naturally involved in the specific movement (e.g. ECR for the extension of the wrist) are no more available
- For this reason, “not- homologous” voluntary movements of the subject have to be coded as prosthesis movements (e.g. extension of the elbow for the extension of the wrist)
- This approach requires a quite long training phase and makes very difficult for the subject to easily control more than two degrees of freedom

EMG control – Muscle and feature selection

TD Feature	Definition	References
Mean absolute value	$MAV_i = \frac{1}{N}\sum_{k=1}^{N}\lvert x_i(k)\rvert$	[46], [50], [52]
Integrated absolute value	$IAV_i = MAV_i * N$	[53]
Variance	$VAR_i = \frac{1}{N}\sum_{k=1}^{N}(x_i(k)-\overline{x_i})^2$	[52], [54]
Mean absolute value slope	$MAVS_i = MAV_{i+1} - MAV_i$	[46]
Willison amplitude	$WAMP_i = \sum_{k=1}^{N} f(\lvert x_i(k) - x_i(k+1)\rvert)$ with $f(x) = 1 \; if x > x_{th}$, 0 otherwise	[54]
Zero crossing	$ZC_i = \sum_{k=1}^{N} f(k)$ with $f(k) = 1 \; if \; x_i(k)*x_i(k+1) < 0$ and $\lvert x_i(k)-x_i(k+1)\rvert > x_{th}$	[46]
Slope sign changes	$SSC_i = \sum_{k=2}^{N-1} f[(x_i(k)-x_i(k-1))*(x_i(k)-x_i(k+1))]$ with $f(x) = 1 \; if x > x_{th}$, 0 otherwise	[55]
Waveform length	$WL_i = \sum_{k=1}^{N-1}(\lvert x_i(k) - x_i(k+1)\rvert)$	[46], [55]
TSD Feature	**Definition**	**References**
Autoregressive coefficients	$x_i(k) = \sum_{j=1}^{N} a_j x_i(k-j)$, n^{th} order AR model	[53], [56]–[58]
Cepstral coefficients	$c_1 = -a_1; \;\; c_i = -a_i - \sum_{k=1}^{i-1}(1-\frac{k}{i})a_n c_{i-k}$ $1 \le k \le n$ and a_i are the AR coefficients	[52]
FD Feature	**Definition**	**References**
Mean of signal frequencies	$FMN_i = \sum_{j=1}^{M}(f_j p_j) \,/ \sum_{j=1}^{M}(p_j)$	[7]
Frequency ratio	$FR_i = \frac{min(FFT(x_i))}{max(FFT(x_i))}$	[7]
TSC or TF Feature	**Definition**	**References**
Short-time Fourier transform	$STFT[k,m] = \sum_{r=1}^{N-1} x[r]g[r-k]e^{-j2\pi mi/N}$ where g, k, and m are the window function, the time sample, and frequency bins, respectively.	[7]
Wavelet transform	Continuous WT (CWT) produces a good frequency resolution Δf in long time windows (low frequencies) and a good time localization Δt at high frequencies $CWT_x(\tau, a) = \frac{1}{\sqrt{a}}\int x(t)\Psi(\frac{t-\tau}{a})dt$ where t and a are the translation and scale parameters and Ψ is the mother wavelet function	[47], [51]
Wavelet packet transform	WPT is a generalized version of the continuous and discrete WT.	[47], [51], [59]

PCA or similar could be necessary to select few more information muscles

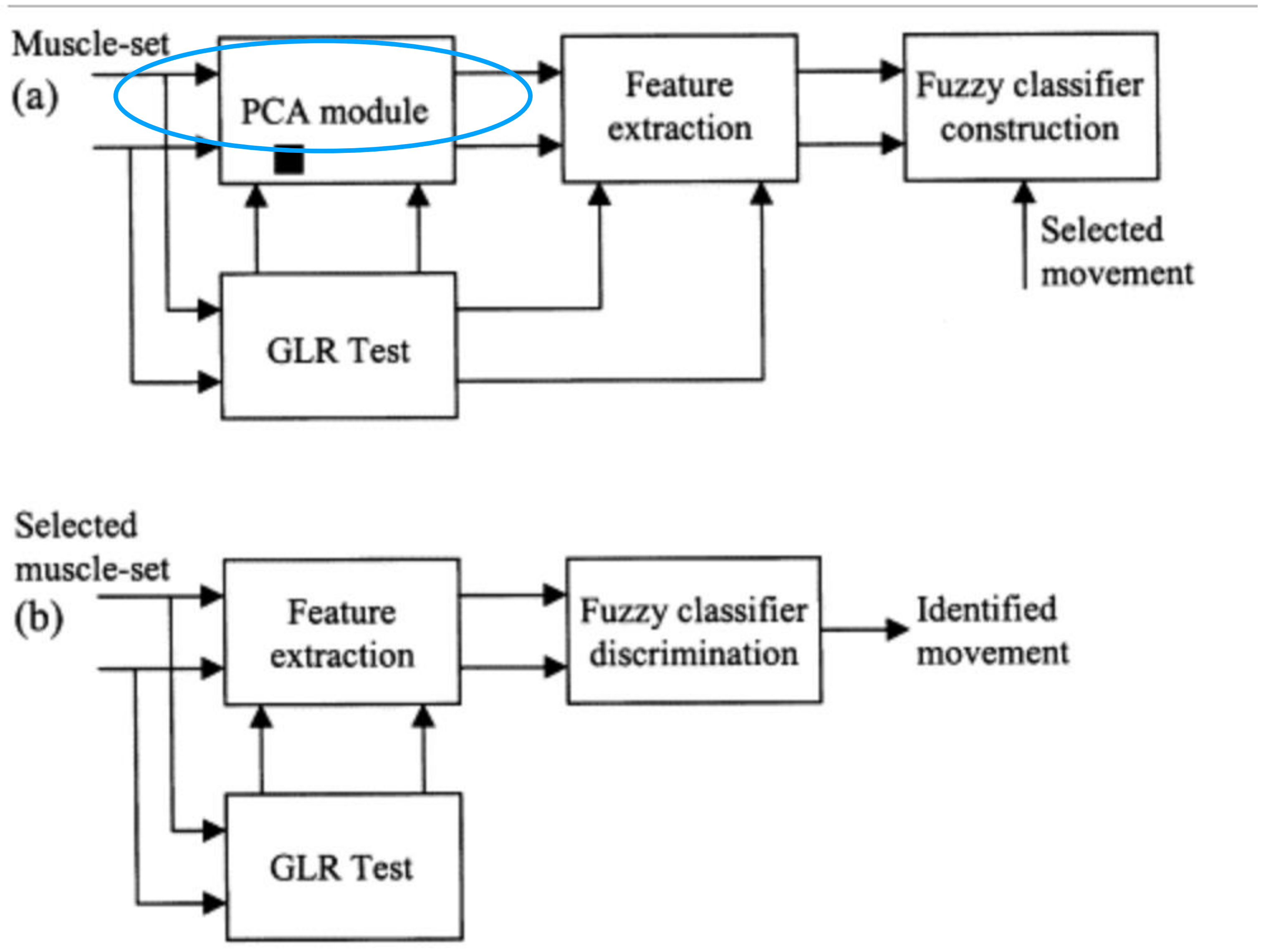

EMG control – Classifier selection

- Supervised learning classifier to link EMG signals (features) to desired hand movements
- More or less anything has been tried (including majority voting)
- Make a fair comparison!!

TABLE IV
SOME PATTERN RECOGNITION BASED CONTROL OF UPPER LIMB PROSTHESIS.
A = amputee subjects, H = healthy subjects, LD = limb deficiency subjects

Classifier	EMG chan-nels	Classes	Features	Subjects involved	References
MLP	2	4	MAV, MAVS, ZC, SSC, WL	9H+6A	Hudgins et al [46]
Fuzzy	2	6	IAV,VAR,AR, CC, adaptive CC	6H	Park and Lee [52]
LDA,MLP	2	4	-	16H	Englehart et al [51]
Fuzzy	2	4	MAV, MAVS, ZC, WL	4H	Chan et al [65]
PCA,LDA	2,4	4,6	-	11H	Englehart et al [47]
PCA,LDA	4	6	STFT, WT, WPT	12H	Englehart et al [12]
-	3,4	3,4	Fuzzy	3H+1A+1LD	Ajiboye and Weir [67]
HMM,MLP	4	6	-	12H	Chan and Englehart [66]
GMM,LDA,MLP	4	6	TD, RMS, AR	12H	Huang et al [68]
LDA,MLP	4	8	WPT	10H	Chu et al [64]
SVm,GDA	3	8	AR, histogram	1H+2A	Liu et al [70]
SVM,LDA,MLP	4	5	single and multi TD/FD	11H	Oskoei and Hu [49]
SVM	7	8	RMS	3H	Shenoy et al [71]
HMM,bayes	4	9	-	10H	Chu and Lee [69]
MLP	12/32	12	MAV, VAR, WL, W	5H+1A	Tenore et al [54]
LDA	12	10	MAV, ZC, WL, SSC	5A	Li et al [72]

EMG control – A little help?

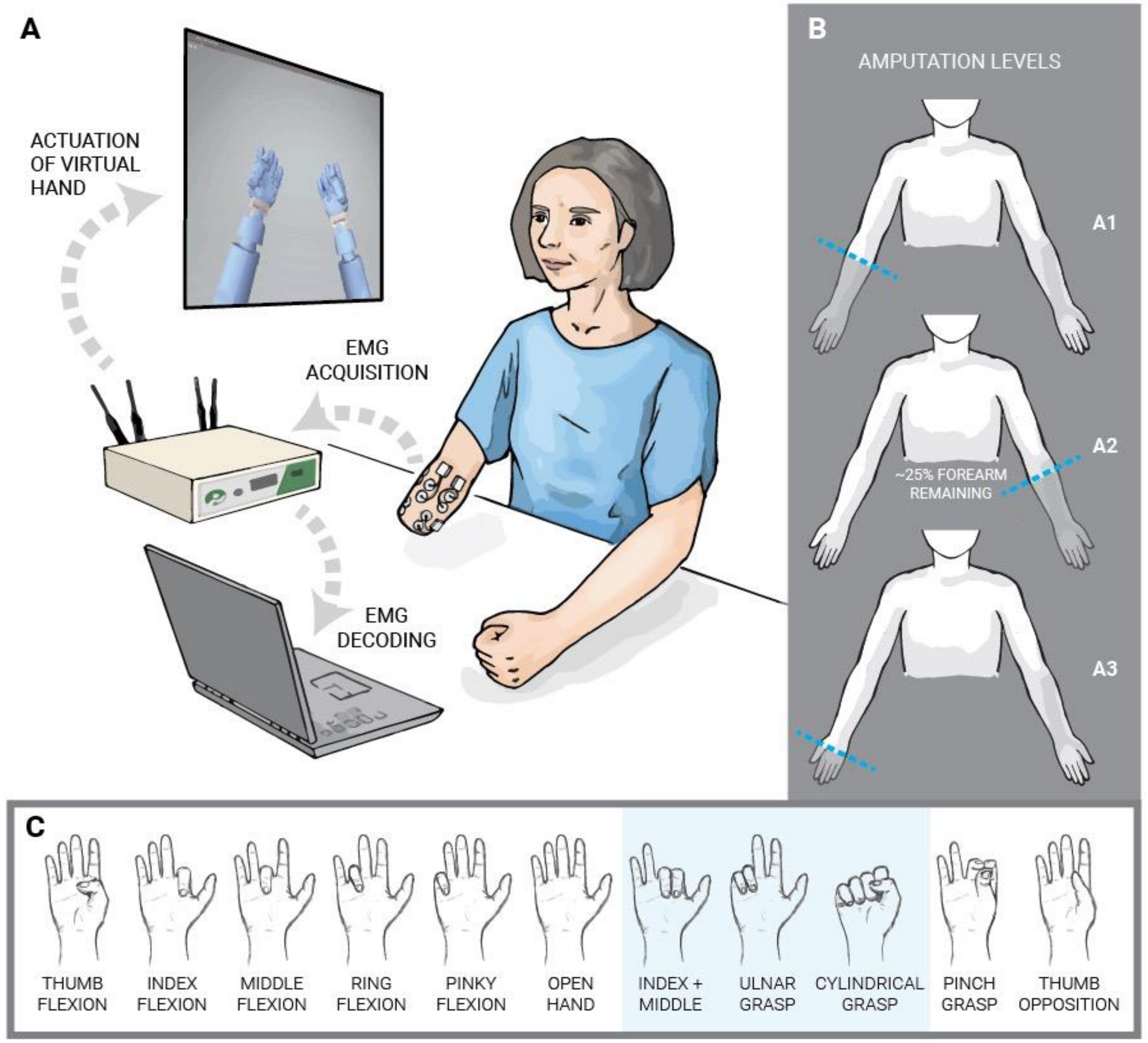

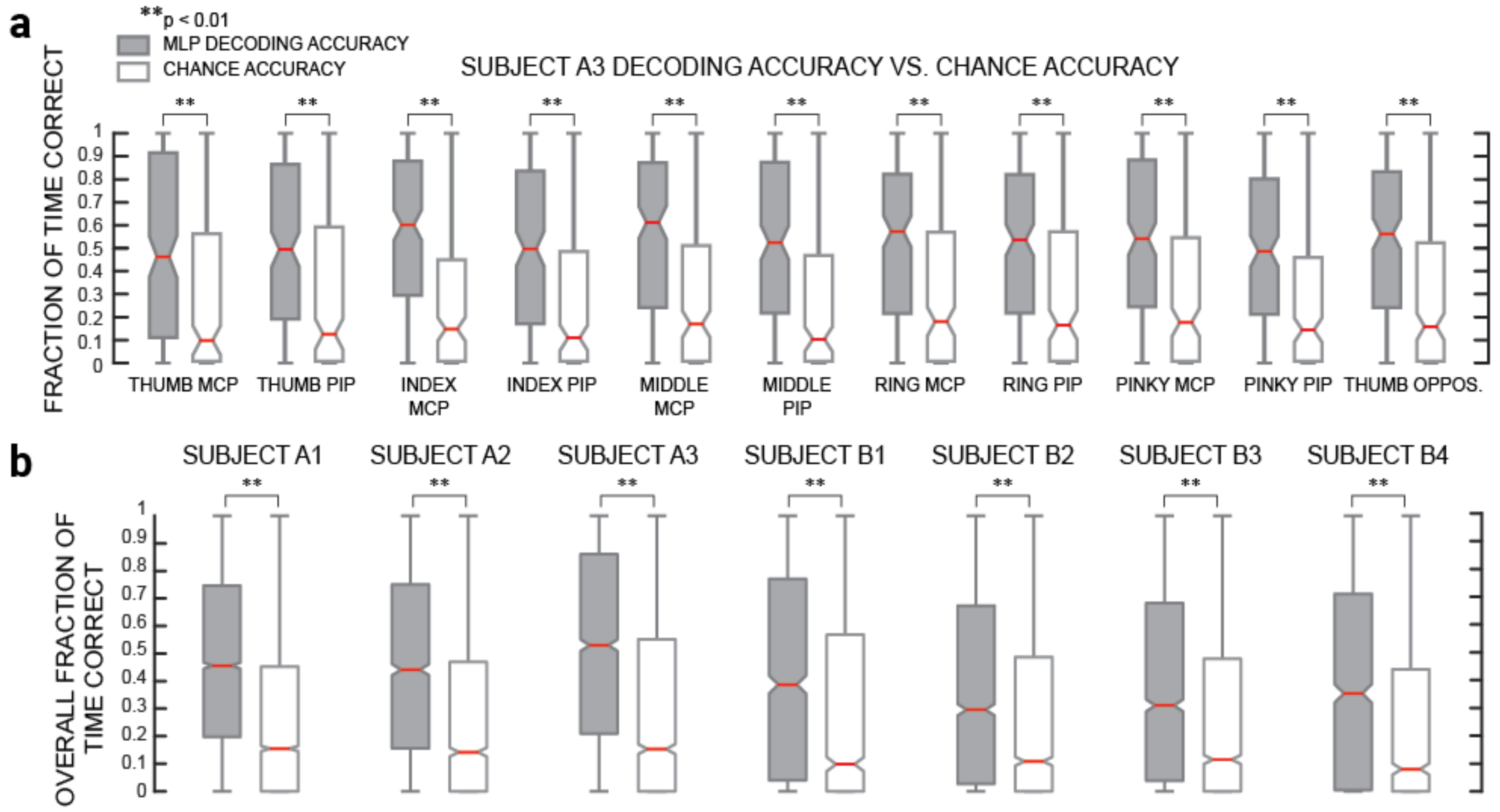

- Single finger decoding using EMG signals
- One implanted patient from UCSC - Loretana
- Two patients from collaboration with hospitals Chuv (Lausanne, CH) and Villa Beretta (Lecco, Italy)

EMG shared control

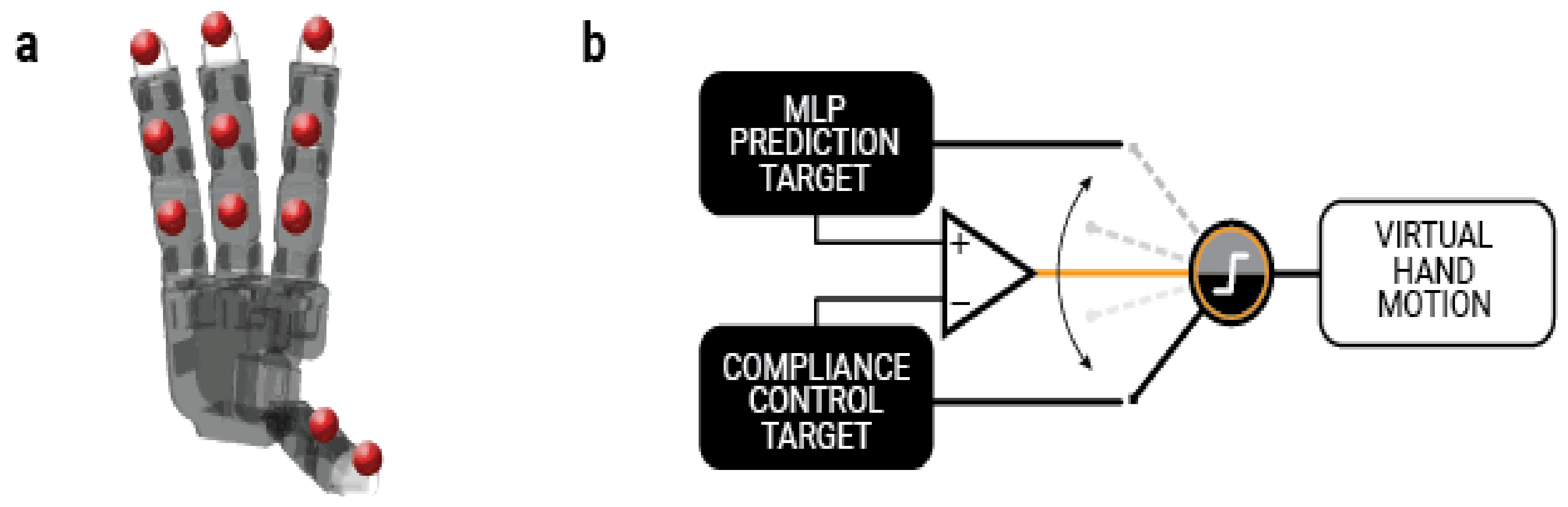

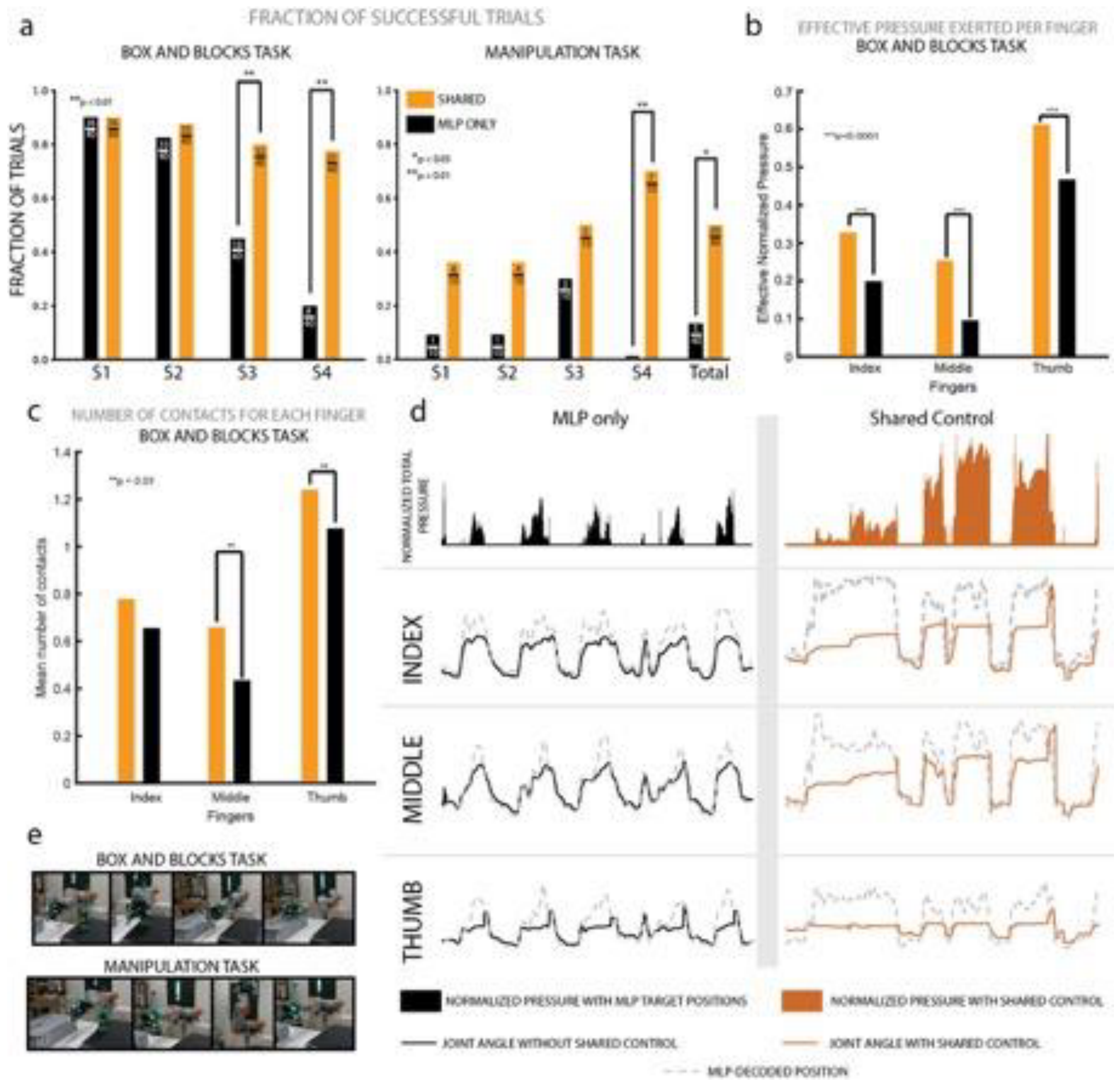

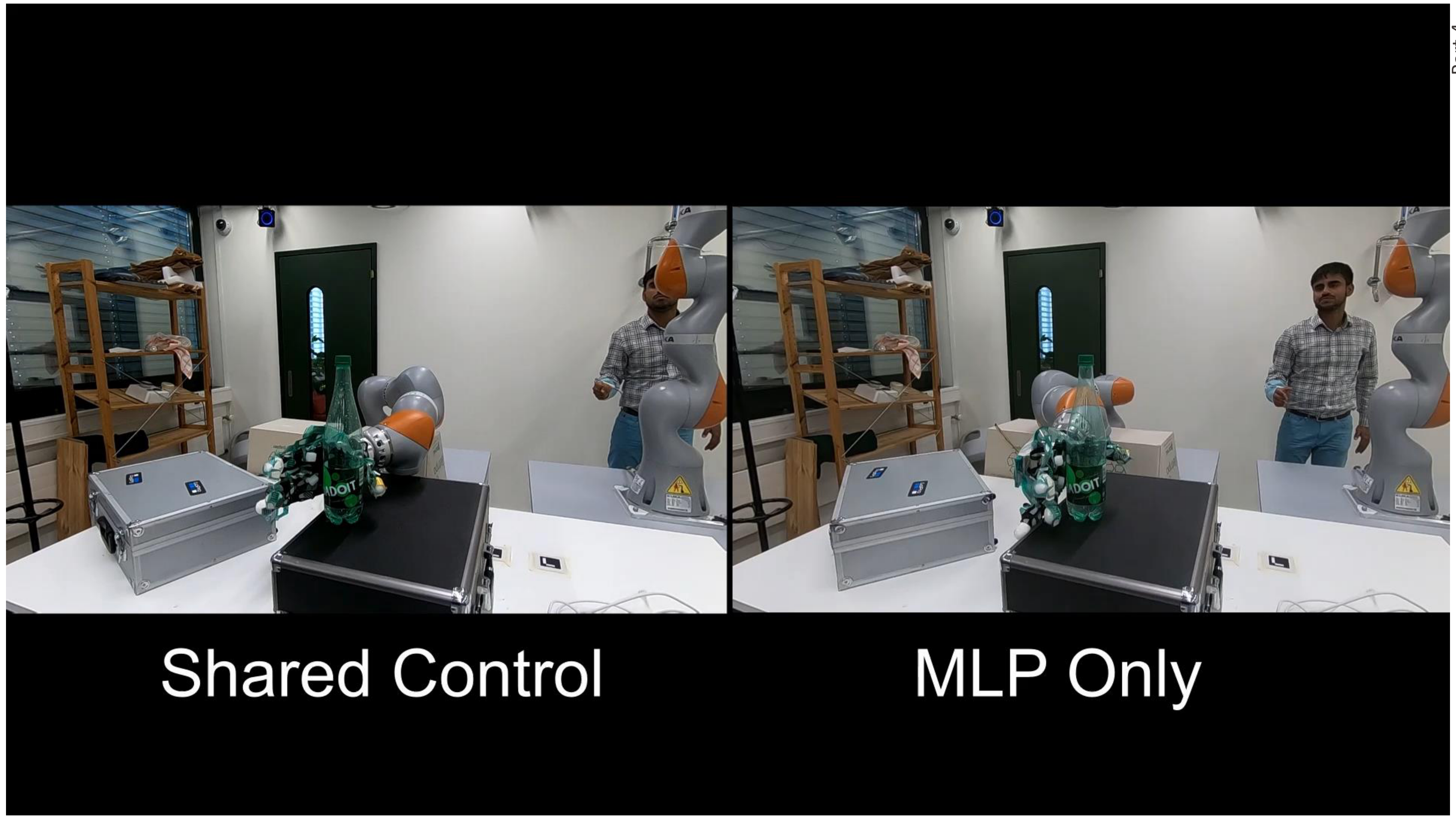

When a hand is not contacting an object, the user controls the robotic hand with the output of EMG decoding

When the hand makes contact with an object, the compliance controller automates hand conformation around the object, allowing a high degree of grasp stability

Intramuscular EMG (iEMG) control

- Clinically available myoelectric control strategies do not allow simultaneous movement of multiple degrees of freedom (DOFs)
- The use of implantable devices that record intramuscular EMG signals could overcome this constraint
- Intramuscular EMG signals can be recorded using percutaneous fine wire electrodes inserted using needles
- The use of iEMG can allow to use proportional control (but of course also pattern recognition)

Smith et al., 2014

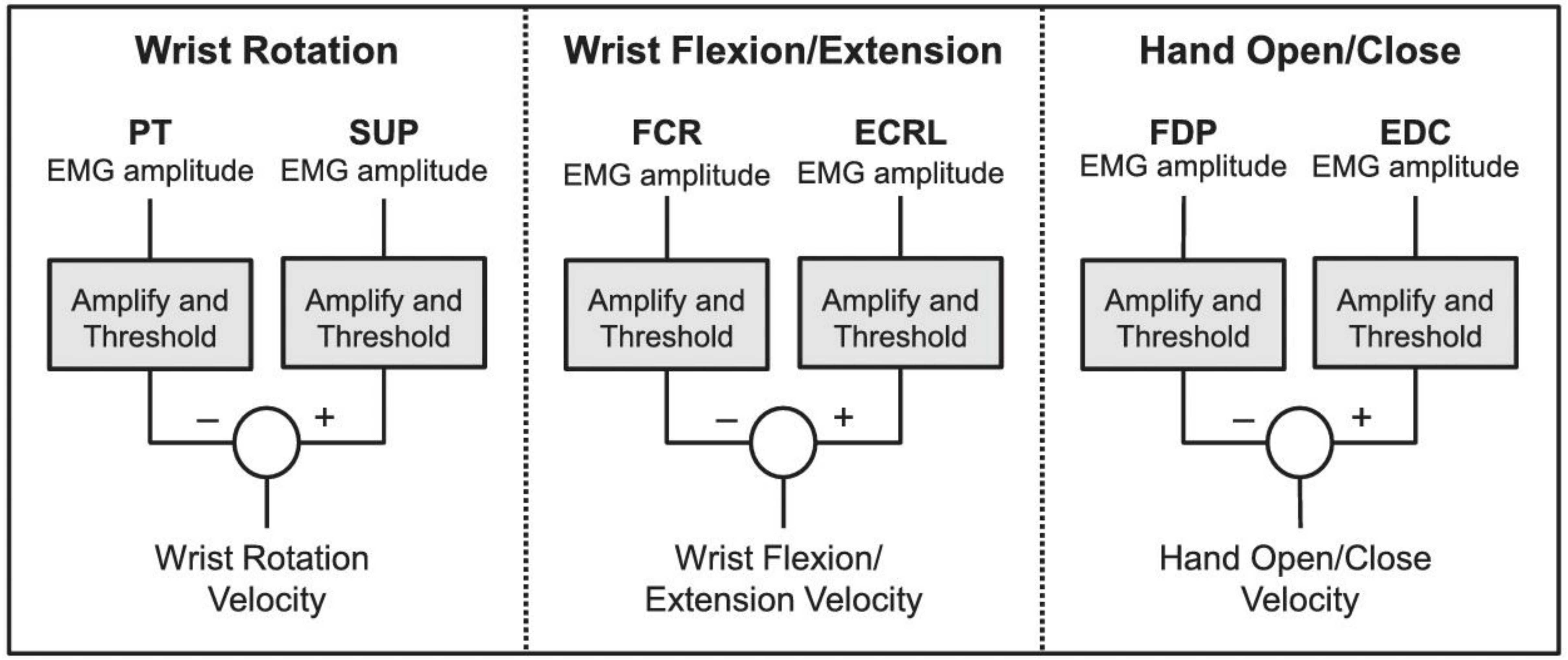

Intramuscular EMG (iEMG) control

- Sense myoelectric signal at its source, so it acts as an amplifier of the neural command.
- Use inductive coupling to pass power into devices and signal out of device w/o breaking the skin

Multifunction Prosthesis Control Using Implanted MyoElectric Sensors (IMES)

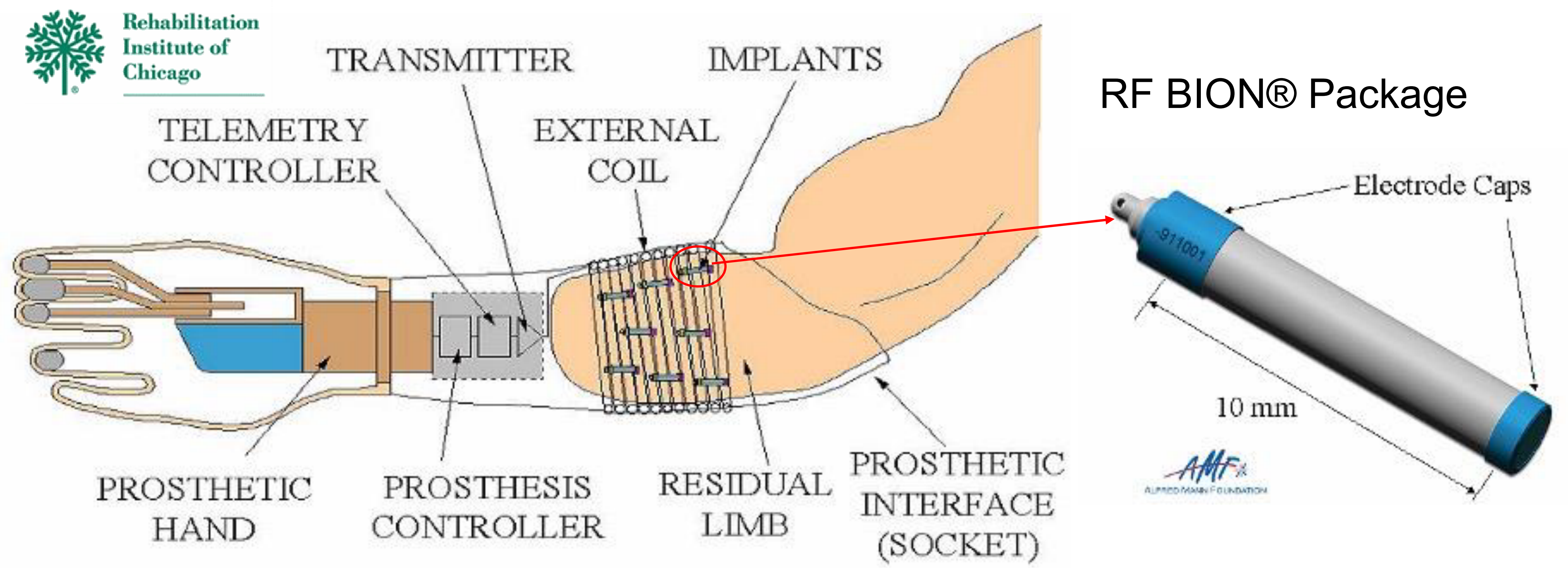

Smith et al., 2014

Targeted muscle reinnervation (TMR)

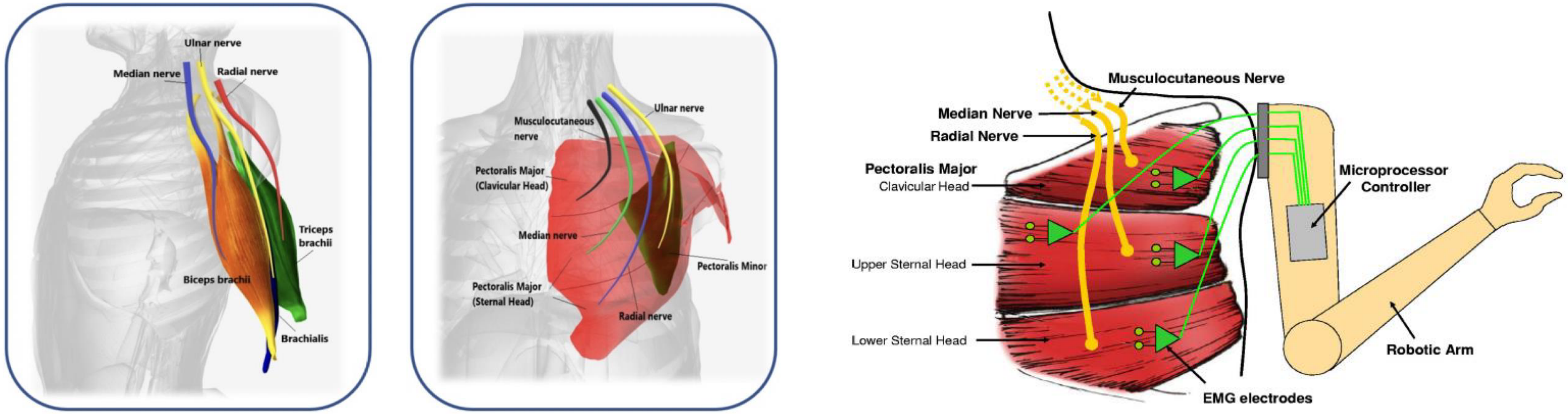

- A surgical technique called targeted muscle reinnervation (TMR) transfers residual arm nerves to alternative muscle sites
- After reinnervation, these target muscles produce electromyogram (EMG) signals on the surface of the skin that can be measured and used to control prosthetic arms

Kuiken et al., 2007

Bidirectional neurocontrolled leg prostheses

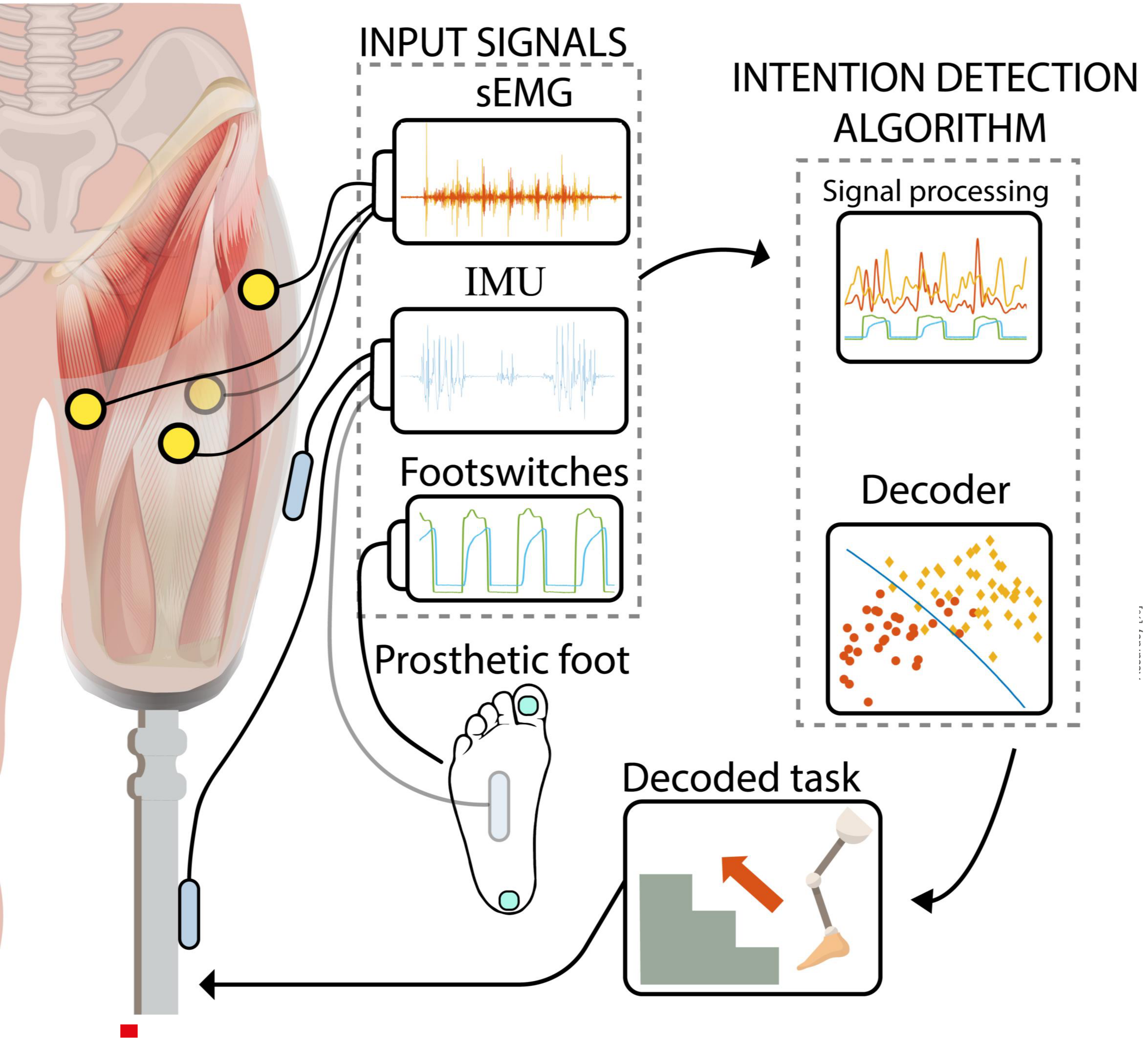

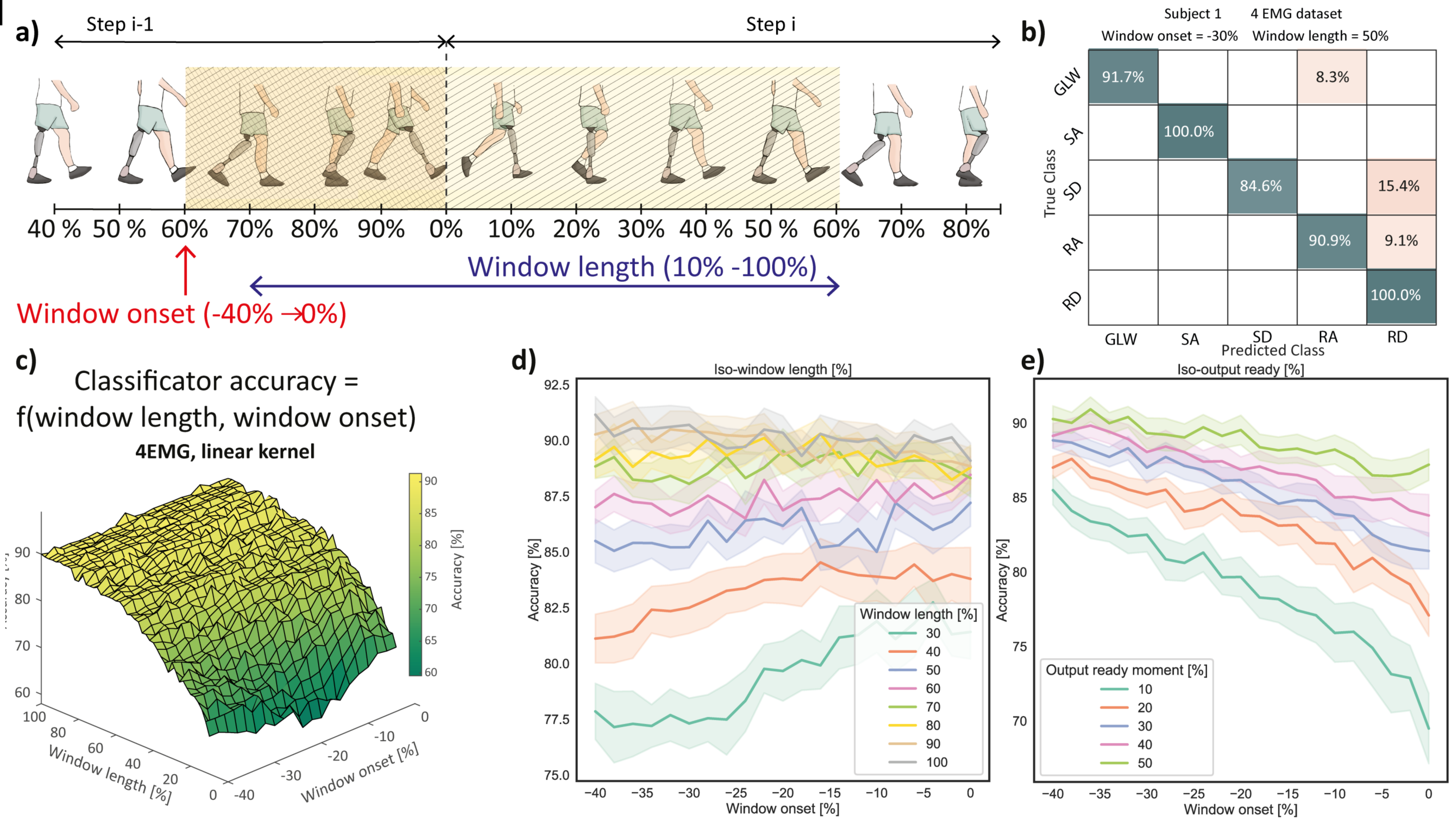

Conclusions

- Artificial limbs can be bidirectionally controlled in several ways
  - Non-invasive interfaces for decoding (EMG, EEG) and encoding (vibrators, transcutaneous electrical stimulation)
  - Invasive interfaces for decoding and encoding (ECoG, intracortical, peripheral implants)
- The choice must be done taking into account the residual skills of the subjects AND their preferences
- The different neurotechnological "tools" must be integrated accordingly